CENTRE FOR BIOPROCESS ENGINEERING RESEARCH
DEPARTMENT OF CHEMICAL ENGINEERING
UNIVERSITY OF CAPE TOWN

The Utilization of Carbon Dioxide by the Microalgal Species *Scenedesmus*

A thesis submitted in partial fulfillment of the requirements for the degree of
Master of Science in Engineering

TRISHA DAYA
AUGUST 2011

Synopsis

Climate change, which is predominantly a result of anthropogenic global warming, is a major concern for humanity. The scientific consensus is that the rise of greenhouse gases, such as CO_2, in the atmosphere has contributed to global warming. The increase in atmospheric CO_2 is due to the burning of fossil fuels and deforestation. In South Africa, 77% of our primary energy needs are supplied by coal and our demand for energy is increasing (Pegels, 2010; www.energy.gov.za). Cultivation of microalgae on flue gas from coal-fired plants and utilization of the algal biomass as an energy source has been proposed as a method for producing CO_2-neutral fuels. At PetroSA's natural gas to liquid fuels plant a CO_2-rich stream at substantially higher CO_2 concentration than typical flue gas is available. While microalgal species which can tolerate pure CO_2 are typically acidophilic thermophiles with low growth rates and low associated CO_2 recoveries, diluted CO_2 streams can be used under broader operating conditions. The selection of a microalgal species for the purposes of production of a CO_2-neutral fuel on a large-scale is influenced mainly by its CO_2 fixation capability and lipid productivity, both of which are a function of biomass productivity. Biomass yield and other morphological and physiological properties are also important as they affect ease of harvesting as well as amenability to anaerobic digestion and adaptability to environmental variations.

In this study, CO_2 utilization by the microalgae *Scenedesmus* sp. was investigated. The aims of this study were:

- To select a CO_2 mass transfer environment applicable to culture *Scenedesmus* sp.
- To compare the capability of CO_2 fixation of *Scenedesmus* sp. to other microalgal species
- To examine the physiological responses of *Scenedesmus* sp. interactively across the range of CO_2 inlet concentrations to delineate the limiting growth process
- To optimize the CO_2 uptake rate and associated biomass productivity, for *Scenedesmus* sp. via manipulation of CO_2, concentration, light intensity and nutrient regime

To achieve the first aim, the CO_2 uptake rates and recoveries were determined for a range of CO_2 inlet concentrations (0.045, 0.12, 0.29, 0.5 and 1% CO_2) and associated dissolved CO_2 saturation concentrations in a well-characterised airlift system. *Scenedesmus* sp. was cultured using modified Bold medium containing 750 $mg.L^{-1}$ $NaNO_3$, and under a light intensity of 282.7 $\mu mol.m^{-2}.s^{-1}$. The CO_2 uptake rates and maximum cell concentrations increased with increasing CO_2 inlet concentrations whereas the CO_2 recoveries decreased. The maximum average CO_2 uptake rate of 0.96 $g.L^{-1}.day^{-1}$ occurred at 1% CO_2. The corresponding CO_2 recovery was 6% and

the maximum cell concentration was 4.29 g/L. The inverse relationship between CO_2 uptake rate and recovery was attributed to the poor solubility of CO_2 in water and the mass transfer limitations of the CO_2 delivery method of active gas transfer. Supplying higher concentrations of CO_2 to *Scenedesmus* sp. (within the range of 0.045% to 1% CO_2) is clearly advantageous with respect to CO_2 assimilation and disadvantageous with respect to CO_2 recovery.

A literature survey was performed to compare the CO_2 fixation capability of *Scenedesmus* sp. with other microalgal species. Comparatively, *Scenedesmus* sp. had a high average CO_2 uptake rate and a low average CO_2 recovery (where authors reported recoveries). An accurate comparison was made between *Chlorella vulgaris* and *Scenedesmus* sp. as both species were cultivated in CeBER internal Loop Air Lift Reactors using the same operating conditions. *Scenedesmus* sp. achieved a two-fold higher maximum average CO_2 uptake rate (0.96 vs. 0.50 $g.L^{-1}.day^{-1}$) and a four-fold higher maximum cell concentration in comparison to *C. vulgaris* (4.29 vs. ~0.9 $g.L^{-1}$). This improvement was attributed to *Scenedesmus* sp.'s superior ability to adapt to the varying light environment. However, this improvement was accompanied by a four-fold lower average CO_2 recovery (6 vs. 26%). These studies clearly highlight the need for extended study on optimization of methods of CO_2 delivery.

To optimize CO_2 uptake rates and recoveries of *Scenedesmus* sp. a 2^3 factorial experiment was designed where the factors CO_2 concentration, external light intensity and nutrient regime were varied by two levels. CO_2 was varied from 0.5 to 1%, external light intensity was varied from 225 $\mu mol.m^{-2}.s^{-1}$ to 560 $\mu mol.m^{-2}.s^{-1}$ and nutrient regime was either standard or fed-batch. The provision of higher light intensities resulted in significant improvements to the average CO_2 uptake rates. The combination of CO_2 supplied at 1% and light supplied at 560 $\mu mol.m^{-2}.s^{-1}$ resulted in the highest average CO_2 uptake rate of 1.84 $g.L^{-1}.day^{-1}$. The corresponding average CO_2 recovery also increased from 6 to 11% and the maximum cell concentration increased from 4.29 to 5.09 g/L. The growth of *Scenedesmus* sp. cultured on 3% CO_2 and 590 $\mu mol.m^{-2}.s^{-1}$ was similar to the growth at 1% CO_2 and 560 $\mu mol.m^{-2}.s^{-1}$. The average CO_2 uptake rates were the same for both conditions hence the predicted CO_2 recovery declined substantially for the 3% CO_2 condition. Increases in CO_2 inlet concentrations beyond 1% CO_2 are unlikely to be beneficial for the range of cell concentrations and light intensities investigated in this study.

Thus far, work at CeBER has demonstrated that *Scenedesmus* sp. has comparatively high lipid productivity, a fast settling rate and can be bio-flocculated with *C. vulgaris* at pH 2.55 within 30 minutes at a recovery of 81% (Griffiths et al., 2011a; Dicks and Harrison, in preparation). This work, demonstrates that *Scenedesmus* sp. has good capability for CO_2 fixation, is adaptable to varying light intensities and can attain high biomass yields. Overall, *Scenedesmus* sp. is a promising candidate for large-scale production of CO_2-neutral fuels.

Plagiarism declaration

I know the meaning of plagiarism and declare that all the work in the document, save for that which is properly acknowledged, is my own.

Signed…….....

Acknowledgements

This work was achieved with the help of several individuals whom I would like to thank.

- To my supervisor Prof. Harrison, for the opportunity to study at CeBER and for academic input and direction
- To Dr Fenner, for her valuable academic feedback and advice throughout this MSc.
- To all algae club members (past and present), for their wonderful work, advice on my work and interesting discussions
- To Melinda Griffiths, for generously teaching me multiple experimental procedures and for sharing her superb algal knowledge with me
- To all CeBER support staff, especially Mrs Fran Pocock and Mrs Sue Jobson, for all the assistance during my work here. A special thank-you to Mr Emmanuel Ngoma, for his efforts with the offgas analyser, for accommodating me in the Fe-S lab and for helping me with numerous other tasks
- To Mr Gary Groenmeyer, for teaching me how to operate the TIC analyser and for accommodating me in the Minerals lab
- To my friends and colleagues, for their positive attitudes, help and encouragement
- To my parents and three older sisters, for their love, support and guidance
- To my boyfriend, for his help with multiple aspects of this MSc. and for his moral support

Financial assistance was kindly provided by the National Research Foundation (NRF) and the Department of Chemical Engineering, U.C.T.

Table of Contents

Table of Figures

List of Tables

Nomenclature

A	Debye-Huckel coefficient	dimensionless
B	Davies B parameter	dimensionless
C	concentration of CO_2 in the bulk liquid	($mol.L^{-1}$)
C*	the liquid-phase concentration of CO_2 in equilibrium with the gas phase	($mol.L^{-1}$)
CR (OG)	CO_2 recovery calculated using offgas data	(%)
CR (X)	CO_2 recovery estimated using biomass data	(%)
I_{avg}	Average Irradiance (PFD)	($\mu mol.m^{-2}.s^{-1}$)
I_{ext}	Average surface Irradiance (PFD)	($\mu mol.m^{-2}.s^{-1}$)
I_z	The intensity of light at depth z	($\mu mol.m^{-2}.s^{-1}$)
I_0	The intensity of light at depth 0	($\mu mol.m^{-2}.s^{-1}$)
I	Ionic Strength	($mol\ L^{-1}$)
k	The attenuation coefficient	dimensionless
F_{CO2}	Flow rate of carbon dioxide	($mg.hr^{-1}$)
K_a	acid dissociation constant	dimensionless
K_La	overall volumetric mass-transfer coefficient of CO_2	(s^{-1})
$K_{0.5}DIC$	concentration of CO_2 and/or HCO_3^- to maintain O_2 evolution at one-half V_{max} in the light	(µM)
$K_{0.5,p}$	affinity constant for CO_2 uptake by photosynthesis	(µM)
$K_{0.5,r}$	affinity constant of RuBisCO for CO_2	(µM)
K_H	Henry's constant for CO_2 in water	($mol.L^{-1}.atm^{-1}$)
m_i	molar concentration	($mol.L^{-1}$)

N_A	rate of mass transfer of CO_2	($gmol.m^{-3}.s^{-1}$)
P_{max}	maximum photosynthetic O_2 evolution	($g.g^{-1}.hr^{-1}$)
PAR	Photosynthetic Active Radiation	($\mu mol.m^{-2}.s^{-1}$)
P_{CO2}	Partial pressure of carbon dioxide in gaseous phase	(atm)
$P_{CO2, CRIT}$	Critical partial pressure of carbon dioxide in gaseous phase	(atm)
PFD	Photon Flux Density	($\mu mol.m^{-2}.s^{-1}$)
PPFR	Photosynthetic Photon Fluence Rate	($\mu mol.m^{-2}.s^{-1}$)
Q_x	Average biomass productivity	($g.L^{-1}.hr^{-1}$)
Q_{CO2}	Average CO_2 uptake rate	($g.L^{-1}.hr^{-1}$)
R	Universal gas constant	($kJ.kmol^{-1}.K^{-1}$)
T	Absolute temperature	(Kelvin)
U_{GR}	Superficial gas velocity in the riser	($m.s^{-1}$)
vvm	Volumetric flow rate ($L.min^{-1}$) per volume of culture (L)	(min^{-1})
y_i	the activity coefficient of species *i*	dimensionless
X	Biomass concentration	($g.L^{-1}$)
z_i	charge of species *i*	dimensionless

Abbreviations and Acronyms

ALR	internal loop Air Lift Reactors
ANOVA	Analysis of Variance
ATP	Adenosine Triphosphate, energy carrying molecule
AZA	Acetazolamide, a weak membrane-permeable CA inhibitor
CA	Carbonic Anhydrase
CeBER	Centre for Bioprocess Engineering Research
Chl	Chlorophyll
CCM	CO_2 concentrating mechanisms
CCS	CO_2 Capture and Storage
Ci	inorganic carbon
dCO_2	dissolved CO_2
dH_2O	distilled water
DW	Dry Weight
DIC	Dissolved Inorganic Carbon
EZA	Ethoxyzolamide, a membrane-permeable CA inhibitor
3NBBM	Bold's Basal Medium, enriched with 3X nitrate and vitamins
NADPH	Nicotinamide adenine dinucleotide phosphate
NO	Nitric Oxide
NO_X	Nitrogen oxide species
PCE	PhotoConversion Efficiency
PE	Photosynthetic energy conversion Efficiency

PFD	Photon Flux Density
PSI	Photosystem I
PSII	Photosystem II
PUT	Putrescine
RuBisCO	Ribulose 1,5 bisphosphate-carboxylase oxygenase
SO_X	Sulphur oxides species
SPM	Spermine
STP	Standard Temperature and Pressure
TIC	Total Inorganic Carbon

Glossary

Adsorption concentration	The selective concentration of one or more components of a gas at the surface of a microporous solid
Anaerobic Digestion	The process whereby volatile organic compounds are broken down by bacteria, in the absence of oxygen, to produce methane and CO_2
Autotroph	Organisms that obtain all the elements they require for growth from inorganic compounds (e.g. CO_2) only
Average Irradiance	The light level experienced by a single cell moving randomly inside the culture
Balanced growth	Occurs when the average concentration of major cell constituents remains constant and the rate of change of these constituents in the population is constant
C3 plants	Plants which use the conventional pathway of CO_2 uptake i.e. RuBisCO catalyzes the fixation of CO_2 to Ribulose 1,5 bisphosphate to form 3-phosphoglycerate
Carbonic Anhydrase	Enzyme which catalyzes the reversible reaction of CO_2 to HCO_3^-
Critical partial pressure of CO_2	The lowest value of CO_2 partial pressure, in the inlet gas, that facilitates a CO_2 gas-liquid transfer rate that is equal to the maximum rate at which CO_2 can be utilized through photosynthesis
Energy Transduction	Process in photosynthesis where the energy of excitation is used to raise an electron to a higher energy orbital such that it becomes a more potent

	electron donor. The transference of this electron to an electron acceptor results in the transformation of light energy to chemical energy
Extremophiles	An organism that lives in extreme environmental conditions
Flocculation	The process by which small micro-organisms destabilize and asexually aggregate within a colloid by approach to the point of zero charge, electrical double layer compression, charge patch neutralization, polymer bridging, hydrophobic interaction, and enmeshment within sweep floc
Heterotroph	Organisms that need organic substrates synthesized by other organisms
Lipid productivity	The product of lipid content and biomass productivity
Mixing time	Time after which the concentration of tracer differs from the final concentration C_f by less than 10% of the total concentration difference (C_f-C_i)
Photoacclimation	Phenotypic adjustments to variations in environmental factors
Photoadaptation	Changes in the genotype that arise in response to variations in environmental factors
Photobioreactor	Closed vessel for phototrophic production where energy is supplied via electric lights
PhotoConversion Efficiency	Measures the fraction of the solar energy that is converted to chemical energy

Photorespiration	The process involving the fixation of O_2 and the evolution of CO_2
Photosynthetic energy conversion Efficiency	Measures the fraction of the PAR solar energy that is converted to chemical energy
Photosynthesis	The process whereby the energy of light is used to oxidize water and simultaneously reduce CO_2 to organic carbon
Photon Flux Density	The number of photons passing through a flat surface per unit of time (considers photons in the PAR region only)
Photosynthetic Photon Fluence Rate	The total no of photons incident per time interval from all directions on a small sphere divided by the cross-sectional area of the sphere (equivalent to PFD)
RuBisCO	Enzyme which catalyzes the fixation of either carbon dioxide or oxygen
Stripping	The transfer of a component from a liquid phase in which it is dissolved to a gas phase
Zeolites	Microporous crystalline solids with well-defined structures. Generally contain silicon, aluminium and oxygen in their framework and cations, water and/or other molecules within their pores

Chapter 1: Introduction

1.1 Background

1.1.1 South Africa: a coal-dependent nation

The atmospheric concentration of carbon dioxide is increasing and is considered to be the main cause of global warming (de Morais and Costa, 2007a). Usage of fossil fuels such as coal is the main contributor to greenhouse gases such as CO_2. From a South African perspective, approximately 77% of our primary energy needs are provided by coal and about 850 g of CO_2 emitted per kWh produced, the South African average is nearly twice as high as industrialized countries (www.energy.gov.za; Pegels, 2010) (Figure 1.1). Additionally, SA's energy demand is expected to reach about 76 GW by 2025 and Eskom, which produces most of SA's electricity (95%), has an installed capacity of 40 GW (Pegels, 2010). At the current rate of production, SA's coal reserves are expected to last at least 50 more years (www.energy.gov.za).

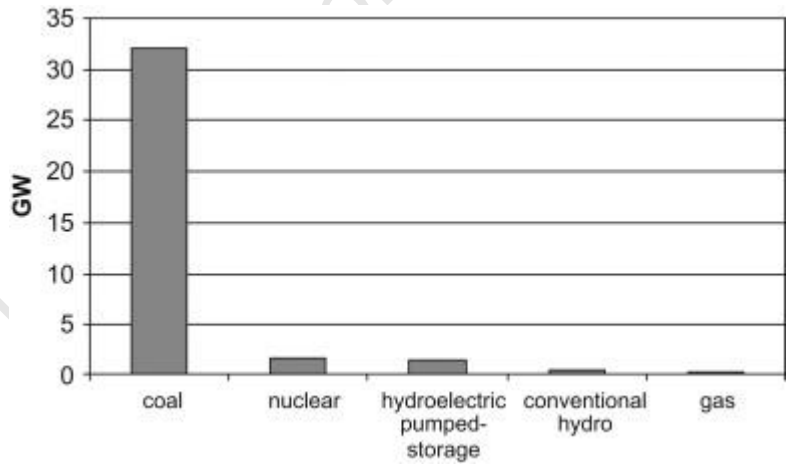

Figure 1.1: Energy mix in SA for electricity production (Pegels, 2010)

1.1.2 Drivers for change

According to the Kyoto Protocol, South Africa (SA) is listed as a non-annex II country which means it does not have binding mitigation targets (www.unfcc.int). However, SA like many

developing countries is most vulnerable to the effects of climate change, especially with regard to water supply, agricultural output and public health (Pegels, 2010). Unlike other developing countries such as India, which has a 1.5 t CO_2-eq per person and China, which has a 3.8 t CO_2-eq per person, SA has a 10.1 t CO_2-eq per person which is cause for concern (Winkler and Marquand, 2009).

1.1.3 South African Renewable Energy Policies

Recent governmental strategies to address the above concerns include the 2003 White Paper on renewable energy, the 2007 Long-Term Mitigation Scenarios, the 2009/ 2010 Renewable Energy Feed-In Tariff (REFIT) and a carbon tax which was implemented in mid-2009. In the long-term scenario, four pathways are outlined (Pegels, 2010). 'Growth without Constraints' is business as usual; 'Start Now', requires positive upfront investments but results in net negative costs; in 'Use the Market' economical devices such as carbon tax are used and 'Reach for the Goal' combines the mitigation efforts of the other 3 scenarios and factors in the use of unknown technology (Pegels, 2010). The only pathway which intersects with the 'Required by Science' scenario, which aims at reducing SA emissions by 30-40% from the 2003 level, is the 'Reach for the Goal' scenario depicted by the grey wedge in Figure 1.2 (Pegels, 2010). This necessitates research into new technology and alternative energy sources, of which algal biofuels are one example.

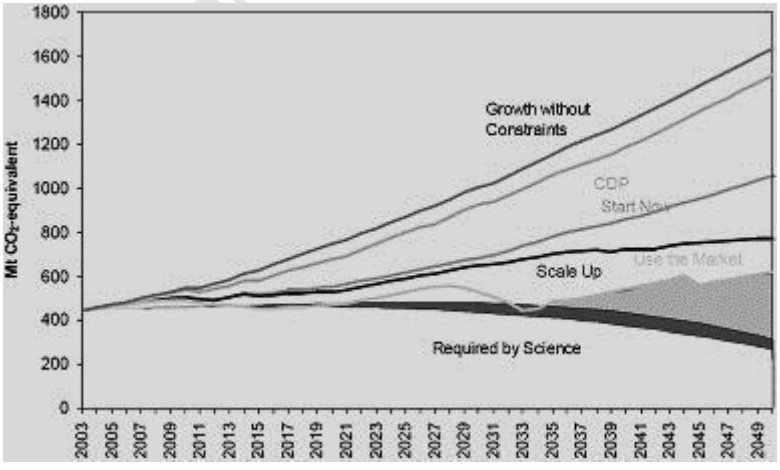

Figure 1.2: SA mitigation options 2003-2050, Long-Term Mitigation Scenarios (Pegels, 2010)

1.1.4 Advantages of algal biofuels

Second generation biofuels such as algal biofuels are of growing interest as they minimize the food versus fuel trade-off. The benefits for using algae versus other plant crops for biofuels are a greater flux tolerance, greater photosynthetic efficiency, faster reproductive cycles, limited nutrient requirements and the ability to adapt to artificial irradiation distributions and intensities (Gordon and Polle, 2007). Other benefits are that energy is not expended in the production of non-photosynthetic supporting structures; it is easier to supply optimal nutrient levels due to the well-mixed aqueous environment and the ability to maintain cell densities at optimal levels with continuous culture systems (Packer, 2009). In exploiting these advantages, the net energy recovery from the biofuel, i.e. the energy generated for use as a ratio of energy required for production, is a key consideration in process selection.

1.1.5 Cultivating algae on flue gas

Approximately 90% of SA's electricity is generated from coal fired plants and this process contributes to a major portion of its CO_2 emissions (www.energy.gov.ac.za). Flue gas typically contains between 3 and 15% CO_2[1]. At PetroSA, where natural gas is converted to liquid fuels, highly concentrated CO_2 streams (approaching 100% CO_2) are available for use (Packer, 2009).

Algal species which are able to tolerate growth at high dissolved CO_2 concentrations resulting from sparging with concentrated CO_2 streams are rare. It has been noted that high concentrations of CO_2 in the inlet gas (>5%) and low pH caused by CO_2 dissolution, suppress algal growth (Kurano et al., 1995; Nielsen, 1955). The acidophilic and thermophilic rhodophytes *Galdieria partita*, *Cyanidium caldarium* and *Cyanidium melorae* showed growth at 50°C, pH 1 and pCO_2 1, while only *G. partita* could proliferate under 50 ppm SO_2 aeration (Kurano et al., 1995). Thus, Kurano et. al. (1995) concluded that *G. partita* would be the most suitable candidate for direct CO_2 fixation of industrially discharged gases without pretreatment.

Direct use of flue gas imposes extreme conditions on microalgae such as high concentrations of CO_2 and the presence of inhibitory compounds like oxides of nitrogen (NO_X) and sulphur (SO_X) (Sung et al., 1999). There are several studies which provide evidence that algae can be cultivated on flue gas, although the biomass generated may be unable to be used for animal and human

[1] Concentration based on a volume to volume basis unless specified otherwise

consumption due to heavy metal accumulation (Borkenstein et al., 2010; Brown, 1996; Doucha, Straka and Livansky, 2005; Douskava et al., 2009; Kadam, 1997; Vunjak-Novakovic et al., 2005).

Additionally, numerous studies evaluated whether a species of algae can tolerate a specified percentage of CO_2 in the inlet gas, however this is a subjective measure owing to the influence of reactor configuration. Few studies provide information linking the cultivation setup (mass transfer coefficient, gas flow rate) to CO_2 recovery, dissolved CO_2 concentration, CO_2 uptake rate, growth rate and productivity of the species (Jacob-Lopes et al., 2009a; Murakami and Ikenouchi, 1997; Sydney, 2010; Usui and Ikenouchi, 1997). This makes it difficult to determine whether the excess CO_2 provided is being sequestered by the algae or used to drive mass transfer. Further the data reported in the absence of rigorous reactor study remains system specific with limited applicability to informing process design and estimating its performance.

It should be noted that the concentration of the CO_2 inlet gas stream (P_{CO2}) is not an indication of the potential of the algal culture system to sequester CO_2, but an indication of the tolerance of that species to pH and CO_2 concentration (Langley, 2010). While the dissolved CO_2 concentration will increase as CO_2 inlet gas concentration is increased, this depends upon the mass transfer properties and the retention time of the gas, within the culture. Above a certain CO_2 inlet concentration, the dissolved CO_2 concentration will reach a saturation limit where the CO_2 transfer rate matches the uptake rate with a small driving force (Chiu et al., 2008). At lower CO_2 inlet concentrations, a steady state dissolved CO_2 concentration is achieved where the CO_2 transfer rate at this driving force is equivalent to the algal species' uptake rate of CO_2. The capability of an algal culture to fix CO_2 at the maximum rate depends on the physiological characteristics of the algal species used, optimization of growth conditions, method of CO_2 supply and physical parameters (temperature, pH etc.) which affect CO_2 solubility and bioavailability (Keffer and Kleinheinz, 2002). A rigorous understanding of these interactions is an essential requirement for the efficient production of algal biomass as an energy product with concomitant CO_2 capture or cycling.

1.2 Hypotheses and Key Questions

Previous work done in the Centre for Bioprocess Engineering Research (CeBER) with the algal species *Chlorella vulgaris* and alkaphilic algal species *Spirulina platensis* revealed that *C. vulgaris* had a maximum average biomass productivity (Q_x) of 12.8 $mg.L^{-1}.hr^{-1}$ and *S. platensis* had a Q_x of 7 $mg.L^{-1}.hr^{-1}$. *C. vulgaris and S. platensis* were cultivated in internal loop Air Lift Reactors (ALRs) at 25 ± 1 °C with 750 $mg.L^{-1}$ and 2500 $mg.L^{-1}$ of $NaNO_3$ respectively (Langley, 2010).

The $P_{CO2,\ CRIT}$, defined 'as the lowest value of CO_2 partial pressure, in the inlet gas, that facilitates a CO_2 gas-liquid transfer rate that is equal to the maximum rate at which CO_2 can be utilized through photosynthesis', was determined to be 0.0012 atm (1200 ppm) for *C. vulgaris* (Langley, 2010).

Hypothesis 1

In comparison to *C. vulgaris*, *Scenedesmus* sp. attains higher cell concentrations. It is predicted that the capability for CO_2 fixation and recovery is greater for this algal species and that a higher $P_{CO2,\ CRIT}$ results.

Key questions

- What is the $P_{CO2,\ CRIT}$ for *Scenedesmus* sp. cultured in ALRs under standard operating conditions?
- What is the effect of CO_2 inlet concentrations, higher than air levels (350-450 ppm) on the parameters:

    a) Maximum average specific growth rate (μ_{max})

    b) Maximum average CO_2 recovery

    c) Maximum average CO_2 uptake rate (Q_{CO2})

    d) Maximum cell concentration (X_{max})

- How does the CO_2 fixation of *Scenedesmus* sp. compare to other microalgal species?

Hypothesis 2

In addition to limitations of CO_2 mass transfer, algal culture in the ALRs is limited by light. By manipulating factors such as light intensity, nutrient concentration and CO_2 inlet concentrations optimum biomass productivity can be approached. This will enhance the CO_2 fixation and recovery of the cultivation system.

Key questions

- What limits the CO_2 fixation of *Scenedesmus* sp.?
- What is the effect of using higher nutrient concentrations, or a different mode of culture on the aforementioned parameters?
- What is the effect of using higher light intensities on the aforementioned parameters?

1.3 Thesis Layout

In Chapter 2, a literature review is presented to outline the relevant theory, to obtain an understanding of the fundamentals of algal biotechnology and to provide insight into the current relevant understanding of microalgal culture and the scope of the research globally. In Chapter 3, the methods, materials and data analysis used in this study are described. In Chapter 4, the effect of CO_2 inlet concentration on various growth parameters are presented and discussed. In Chapter 5, experiments designed to optimize the CO_2 utilization by studying the interactions between light, nutrient and CO_2 availability are presented and discussed. The conclusions of this study are presented in Chapter 6 and their significance and limitations are discussed.

Chapter 2 : Literature Review

2.1 The biology of algae

2.1.1 Introduction to algal biology

Algae are photosynthesizing O_2 evolving organisms that have evolved from independent evolutionary lines (polyphyletic) (Figure 2.1). The term algae refers to both macroalgae and microalgae with the latter accounting for the majority of the existing species. The huge diversity of algal strains arises from the polyphyletic roots of algae, making classification difficult. According to Van Der Hoek's scheme they are classified under the two kingdoms Prokaryota eubacteria and Eukaryota with two and nine divisions attributed to these kingdoms respectively (Barsanti and Gualtieri, 2006). Algae within different divisions are characterized by their accessory pigments that impart a red, blue, or golden-brown colour. Additionally, they have chemically different cell walls and storage products, distinctive forms of motility or numbers of flagella, and distinctive ultrastructural features (Stevenson et al., 1996).

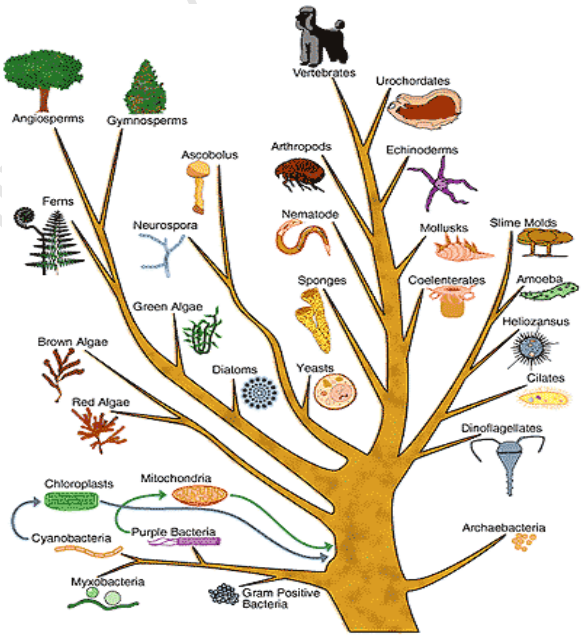

Figure 2.1: Evolutionary Tree (http://gapanalysis.ncbi.gov)

Algae can occur aquatically or sub-aerially with sizes ranging from 0.2-20 µM in diameter for picoplankton, to 60 m length fronds of giant kelps. Owing to the large diversity of strains, algae can tolerate a broad range of pH, temperature, turbidity and O_2 and CO_2 concentrations. Algae that thrive in acidic and alkaline conditions, or under high osmotic stress, are known as acidophilic, alkalophilic and halophilic species respectively. The mode of algal reproduction may be vegetative (binary division), asexual (production of motile spores) or sexual (production of gametes) (Barsanti and Gualtieri, 2006). This literature review will focus on phototrophic microalgae, with emphasis on the green microalgae, *Scenedesmus*.

2.1.2 The microalga *Scenedesmus*

Microalgae of the family *Scenedesmaceae* are unicellular and reproduce asexually. *Scenedesmus* cultures are freshwater species which grow rapidly, have simple nutritional needs and are easy to maintain in the laboratory (Trainor et al., 1976). The indigenous culture which is used in this study has not been designated to a species and will be referred to as *Scenedesmus* sp.

2.2 Requirements for microalgal culture

2.2.1 Light

Light is one of the principal requirements for photosynthesis, which is essentially the transduction of light energy to chemical energy (Garrett and Grisham, 2005). Most algae require light for growth and are thus labeled phototrophic. Algae also use light for information sensing processes. Both the sensing process and photosynthesis require the absorption of photons, by electrons of chromophore molecules, in order to excite the electrons to a higher orbital increasing the capability of the molecule to do work (Barsanti and Gualtieri, 2006). All algal divisions have the chromophore chlorophyll *a*, but different divisions can also have chlorophyll *b*, *c*, and/or *d* (Stevenson et al., 1996).

The relationship between light and photosynthesis can be described by the Photosynthesis-Irradiance response (P-I) curve which has three characteristic regions: light limited photosynthesis, light saturated photosynthesis and photoinhibition (MacIntyre et al., 2002). Photosynthesis can be measured as rates of carbon accumulation or oxygen evolution, and either measurement can be converted into the other using the photosynthetic quotient (molar ratio of O_2 evolved to CO_2 assimilated) (Anderson, 2005).

- ***Light Limited photosynthesis***

  The rate of photosynthesis increases linearly with increasing Photon Flux Density (PFD) (Barsanti and Gualtieri, 2006). The rate of photon absorption determines the rate of steady-state electron transport from H_2O to CO_2 (Barsanti and Gualtieri, 2006). The relatively low light intensities are insufficient to support the maximum rate of the light dependent reactions, hence photosynthesis is limited.

- ***Light Saturated photosynthesis***

  The rate of photosynthesis ascends with the increasing PFD whereupon it plateaus to a maximum level. Any further increase in PFD cannot be utilized, since the rate of photon absorption exceeds the rate of steady-state electron transport from H_2O to CO_2 (Barsanti and Gualtieri, 2006).

- ***Photoinhibition***

  Excessively high PFDs results in a decline in the photosynthetic rate. This is perhaps due to the fact that the excess energy is dissipated as fluorescence and heat (non-photochemical quenching), which may result in free radicals which damage Photosystem II (Eriksen, 2008; Schenk et al., 2008).

2.2.1.1 Light dependent reactions of photosynthesis

In photosynthesis a charge separation is produced between the photo-excited molecule of a chlorophyll molecule (electron donor) and an electron-deficient molecule (electron acceptor). As depicted in Figure 2.2 both Photosystem I (PSI) and Photosystem II (PSII) contain light harvesting complexes, which have maximal light absorption at 700 and 680 nm respectively (Garrett and Grisham, 2005). Excitation energy (from light) is transferred to the photosynthetic reaction centres of PSI and PSII via a network of pigments. PSII uses the energy to split water into protons, electrons and oxygen. The electrons are passed along the electron transport chain

and the protons are simultaneously released into the thylakoid lumen, which generates a proton gradient that drives ATP production. At PSI, the spare protons and electrons are used to regenerate NADPH. NADPH and ATP are used in the Calvin cycle and other biochemical pathways to produce sugars, starch, oils and other bio-molecules that are needed to produce bioethanol, biodiesel and biomethane and other biofuels. With some species e.g. *Chlamydomonas reinhardtii* the protons and electrons are alternatively used to drive the direct photo-production of biohydrogen (Figure 2.2) (Barsanti and Gualtieri, 2006; Schenk et al., 2008).

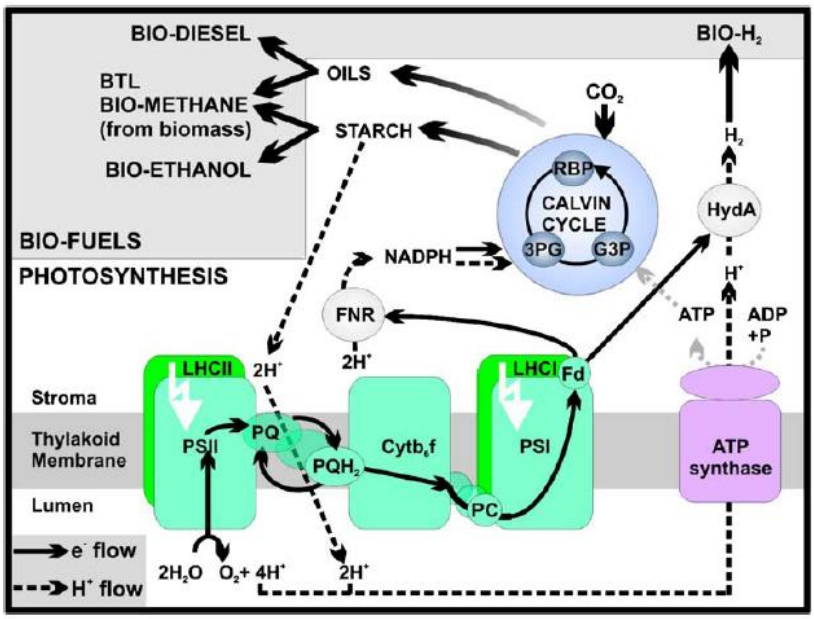

Figure 2.2: Photosynthesis schematic (Schenk et al., 2008)

2.2.1.2 PhotoConversion Efficiencies

PhotoConversion Efficiency (PCE) is a measure of the fraction of the total solar energy that is converted to chemical energy. Only light within the PAR region (400-740 nm) of the light spectrum can be absorbed by algae, which is why Photosynthetic conversion Efficiency (PE) which considers only the PAR solar energy, is occasionally used in lieu of PCE (Posten, 2009). Figure 2.3 illustrates the spectral irradiance profile of sunlight in the USA which indicates that the majority of energy available from sunlight is within the PAR region.

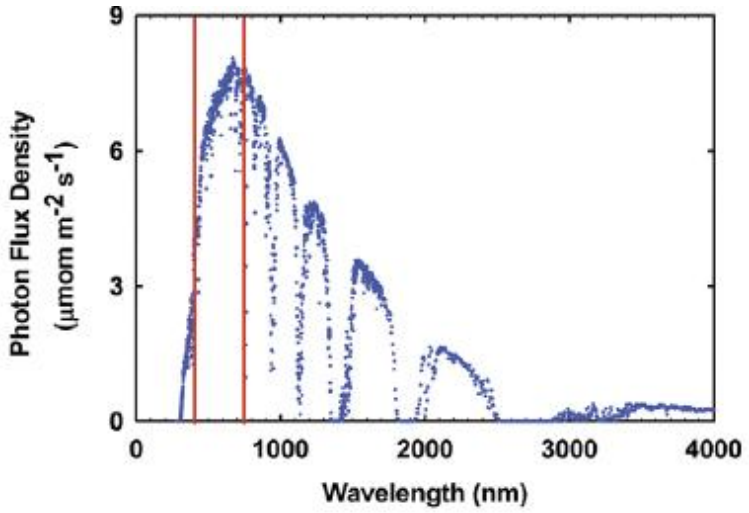

Figure 2.3: Photon flux density of the average spectrum of the 48 continuous states of the United States over a period of one year (Zhu, Long and Ort, 2008)

(PAR region flanked by red lines)

Radiation attenuation phenomena include the absorption of specific wavelengths by photosynthetic and accessory biomass pigments and by the biomass itself; light scattering; and preferential absorption of selective wavelengths (Fernández *et al*., 1997). About 95% of the PAR that is provided to the algal cell is mainly lost due to the absorption by components other than chloroplasts and the ineffectiveness of the transduction of light energy into chemical energy (Barsanti and Gualtieri, 2006). For instance, approximately 10% of PAR is reflected due to the weak absorbance of chlorophyll in the green spectrum (Barsanti and Gualtieri, 2006). Additionally, energy loss occurs due to rapid relaxation of higher excited states of chlorophyll, differences between energy trapping at the reaction centres and carbohydrate production, photorespiration and mitochondrial respiration (Zhu *et al*., 2008). Microalgae have higher PEs than higher-order plants. C3 plants have a theoretical maximum PE of solar radiation of 4.6% at 30 °C while the highest reported value demonstrated practically is 2.4% (Zhu *et al*., 2008). Posten (2009) reported that practically achieved values of PCE/PE for microalgae are around 5/10% respectively.

2.2.1.3 Light regimes

In this context, light regime refers to the numbers of hours of light the algal culture receives per day i.e. under a continuous light regime (0:24) the algal culture receives 24 hrs of light per day. Jabob-Lopes *et al*. (2009b) evaluated the effect of this on biomass production and CO_2 fixation rates by the cyanobacterium *Aphanothece microscopica Nägeli* cultured in a bubble column photobioreactor. The authors found that maximum values of volumetric productivity, maximum

cell concentration and carbon dioxide fixation rate were obtained under a continuous light regime. These values were not significantly different to a 2:22 photoperiod but were significantly different to photoperiods ranging from 24:0 to 4:20 (with increments of 2 hrs). When a mixed culture of *Scenedesmus caribeanus* and *Chlorella vulgaris* was cultivated under a continuous light regime in a helical tubular photobioreactor, the biomass production was higher than when the mixed culture was cultivated with a 12:12 hr light dark cycle (Westerhoff *et al*., 2010).

2.2.2 Nutrients

Algae require the major nutrients nitrogen, phosphorus, sulphur, potassium and magnesium for growth and the role of these nutrients in the cell will be briefly outlined (Wang *et al*., 2008). Secondary to carbon, nitrogen is quantitatively the most important nutrient and is needed for protein synthesis (Becker, 2004). It can be supplied in the form of nitrate, ammonia, urea, nitrite, or in the case of certain cyanobacteria, elemental nitrogen (N_2) from the atmosphere (Barsanti and Gualtieri, 2006). Ammonia and urea are less expensive and need less energy to be assimilated into the algal cell in comparison to nitrate and nitrite (Wang *et al*., 2008). The assimilation of nitrogen sources changes the pH e.g. using ammonia as the sole nitrogen source may lower the pH to 3 (Becker, 2004). Light stimulates the uptake and assimilation of inorganic nitrogen (Becker, 2004).

Phosphorus is needed for energy transfer, nucleic acid synthesis, protein synthesis and reactions that are associated with cell division. Both phosphorus and sulphur are vital to all cells as they are components of certain amino acids, and both require energy for uptake by the cell (Borchardt, 1996). Potassium serves as a cofactor for several enzymes and is involved with protein synthesis and osmotic regulation and can possibly be substituted by sodium (Becker, 2004). Magnesium is needed for formation of chlorophyll and also has a role in the aggregation of ribosomes into functional units and for the formation of catalase (Becker, 2004). Calcium ions play a role in the maintenance of cytoplasmic membranes, salt formation with colloids and the precipitation of $CaCO_3$ (Becker, 2004). The aforementioned nutrients viz. nitrogen (in the form of nitrates), calcium, magnesium, sulphur, phosphorus and sodium form the major components of the Bold's Basal medium (3NBBM) used for culturing *Scenedesmus* sp. (Appendix A). The minor components of the media are added in Provosoli's trace metal solution (PIV metal solution) and the filtered vitamins cyanocobalamin (B_{12}) and thiaminhydrochloride (B_1) are added after the medium is autoclaved (Anderson, 2005). Iron is the main component of the PIV solution; it is needed for the formation of cytochromes (ferrodoxin) and affects the synthesis of phycocyanin and chlorophyll. The remaining constituents of the PIV metal solution are the trace elements,

manganese (part of PSII), zinc, cobalt (cofactor of B_{12}), molybdenum and EDTA (chelating agent) (Garrett and Grisham, 2005). The vitamin B_1 is a precursor of the enzyme thiamine pyrophosphate, a coenzyme involved in reactions of carbohydrate metabolism and the vitamin B_{12} forms coenzymes which participate in 3 types of reactions (Garrett and Grisham, 2005).

2.2.3 Carbon Dioxide

Carbon is the major requirement for algal growth; approximately 1.8 kg of CO_2 is needed for the production of 1 kg of algae (Moroney and Somanchi, 1999). Algae acquire carbon via two main methods: autotrophy and heterotrophy. Heterotrophic algae can utilize organic carbon sources such as sugar, molasses, acetic acid and hydrocarbons and many algal species can switch between autotrophy and heterotrophy (Becker, 1994). *Scenedesmus* sp. is an obligate photoautotroph and the theory of phototrophic CO_2 fixation will be overviewed.

2.2.3.1 CO_2 fixation during photosynthesis/ 'Light-independent' reactions

During photosynthesis there are two main sets of reactions that occur. The first involve the 'light-dependent' reactions (Section 2.2.1.1) and the second involves the 'light-independent' reactions. CO_2 is fixed during the 'light-independent' reactions into sugars, using the energy from ATP and the reducing power of NADPH (Barsanti and Gualtieri, 2006). Under nutrient saturated conditions the absolute rate of light-saturated photosynthesis is limited by carbon fixation rather than electron transport (Sukenik *et al*., 1988). The enzyme RuBisCO (Ribulose Bisphospate Carboxylase/Oxygenase) can catalyze either CO_2 or O_2 fixation to Ribulose Bisphosphate (Moroney and Somanchi, 1999). O_2 is a competitive substrate (Moroney and Somanchi, 1999). In addition to catalyzing one of the reactions of photorespiration, RuBisCO works very slowly (catalyzing 3 molecules per second) and under standard atmospheric conditions RuBisCO operates at less than 30% of its maximum capacity (Moroney and Somanchi, 1999). Thus, for carboxylation to be favoured, it is necessary to keep the partial pressure of CO_2 high and to use moderate temperatures and light intensities (Barsanti and Gualtieri, 2006). However, the percentage of CO_2 in air is less than 0.04% and when water is in equilibrium with the atmosphere at pHs above 7, CO_2 can account for less than 1% of total inorganic carbon (C_i) (Becker, 1994; Colman *et al*., 2002). To remedy the problem of CO_2 limiting growth rates, most algal species possess CO_2 concentrating mechanisms (CCMs).

2.2.3.2 Carbon Concentrating Mechanisms (CCMs)

CCMs are needed when surrounding CO_2 concentrations are low and the rate of diffusion limits the availability of CO_2/HCO_3^- to the cell. The expression of the CCM is controlled by the partial pressure of CO_2 in the air that is passed through the culture medium (Colman *et al*., 2002). Microalgae with active CCM's specifically package RuBisCO in pyrenoids, which serve as a location in which an elevated CO_2 environment can be created such that CO_2 can out-compete O_2 at the active site of RuBisCO (Moroney and Somanchi, 1999). CCM's involve the activity of the external carbonic anhydrase (CA) enzyme and/or active CO_2 /HCO_3^- transporters (Colman *et al*., 2002). Certain algal species possess active transport systems for the uptake of HCO_3^- and CO_2. For formation of the CO_2 active transport system (CO_2 pump) light is required, whereas the HCO_3^- pump becomes partially activated in the dark which suggests that the ATP is provided by mitochondrial respiration (Colman *et al*., 2002; Thielmann *et al*., 1990).

Scenedesmus obliquus uses a CO_2-pump in combination with an external CA at pH 5 to 8 and uses an ATPase linked HCO_3^- transporter at pH 7 to 11 (Figure 2.4) (Thielmann *et al*., 1990). With air-adapted *Scenedesmus*, the $K_{0.5}$DIC (concentration of CO_2 and/or HCO_3^- needed to maintain O_2 evolution at one-half V_{max} in the light) was 5 µM at pH 5-8 and for CO_2-grown cells the $K_{0.5}$DIC was approximately 40 µM (Thielmann *et al*., 1990). At pH's 7-11 when the HCO_3^- transporter is activated the $K_{0.5}$DIC decreased from about 7300 µM for high-CO_2 grown cells to about 10 µM for air-adapted cells (Thielmann *et al*., 1990). The implication of this is that the CCM's of high-CO_2 grown cells will either be non-operational or only partially expressed when the culture is fed with concentrated CO_2.

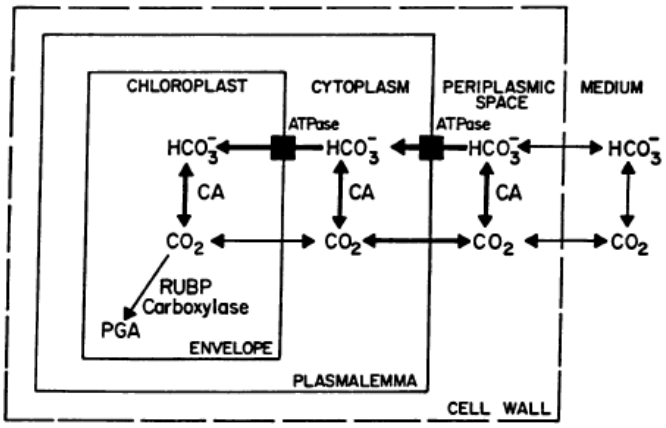

Figure 2.4: Proposed model for inorganic carbon accumulation by *Scenedesmus obliquus* (Thielmann *et al*., 1990)

2.2.3.3 CO_2 solubility in water

Determining the solubility of CO_2 in the cultivation media is necessary as this will determine the amount of carbon which is available for the growth of algae cells. The parameters pH, temperature and the concentration of the nutrients in the medium affect the solubility and the speciation of CO_2. According to Henry's Law (Equation 2.1), CO_2 dissolves in water to an extent determined by its partial pressure (P_{CO2}), temperature and by the interaction of dissolved CO_2 with other solutes in the water (Carroll and Mather, 1992).

$$[CO_2] = P_{CO_2} / K_H \tag{2.1}$$

The Henry's law constant (K_H) can be determined, for low pressure data (< 1 MPa), by the correlation developed by Carroll and Mather (1992).

$$\ln\left(\frac{K_H}{MPa}\right) = -6.8346 + 1.2817 \times \frac{10^4}{T} - 3.7668 \times \frac{10^6}{T^2} + 2.997 \times \frac{10^8}{T^3} \tag{2.2}$$

CO_2 solubility increases with increasing pressure and decreases with increasing temperature, within the 0-100°C range as depicted in Figure 2.5 (Hangx, 2005). At lower temperatures CO_2 will become more soluble owing to the thermodynamics of the reaction i.e. gas has a lower tendency to escape (Carroll and Mather, 1992). Also, the solubility of CO_2 is higher in fresh water than in salt water (Loewenthal and Marais, 1973). At a room temperature of 25 °C, the solubility of CO_2 in water at a P_{CO2} of 101.325 kPa is given as a 0.622 X 10^{-3} mole fraction (Carroll and Mather, 1992). Thus, feeding 100% CO_2 to water at STP would result in a CO_2 saturation concentration (C*) of 1.54 $g.L^{-1}$.

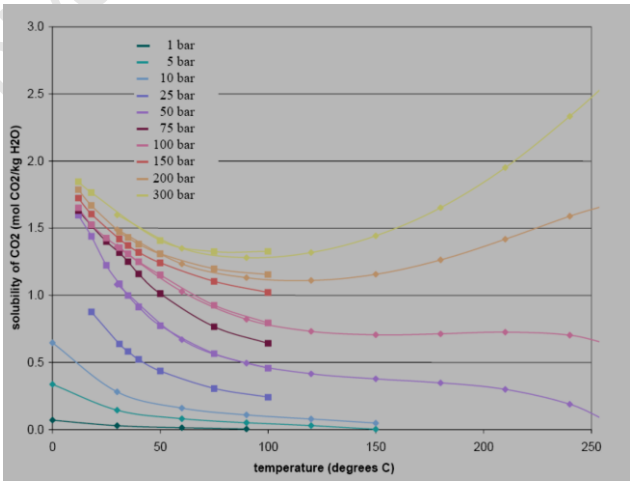

Figure 2.5: The solubility of CO_2 in water as a function of temperature and pressure (Hangx, 2006)

2.2.3.4 Speciation of CO_2

Carbon dioxide is a water soluble gas which can exist in water as the species carbonic acid (H_2CO_3), bicarbonate (HCO_3^-), carbonate (CO_3^{2-}) and solvated CO_2 (dCO_2) (Equation 2.3). The pH of the media will affect the speciation of dCO_2 (Figure 2.6) and this influences the mass transfer of CO_2 as the rates of dissolution of the different species vary (Bailey and Ollis, 1986; Loewenthal and Marais, 1973).

$$CO_2 + H_2O \rightleftarrows H_2CO_3 \rightleftarrows H^+ + HCO_3^- \rightleftarrows 2H^+ + CO_3^{2-} \qquad (2.3)$$

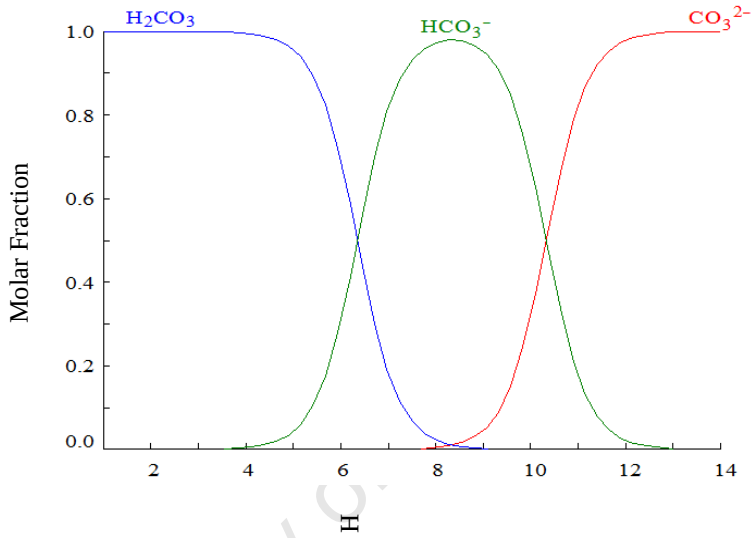

Figure 2.6: The pH dependency of the $CO_2/HCO_3^-/CO_3^{2-}$ equilibrium

(Speciation diagram generated with the thermodynamic package Medusa/Hydra. Total CO_3^{2-}=10 mM and T=25 °C)

The process is as follows:

$$CO_2 + H_2O \rightleftharpoons H_2CO_3 \qquad (2.4)$$

CO_2 dissolves in water to form carbonic acid (Equation 2.4). Carbonic acid is a weak polyprotic acid which has a dissociation constant (Ka_1) of 4.5 X 10^{-7} and a Ka_2= 4.7 X 10^{-11} at 25 °C, these small values indicate that the extent of dissociation of hydrogen ions from carbonic acid is low, and that the first proton is dissociated more readily than the second proton (Silberberg, 2003). The ratio of H_2CO_3: CO_2 at equilibrium is very small i.e. less than 0.002 (Gibbons and Edsall, 1963).

Carbonic acid dissociates in two steps:

$$H_2CO_3 + H_2O \rightleftharpoons H_3O^+ + HCO_3^- \quad \text{pKa of 6.35} \tag{2.5}$$

$$HCO_3^- + H_2O \rightleftharpoons H_3O^+ + CO_3^{2-} \quad \text{pKa of 10.33} \tag{2.6}$$

The dissociation constant refers to the sum of the H_2CO_3 and dissolved CO_2 (Loewenthal and Marais, 1973). The ratio of H_2CO_3: HCO_3 is 0.005 or less. Therefore, H_2CO_3 can be neglected in the overall reaction (Gibbons and Edsall, 1963). The carbonate can also combine with divalent cations e.g. Mg^{2+} and Ca^{2+} to form insoluble carbonates which drives the forward reaction (Equation 2.6), resulting in acidification (Loewenthal and Marais, 1973). As previously mentioned both calcium and magnesium are present in the culture medium (3NBBM) of *Scenedesmus* sp. and the availability of these ions to combine with CO_3^{2-} will depend on the extent of their uptake by the cell.

$$CO_2 + H_2O \underset{k'_{13}}{\overset{k'_{31}}{\rightleftharpoons}} HCO_3^- + H^+ \tag{2.7}$$

$$K'_1 = \frac{k'_{31}}{k'_{13}} = \frac{(H^+)(HCO_3^-)}{(CO_2)} \tag{2.8}$$

Gibbons and Edsall, (1963) calculated the rate constants hydration (k'_{31}) and dehydration (k'_{13}) of CO_2 with different phosphate buffer concentrations and demonstrated that an increased HPO_4^{2-} concentration results in an increased k'_{31} i.e. the hydration reaction. The concentration of phosphate ions in the 3NBBM media is ~1 mM and would only marginally affect the rate of CO_2 hydration.

Water dissociates into Hydrogen and Hydroxyl ions

$$H_2O \rightleftharpoons H^+ + OH^- \quad (K_w \text{ at STP} = 10^{-14} \text{ mol}^2.\text{dm}^{-6}) \tag{2.9}$$

Above pH 7 at 25°C, it is necessary to take account of this reaction (Gibbons and Edsall, 1963)

$$H_2CO_3 + OH^- \rightleftharpoons HCO_3^- + H_2O \tag{2.10}$$

The basic component (B) of many buffers has a catalytic effect on CO_2 dissolution (Gibbons and Edsall, 1963):

$$H_2CO_3 + B \rightleftharpoons HCO_3^- + HB \tag{2.11}$$

The implication of the aforementioned information is that a pH value somewhere within the region of 6 to 9 would be optimal for cultivation of *Scenedesmus* sp. In this pH range the majority of carbon is in the form of bicarbonate which can be readily utilized by *Scenedesmus* sp. (Figure 2.6). Lower pHs would result in a slower rate of CO_2 dissolution, while higher pHs would result in the predominance of carbonate, which cannot be used by *Scenedesmus* sp.

The dissociation equilibrium equations which have been outlined above can be used to calculate the inorganic carbon concentration (C_i) of the solution according to the method described by Ferreira *et al*. (1998).

2.3 Considerations for culturing microalgae on flue gas/high CO_2 concentrations

As discussed in the introduction (Section 1.1.5) there is extensive interest in the ability of algae to utilize CO_2 from flue gas i.e. ***biomass-based CCS*** (Section 2.4.1). It has been suggested that high concentrations of CO_2 (>5%) causes acidification of the cellular content which suppresses algal growth (Kurano *et al*., 1995; Nielsen, 1955; Seckbach and Libby, 1971). Considering that flue gas contains between 3 to 15% CO_2 it is important to understand the responses of various microalgal species to higher CO_2 concentrations.

2.3.1 Influence of flue gas composition on microalgal culture

Components of flue gas include CO_2, water vapour, NOx, SOx and metals such as nickel, vanadium and mercury (Packer, 2009). The main benefit of using flue gas to culture algae is that a carbon-free nutrient medium could be used as the carbon requirement will be provided for by CO_2 (de Morais and Costa, 2007b). Chelf *et al*. (1993) investigated whether the nitrogen and water vapour in flue gas could contribute to the nitrogen and water needs of the algae respectively. Assuming that 10 kg of NOx are emitted per ton of coal combusted and not accounting for the poor solubility of oxides of nitrogen in water, they calculated that the nitrogen oxides can provide 6.1% of the nitrogen required for algal yields of 50 $g.m^{-2}.day^{-1}$. Assuming that all hydrogen in the fuel would be converted to water during combustion and that all water in the fuel would end up as water vapour in the flue gas; Chelf *et al*. (1993) calculated that the flue gas could contribute only

1.5% of the daily water requirement. On the basis of their preliminary calculations they concluded that 'flue gas will have very little impact on the nitrogen requirement, water requirement, salinity, or temperature of algal ponds'. This conclusion would only hold for similar operating conditions. The concentrations of the components within the flue gas, size and proximity of the culture vessel and characteristics of the algal species would need to be considered. It should be noted that high concentrations of NO_X and SO_X in the flue gas may cause acidification of the algal culture. Also, concentrations of above 1 ppm nickel and 0.1 ppm of vanadium decrease algal productivity while mercury can be remediated by certain algal species (Packer, 2009). Thus, denitrification and desulphurisation may be necessary for pre-treatment of flue gas along with cooling and dedusting (Chelf *et al*., 1993; Packer, 2009). Alternatively, the concentrations of the nutrients would need to be adjusted and nitrogen may need to be provided as KNO_3 instead of NH_4 to increase the pH or the pH would need to be controlled (Becker, 2004).

2.3.2 Impact of high CO_2 on microalgal physiology

High CO_2 concentrations[2] lead to several changes in plant physiology and metabolism including the reduction of stomatal density, the decline of photorespiration and dark respiration, and the increase in the C/N ratio. Initially RubisCO acts as a carboxylase and the photosynthetic rate is increased which leads to higher carbohydrate production and increase in biomass (Figure 2.7; Logothetis *et al*., 2004). However, in higher order plants it has been noted that the longer the exposure to high CO_2 the more the situation becomes inverted i.e. the photosynthetic rate declines, carbohydrates accumulate in the chloroplasts and RubisCO levels decrease (Logothetis *et al*., 2004).

The green algal species, *Chlamydomonas acidophilia Negoro* responded to high CO_2 concentrations (5%) by switching off its CCM, reducing its RuBisCO content and increasing its affinity constant for CO_2 uptake by photosynthesis ($K_{0.5,p}$), maximum quantum yield and maximum photosynthetic O_2 evolution (P_{max}) (Spijkerman, 2008). The increased growth rate at higher CO_2 concentrations was attributed to the higher P_{max} (Spijkerman, 2008). It has been suggested that under optimal light and nutrient conditions, the metabolic energy that would have been used for the CCM is used for metabolic processes related to growth in high CO_2-acclimated cells instead (Spijkerman, 2008).

[2] High CO_2 is referred to as a CO_2 concentration which is considerably higher than the atmospheric CO_2 concentration. In 2010 the annual atmospheric CO_2 concentration was 389.78 ppm (~0.04%) (Tans and Keeling, 2010)

Scenedesmus cultures responded to high CO_2 concentrations and high light conditions with an increase in the Chl *a*/Chl *b* ratio (a higher Chl *a*/Chl *b* ratio correlates with cells with smaller sized LHCII) and a higher Putrescine/ Spermine (PUT/SPM) ratio. The polyamines (PUT/SPM) regulate the structure and functioning of photosynthetic apparatus (Logothetis *et al*., 2004). However, the resulting high cell density caused a decrease in the amount of light available per cell. As the RuBisCO levels decreased, the photosynthetic rate gradually decreased, the Chl *a*/*b* ratio decreased and the produced carbohydrates accumulated inside the chloroplasts in the form of large starch grains. Seckbach and Libby (1971) reported that the CO_2-treated cells of *Cyanidium caldarium* and *Scenedesmus* sp. were larger in size than the non CO_2-treated cells. According to these authors, the electron-micrographs of the CO_2-treated cells of *C. caldarium* 'seemed to contain a larger number of storage granules in comparison to the air-treated cells'.

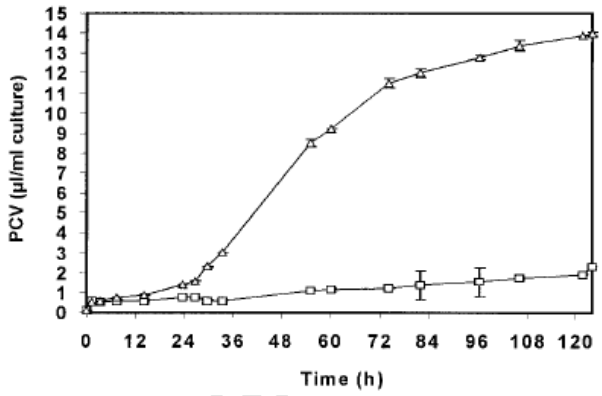

Figure 2.7: Biomass increase of *S. obliquus* cultures grown autotrophically at 0.03% CO_2 (squares) and at 10% CO_2 (triangles) under 235 µmole.m^{-2}.s^{-1} of light (Logothetis *et al*., 2004)

Miyasaka *et al*. (1998) screened twenty-five green algal strains on the basis of organic compound productivity, and of these the marine *Chlamydomonas* sp. strain W-80 was selected for its ability to excrete large amounts of glycerol in the culture medium when cultured with high concentrations of CO_2. The final concentration of glycerol after dark and anaerobic fermentation was 2.29 g.L^{-1}. This concentration is lower than the 4 g.L^{-1} produced by *Chylamydomonas reinhardtii* which excreted glycerol when subjected to osmotic stress; however that is a two-step process. It is unlikely that glycerol will be industrially produced by either of these approaches as the glycerol market is saturated due to its production as a byproduct in biodiesel production (Galan *et al*., 2009). However, the production of glycerol and starch under conditions of high CO_2 concentrations is relevant, as these storage materials serve the purpose of controlling nutrient

uptake via osmotic regulation (Ben-Amotz and Avron, 1973; Seckbach and Libby, 1971). Seckbach and Libby (1971) mentioned that the presence of starch should reduce nutrient uptake and found that the *C. caldarium* CO_2-treated cells, have a lower elemental percentage for many of the 17 elements tested, in comparison to the air-treated cells.

2.3.3 Characterization of microalgal species which are tolerant to high CO_2

An enhancement in the maximum growth rate (μ_{max}) due to higher CO_2 concentrations has been described for many algal species (Spijkerman, 2008). As a result of a screening process for microorganisms which have 'superb capability for CO_2 fixation', Michiki, (1995) characterized 13 new microalgal species, 11 of which are green algae (Table 2-1).

Table 2-1: High CO_2-tolerant algal species (reproduced from Michiki, 1995)

Microalgae	Temp. (°C)	pH	CO_2 (%)	Salt Conc. (%)	X_{max} (g/L)	μ in linear phase (day^{-1})	Axenic or Unialgal	Remark
Chlorococcum littorale Marine green algae	15-27	4-9	70	1-10	4.1	.47	Axenic	High CO_2 fixation rate (4 g CO_2/L/day), densely culturable (14.4 g/L), new species, soon settles
Chlorococcum dorsiventrale Marine green algae	15-27	4-9	60	1-10	3.8	.42	Axenic	Very similar in morphology and characteristics to *C. littorale*, new species, soon settles
Galdieria sp. Red algae from hot spring	50	1-4	100	0-4.5	3.7	.14	Axenic	Low pH, high CO_2, high temp. and SO_2 tolerant strain, growing not faster than *C. littorale*
Prasinococcus capsulatus Marine Prasinophyte	20-30	7-9	3	2-3			Unialgal	Accumulates large amount of extracellular polysaccharides, new genus, new species
Lepidochloris sphaerica Marine green algae	15-30	4-10					Unialgal	Accumulates large number of starch granules inside the cell, new genus, new species
Viridiella sp. Green alga	15-42	2-6	100	0-8		.36	Axenic	Accumulates lipid granules inside the cell, new species high temp. (42 °C) and high CO_2 tolerant
Chlorella sacchalophila Green alga	15-30	3-9	40	1.5-6	5.7	1.2	Axenic	Low pH tolerant, greater maximum cell conc. than *C. littorale* at 5% CO_2
Chlorella sp. (UK001) Green alga	25-40	3.5-9	40	0	3.5	.81	Axenic	High growth ability, high temp. tolerant (40 °C), dispersible
Chlorella sp. (A-2) Green alga	30-40	5.5-7	40	0	3.8	.49	Unialgal	High growth ability, high temp. tolerant (40 °C), dispersible
Chlorella sp. (H-84) Green alga	45	5-9	60	0-1.5	2.1		Unialgal	High growth ability, high temp. tolerant (40 °C), dispersible
Chlorella sp. (L-1) Green alga	40	5-9	40	0-1.0		.1	Unialgal	High temp. tolerant (40°C), dispersible
Scenedesmus acuminatus Green alga	35	5-6	60	0	0.7		Unialgal	High CO_2 tolerant (60 °C), dispersible
Synechococcus lividus Cyanophyte	40-55	8.2	5	0			Unialgal	High pH (8.2) tolerant, high CO_2 tolerant (60%), dispersible

The green algae are predominantly from the *Chlorococcum*, *Chlorella* and *Scenedesmus* genera (Table 2-1). Interestingly, Seckbach and Libby (1971) identified algal species from the aforementioned genera, in addition to *Cocomyxa* sp., as species which survived after a pure CO_2 (100%) treatment. These authors performed experiments with one of the surviving species Zav-9 (*Scenedesmus* sp.). Zav-9 thrived under the 100% CO_2 treatment; the cell concentration continued to increase for the 30 day period and reached 3.65 $g.L^{-1}$ in comparison to the 1.19 $g.L^{-1}$ obtained with the air treatment.

Chloroccum littorale was identified as a fast growing algal species which could tolerate high CO_2 concentrations. Its maximum cell concentration of 4.9 $g.L^{-1}$ at 20% CO_2 was lowered to 4.1 $g.L^{-1}$ at 70% CO_2 (Table 2-1) (Kurano *et al*., 1995). When air-grown *C. littorale* cells were exposed to CO_2 concentrations of more than 20%, a lag period of 1-4 days preceded active photosynthesis. The intracellular pH value dropped from 7 to 6.4 when these cells were exposed to 40% CO_2 for 1-2 hrs. However, this decrease did not occur in the presence of ethoxyzolamide (EZA), a CA inhibitor. However, the air-grown cells of *Chlorella* sp. UK001 and the CO_2-adapted cells grew in 40% CO_2 without any lag period. The CA activity was much lower in this species than in *C. littorale* 18 units.$(mL\ PCV)^{-1}$ vs. 1088 units.$(mL\ PCV)^{-1}$. This led the authors to conclude that intracellular CA caused intracellular acidification and hence inhibition of carbon fixation when air-grown *C. littorale* cells were exposed to extremely high concentrations of CO_2 (Satoh *et al*., 2001). From this it can be inferred that when examining the effects of culturing algae with high CO_2 concentrations, it is important to maintain the stock culture on a P_{CO2} higher than air, particularly when the algal species has a CCM.

A 28-day run of a *Chlorella Tx 71105* chemostat with pure CO_2 supplied at 3.3 $mL.min^{-1}$ revealed that during the first 6 days, the effluent gas contained more than 96% O_2. On the 12^{th} day a temperature rise from 37 °C to 39 °C was noted, and on the 13^{th} day a concentration of 32% CO_2 in the effluent gas was observed. The gas flow was subsequently turned off for 3.5 hrs, and the effluent gas contained 97.8% O_2 half an hour after resumption of CO_2 addition. In the last 6 days of the experiment, when no alterations were made, it was observed that wall growth occurred which coincided with the concentration of the CO_2 in the effluent gas reaching 18%. The mean biomass concentration of *Chlorella Tx 71105* was 2.49, 2.71, 3.15 $g.L.day^{-1}$ when cultured with 100, 71 and 41% CO_2 respectively (Geckler *et al*., 1962). These cell concentrations are reasonably similar to those obtained with the other species of *Chlorella* (Table 2-1).

Galdieria sp. was highlighted in Table 2-1 as a species which can tolerate 100% CO_2. Kurano *et al*. (1995) identified *Galdieria partita* along with *Cyanidium caldarium* and *Cyanidioschyzon melorae* as species which could grow at 50 °C, pH 1, P_{CO2} 1(unit unspecified) and 50 ppm of

nitric oxide (NO). Of the three extremophiles mentioned above only *G. partita* could tolerate aeration of 50 ppm SO_2. Experiments with *C. caldarium* by Seckbach and Libby (1971) revealed that *C. caldarium* could tolerate 10 atm of CO_2 but not 50 atm CO_2. Growth of *C. caldarium* continued under 49 atm Argon and 1 atm of CO_2. Thus, it can be concluded that growth was arrested due to the high CO_2 concentration effect and not the high pressure effect. However, these species have low growth rates (Table 2-1) and from this it can be inferred that productivity and CO_2 recovery will be low (Satoh *et al*., 2001).

2.3.4 Impact of high CO_2 on pH

The disadvantage of growing algae on high percentages of CO_2 is that maintenance of the pH balance within the culture is difficult. Acidification of the medium will occur when the rate of CO_2 dissolution in water is greater than the rate of CO_2 uptake by the algae (Geckler *et al*., 1962). This is dependent on the partial pressure of CO_2, the concentration of cation available for combination with carbonate or bicarbonate ions, and the equilibria between molecular and ionic species in solution (cf. Section 2.2.3.4) (Geckler *et al*., 1962). If the uptake rate of CO_2 is greater than the dissolution rate, alkylation will occur due to the excretion of OH^- ions by the algae into the medium (Becker, 2004; Geckler *et al*., 1962). The pH needs to be maintained within a certain range to achieve optimal growth of the microalgae and to prevent depletion of carbon in the medium (Becker, 1994). A pH controller can be used to measure the pH of the medium and can be programmed to respond by adding acid (CO_2) or alkali (Becker, 2004).

2.4 CO_2 cycling

2.4.1 CO_2 capture and storage

CO_2 capture and storage (CCS) is 'a process consisting of the separation of CO_2 from industrial and energy-related sources, transport to a storage location and long-term isolation from the atmosphere' (Abanades *et al*., 2005). The concept involves capture of CO_2 from a large point source, compression and transportation for storage. Large point sources include Fossil fuel facilities, Power plants, Cement production plants, Refineries, Iron and Steel industry,

Petrochemical industry, Oil and Gas processing plants, Other sources and Biomass energy facilities (each source produces more than 0.1 billion kg of CO_2 per year; listed in order of decreasing CO_2 emissions) (Abanades *et al*., 2005). From an environmental perspective CCS is promising; a lifecycle assessment (LCA) by Pehnt and Henkel (2009) demonstrated that there are substantial reductions (~80%) of greenhouse gases (GHG) for plants with CCS vs. plants without CCS. For other environmental categories and in terms of cumulative energy demand CCS looks less attractive but this is dependent upon the separation task and details of the process (Pehnt and Henkel, 2009). The economics of CO_2 fixation by algae and CCS in general are influenced by multiple factors such as technical development, regulatory issues, current market price of oil/gas, the implementation of emission reduction mechanisms such as cap and trade, carbon taxes, voluntary funding markets and the emergence of other renewable energy technologies (*s.l.* Pehnt and Henkel, 2009).

2.4.1.1 CO_2 capture

The capture of CO_2 can be divided into the categories Post-combustion, Pre-combustion, Oxyfuel combustion and Industrial process stream capture which are described below according to Thambimuthu *et al*., 2005.

- ***Post-combustion capture*** occurs after combustion of the fuel, when the flue gas is passed through equipment which separates the CO_2.
- ***Pre-combustion capture*** involves reacting a fuel with O_2/air to yield a synthesis gas (syngas) composed of carbon monoxide (CO) and hydrogen (H_2). The CO is reacted with stream to form CO_2 and H_2, viz. the water-gas shift reaction (Hufton *et al*., 2005).
- ***Oxy-fuel combustion capture*** involves recycling CO_2 flue gas by mixing it with pure O_2. This serves the purpose of reducing the flame temperature and results in a nitrogen-free flue gas with water vapour and a high concentration of carbon dioxide as its main components.
- ***Industrial process stream*** capture occurs as a result of purification of natural gas, production of hydrogen containing synthesis gas for the manufacture of ammonia, alcohols and synthetic liquid fuels.

When CO_2 is unavailable as a byproduct from industrial processes, alternate methods for capturing CO_2 from flue gas are needed (Chapel *et al*., 1999). A brief description of the preferred currently applicable technologies used in the separation tasks is provided (bold text, Table 2-2).

- ***Separation with sorbents/solvents***

  The separation occurs by contacting a solid sorbent (e.g. lime/sodium carbonate) with CO_2 to form a salt (limestone/sodium bicarbonate). However, this adds exorbitant costs to the coal production process ($176.ton^{-1}$ and $1400.ton^{-1}$ coal respectively). In addition, more CO_2 is released during the process of manufacturing lime, than can be captured from flue gases (Chelf *et al*., 1993). Separation with solvents (e.g. monoethanolamine (MEA)/ ammonia (NH_3)) involves scrubbing the CO_2 from the flue gas, in an absorber. MEA is traditionally used industrially despite being a more expensive and less effective absorbent than ammonia (Yeh and Bai, 1999). The MEA product solution is heated in the stripper to desorb the CO_2 and the regenerate the MEA (Wang *et al*., 2008). Alternatively the amine solution can be regenerated by algae culture (Hsueh *et al*., 2007). Due to the low partial pressure of CO_2 in flue gases either a large flow of absorbents is required or an absorbent with a higher activity is needed, which tends to result in an efficiency penalty or added cost (Thambimuthu *et al*., 2005).

- ***Membrane separation***

  CO_2 is separated by the selective permeation of a gas through membranes. Membranes could potentially be used in the MEA scrubbing process, to improve the absorber and stripper processes by increasing the mass transfer area in a given volume (Stewart and Hessami, 2005;Thambimuthu *et al*., 2005). The flow of gas across the membrane is aided by a high pressure stream (Thambimuthu *et al*., 2005). This requires compression and heat exchange which is costly. An additional disadvantage is that an impure O_2 product is produced. There are currently no known commercial applications (Chapel *et al*., 1999).

- ***Distillation of a liquefied gas stream***

  A series of compression, cooling and expansion steps are used to convert gas to liquid. The liquid stream can then be separated by distillation and the oxygen stream can be used in oxy-fuel combustion and pre-combustion capture (Thambimuthu *et al*., 2005).

Table 2-2: Relevant CO_2 capture technology for separation process (Thambimuthu et al., 2005)

Separation task	Process streams*		Post-combustion capture		Oxy-fuel combustion capture		Pre-combustion capture	
	CO_2/CH_4		CO_2/N_2		O_2/N_2		CO_2/H_2	
Capture Technologies	**Current**	**Emerging**	**Current**	**Emerging**	**Current**	**Emerging**	**Current**	**Emerging**
Solvents (Absorption)	**Physical solvents** **Chemical solvents**	Improved solvents Novel contacting equipment Improved design of processes	**Chemical solvents**	Improved solvents Novel contacting equipment Improved design of processes	n. a.	Biomimetic solvents, e.g. hemoglobine-derivatives	**Physical solvent** **Chemical solvents**	Improved chemical solvents Novel contacting equipment Improved design of processes
Membranes	**Polymeric**	Ceramic Facilitated transport Carbon Contactors	Polymeric	Ceramic Facilitated transport Carbon Contactors	Polymeric	Ion transport membranes Facilitated transport	Polymeric	Ceramic Palladium Reactors Contactors
Solid sorbents	Zeolites Activated carbon		Zeolites Activated carbon	Carbonates Carbon based sorbents	Zeolites Activated carbon	Adsorbents for O_2/N_2 separation, Perovskites Oxygen chemical looping	Zeolites Activated carbon Alumina	Carbonates Hydrotalcites Silicates
Cryogenic	Ryan-Holmes process		Liquefaction	Hybrid processes	**Distillation**	Improved distillation	Liquefaction	Hybrid processes

2.4.1.2 CO_2 storage

Proposed methods for CO_2 storage/ 'sequestration' include: CO_2 injection into, the ocean, deep saline formations, coal seams, terrestrial habitats and depleted oil and gas reservoirs; mineral carbonation and oceanic fertilization (Figure 2.8) (Abanades *et al*., 2005; Packer, 2009; Stewart and Hessami, 2005). Geological storage which is the injection of CO_2 in a dense form into a rock formation below the earth's surface is ongoing in multiple industrial-scale projects (Abanades *et al*., 2005). CO_2 injection is also used for enhanced oil recovery (EOR), enhanced gas recovery (EGR) and enhanced coal bed methane recovery, although it needs to be captured from the product stream (Abanades *et al*., 2005). Meanwhile, the technology of ocean storage is still in the research phase due to its lower expected retention rate in comparison to geological storage and environmental concerns such as pH effects (Abanades *et al*., 2005; Stewart and Hessami, 2005).

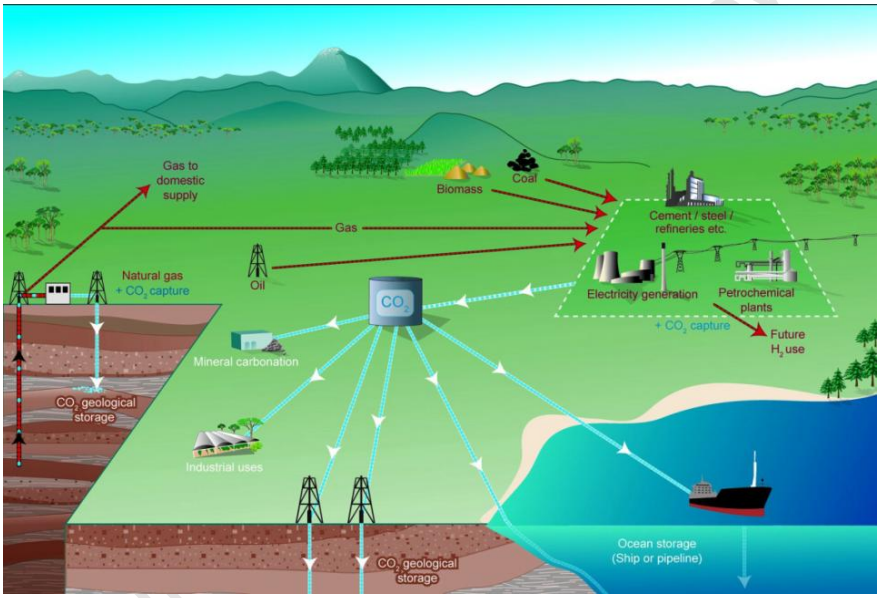

Figure 2.8: Schematic diagram of possible CCS systems (Abanades *et al*., 2005)

2.4.1.3 CO_2 transport

Pipelines are the mostly commonly used method for CO_2 transport. When the CO_2 needs to be transported over large distances or overseas ships are used instead. Gaseous CO_2 is normally compressed to a pressure above 8 MPa to increase its density which makes it easier and less costly to transport (Abanades *et al*., 2005). An economic model comparing the costs of directly pumping flue gas into an algal pond versus recovery of CO_2 using the MEA process prior to pumping the CO_2 in the algal pond, revealed that the latter option was significantly less expensive. A transportation distance of 100 km was assumed and the differences were attributed

to the compression and concentration cost of a sevenfold higher gas volume (Kadam, 1997). The implication of this is that it is necessary to minimize the distance between the algal cultivation unit and the flue gas supply in order to reduce transportation costs and avoid use of a capture technology. Once the CO_2 arrives at the site it can be supplied to the algal culture by one of two methods, active gas transfer or passive gas transfer.

2.4.2 CO_2 supply methods to algal culture

2.4.2.1 Active gas transfer

Active gas transfer is achieved by sparging small gas bubbles into the medium or spraying the liquid through the gas phase (Becker, 2004). The simplest way to distribute CO_2 into the culture is through sintered stones (spargers) or pipes as shown in Figure 2.9A (Becker, 2004; Carvalho and Malcata, 2001). The problem with this method is that the retention time of the bubbles is too short to allow for the complete absorption of the CO_2, when using shallow ponds (Becker, 2004). To increase the retention time of CO_2, (transparent) plastic sheets can be submerged in the pond (Figure 2.9B) or CO_2 can be injected against the downward flow of the suspension in air-lift reactors (Becker, 2004). The problem with systems A and B is that fouling of the gas transfer devices (e.g. sparger) can occur which would impede CO_2 transfer (Carvalho and Malcata, 2001). The third system combines agitation and aeration, CO_2 is added in a special chamber wherein algal suspension is pumped as shown in Figure 2.9C (Becker, 2004). This provides high turbulence and good CO_2 transfer rates can be established (Becker, 2004). The disadvantage of the active gas transfer method is that it fails to adjust the amount of CO_2 supplied to the actual requirement of the growing algae (Becker, 2004).

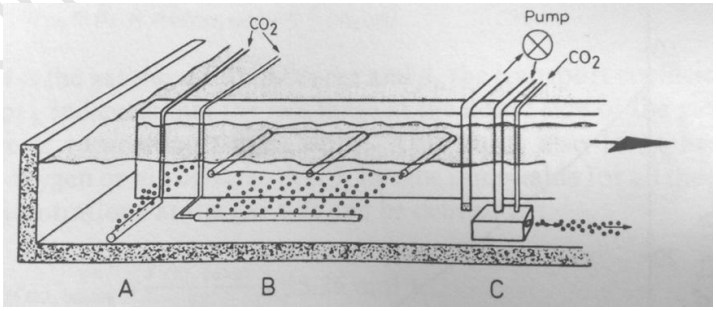

Figure 2.9: Different systems for CO_2 aeration in algal ponds (Becker, 2004).

A, sintered stone; B, porous pipe under submerged plastic sheets which traps the CO_2 bubbles and increases contact time between gas and water; C, pressure pump which injects air/ CO_2

2.4.2.2 Passive gas transfer

Passive transfer involves the creation of large contact areas between a CO_2 stream and the surface of the culture medium. An open vessel is introduced upside down into the algal suspension and filled with CO_2 via a supply hose and as it floats along the pond it distributes CO_2 by simple diffusion. This floating CO_2 injector is simple to construct and is effective for shallow ponds. A disadvantage is that the CO_2 is continuously diluted with photosynthetically produced O_2 and atmospheric N_2. Another method of passive gas transfer of CO_2 to the algal culture is counter-current carbonation (Figure 2.10). In this method the gas is pumped against gravity into the algal culture while the culture is pumped in from the opposite end of the column. The flow rate of the algal culture is adjusted so that the gas bubbles remain in the water until fully absorbed. The efficiency of gas transfer for this method is not very high which leads to wastage of CO_2 and compression energy (Becker, 2004).

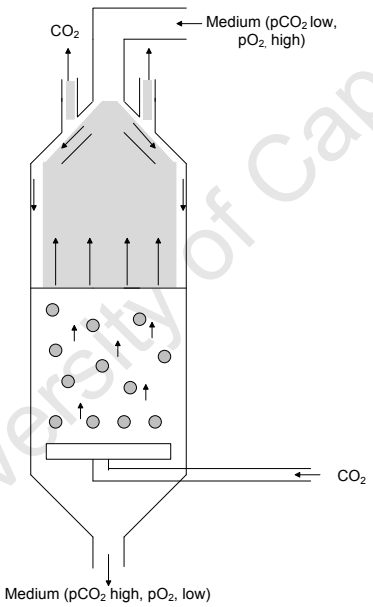

Figure 2.10: Schematic diagram of a carbonation column (reproduced from Becker, 2004)

2.4.3 Potential CO_2 release from algal products

As the renewed interest in industrial scale cultivation of microalgae is due largely to the interest in using lipids from microalgae for conversion to biodiesel it is necessary to realise that the CO_2 that was temporarily stored in the microalgae biomass will be released when the biodiesel is used.

However, using biodiesel in lieu of petroleum fuels results in fewer emissions to the environment and the process has the capability to be carbon neutral (Campbell, 2008). Alternatively the CO_2 can be trapped if the algal biomass is used for products such as those which are discussed in the section below.

2.4.3.1 General uses of algal biomass

The algal cell uses low cost substrates to accumulate biomass (Figure 2.11). A diverse array of products can be produced from the different fractions of the cell constituents. The variation of growth conditions can alter the proportion of the cell constituents (Becker, 2004). Many algal species produce all twenty amino acids and contain a high percentage of protein (8-71% of dry matter) and about 10% of non-protein nitrogen (Becker, 2004). Thus, certain algal species are a good feedstock for both human and animal consumption, as they provide nitrogen and amino acids which can be assimilated into protein (Barsanti and Gualtieri, 2006). Waxes, hydrocarbons, glycerol, vitamins, alginates, agar, carrageen, carotenoids and phycobiloproteins are also produced by algae. The amounts of these products are dependent upon the algal strain and culture conditions (Becker, 2004).

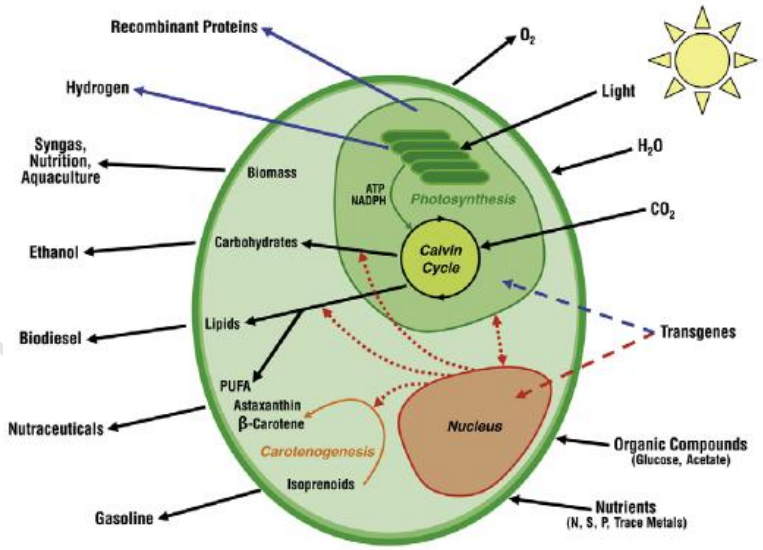

Figure 2.11: Commercially important metabolic pathways in microalgae (Rosenberg, 2008)

2.4.3.2 Algal biomass for energy production

Algal biomass can be used as a substrate to generate energy via four processes (Figure 2.12). The thermochemical conversion process and direct combustion process will not be discussed here, as these are energy intensive, expensive processes. Gasification and pyrolysis require temperatures of 800-900°C and 500°C respectively and liquefaction requires high pressures and hydrogen (Wang *et al*., 2008; Haiduc *et al*., 2009).

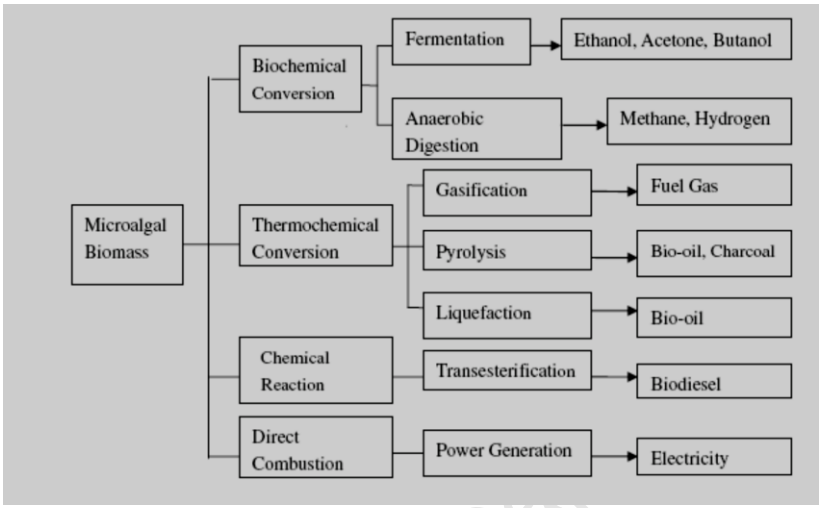

Figure 2.12: Energy production via microalgal biomass conversion using biochemical, thermochemical, chemical, and direct combustion processes (Wang *et al*., 2008)

2.4.3.3 Production of algal biodiesel by transesterification of biomass

Algae have the capability to accumulate high amounts of lipids as a fraction of their cell mass (Becker, 2004). Both the fatty acid profile and lipid productivity are key factors to consider when selecting an algal strain for biodiesel production (Griffiths and Harrison, 2009; Yoo *et al*., 2010). *Botyrococcus braunii* has a lipid productivity of 5.51 ± 1.53 $mg.L^{-1}.day^{-1}$ and a lipid profile containing 44.9 ±0.4 % oleic acid (w/w total fatty acids) when grown with 10% CO_2 (Yoo *et al*., 2010). This makes it amenable to the production of biodiesel by transesterification with an alkaline catalyst and excess alcohol (Yoo *et al*., 2010). Perturbations to the growth conditions can alter the lipid profile of the algae (Becker, 1994). For example, nitrogen limitation can increase the lipid content of algal cells and alter the lipid profile (Griffiths and Harrison, 2009; Griffiths *et al*., 2011a). Of 11 microalgal species tested in the CeBER laboratory, *Scenedesmus* sp. had the highest average lipid productivity (6 $mg.L^{-1}.day^{-1}$) when cultured under low nitrogen conditions as a batch culture in ALRs (Griffiths *et al*., 2011a). However, the difficulties involving the extraction of lipids with solvents and the high costs incurred require technological advances before commercial production is feasible.

2.4.3.4 Production of solvents and methane

Dunaliella species accumulate glycerol in response to its highly saline environment. When 5 species of *Dunaliella* were grown in 2 M NaCl with 24 mM $NaHCO_3$, or 3% CO_2 at 28°C, 4 of the species produced ca. 10-20 mg of glycerol per liter of culture. When supplemented with 4% glycerol, *Clostridium pasteurianum* converted this to ca. 16 g of mixed solvents per litre (Nakas, 1983). This compares favourably with the classical fermentation method using *Clostridium acetobutylicum* which produces between 10 to 20 g of mixed solvents per litre (Nakas, 1983).

Alternatively, algal biomass can be broken down by anaerobic bacteria to generate methane and CO_2 (Sialve *et al*., 2009). If the lipid content of the algae cell is less than 40%, then anaerobic digestion is preferable to transesterification of biomass from an energy balance standpoint (Sialve *et al*., 2009). The methane can be used as an energy source for the process or can be added to the national electricity grid. Species from the genus *Scenedesmus* typically have recalcitrant cell walls and are thus less amenable to anaerobic digestion in comparison to other microalgal species such as *S. platensis* (Wiltshire *et al*., 2000).

2.5 Algal cultivation vessel

2.5.1 Ponds

For large-scale cultivation, algae can be grown either in ponds or in reactors. Ponds are either ***Circular***, with agitation provided by a rotating arm; ***Oblong forms (raceways)***, with agitation provided by a paddle wheel, propeller, air-lift pumps or ***Sloping***, where mixing is achieved by pumping and gravity flow (Becker, 2004). The main advantage of using ponds is that they are technologically simple although not necessarily cheap due to high downstream processing costs (Lee, 2001). Ponds are only suitable for culture of fast-growing algal strains or strains which grown in an extreme culture environment, as they are open to contamination. Even, fast-growing algal cultures are still susceptible to bacterial or other forms of biological contamination (Lee, 2001). They are also subject to the weather conditions of their environment and this often results in excess evaporation (Becker, 2004). The disadvantage of using ponds with regard to culture with flue gas is that excessive CO_2 injected into a pond will likely lead to evaporative loss of CO_2 i.e. low CO_2 recovery. According to Becker (2004) the use of plastic covers to improve gas transfer (as discussed in Section 2.4.2.1) has not been verified yet and according to Carvalho and

Malcata (2001) considerable amounts of CO_2 escape from the ends of the plastic sheets to the atmosphere.

2.5.2 Photobioreactors

In contrast, photobioreactors do not allow direct exchange of gases or contaminants between the algal culture and the atmosphere. Thus, loss of water by evaporation is less. The main advantage of using reactors is the ability to control culture conditions such as pH, temperature, and O_2 and CO_2 concentrations, which can result in higher productivities. In reactors, CO_2 can be recycled back to the culture medium. However, reactors typically require high capital investment and are more expensive to run (Barsanti and Gualtieri, 2006). There are three main types of photobioreactors, namely ***tubular, flat panel*** and ***column*** photobioreactors (stirred tank reactor, bubble columns, ALRs) (Eriksen, 2008). The characteristics of these photobioreactors will not be discussed here as reactor design was not part of this study. A previous CeBER student expressly designed ALRs for sterile algal culture and confirmed that reproducible growth data could be obtained for these five reactors (standard deviation of 5% for growth data) (Langley, 2010). These ALRs were used in study. Operational parameters such as providing homogeneous distribution of light to the algal culture, mass transfer, gas exchange and mixing will be discussed as these pertain to CO_2 sequestration of algae cultured in photobioreactors (Schenck, 2008).

2.5.2.1 Light supply

The amount of illumination that each algal cell is exposed to is affected by factors such as incident light intensity, reactor design, cell density, pigmentation of cells and mixing patterns (Eriksen, 2008). The productivity of photoautotrophic cultures in bioreactors is primarily limited by light (Eriksen, 2008). Light supply is complicated by the fact that the light intensity within the reactor becomes a function of the biomass concentration and culture depth (Jacob-Lopes *et al*., 2009b; Becker, 2004). A further complication for a dense algal culture is that each cell, experiences fluctuating light/dark variations according to the movement of the currents in the liquid medium (Eriksen, 2008). The provision of low light intensities may result in higher PE's but the biomass productivity is reduced due to central, light-deprived zones. The provision of high light intensities may lead to photoinhibition and may increase the operational and equipment costs (Eriksen, 2008). It would be useful to adjust the light intensities as the cell numbers and cell pigment concentration increases by using a photobioreactor with on-line optimization of light intensity. Eriksen *et al*. (1996) control the pH of a *Synechococcus* culture with CO_2 additions and

then use these measures to change the light intensity of the surrounding light banks. They found that in comparison to batch cultures with a fixed light intensity the productivity was higher.

2.5.2.2 CO_2 mass transfer theory

The transfer of CO_2 from the gas bubble to the algal cell involves passage through at least seven resistances including the gas-liquid interface, stagnant regions, bulk liquid and the cell wall (Bailey and Ollis, 1986). Not all of these resistances are significant; for poorly soluble gases with a well-mixed bulk region, the liquid-phase mass transfer resistance dominates i.e. the major resistance is the liquid film surrounding the gas bubble (Carvalho and Malcata, 2001; Doran, 1995). The rate of mass transfer is dependent upon the interfacial area, a; the liquid mass transfer coefficient, K_L and the CO_2 concentration driving force (C*-C) (Equation 2.12) (Carvalho and Malcata, 2001; Doran, 1995) .

$$\frac{dC}{dt} = K_L a(C^* - C) \tag{2.12}$$

The mass transfer coefficient (K_La) is dependent upon the size and number of bubbles and this is affected by factors such as gross flow patterns, medium composition, stirrer speed and gas flow rate. A typical value for a K_La in fermenters is in the range of 0.002-0.25 s^{-1}. This can be obtained using mass transfer correlations or experimentally (Doran, 1995). High concentrations of CO_2-enriched air (P_{CO2}) will drive mass transfer and will compensate for a low K_La i.e. less area will be required for gas exchange, gas flow rate can be reduced etc. (Equation 2.1 and 2.12) (Geckler, *et al*., 1962). However, as previously mentioned excessively high concentrations of CO_2 can be harmful to the algae and will result in reduced CO_2 recovery (Cheng *et al*., 2006).

2.5.2.3 Mass Transfer/ Gas Exchange

Improving CO_2 mass transfer is a key factor in cultivating micro-algae; if CO_2 is distributed uniformly within the algae culture, optimum photosynthetic rates will be promoted and algal productivity increased (Hsueh *et al*., 2007). The CO_2 concentration in the reactor, the effect caused by the reaction of dissolved CO_2 with OH^- to produce bicarbonate, and the mixing regime are the three main factors to consider for CO_2 transfer from the gas stream to the culture medium (Becker, 2004).

Several authors used hollow-fiber modules for algal culture on the premise that an increase in the interfacial area of contact available for gas exchange, will improve the mass transfer (Carvalho and Malcata, 2001; Cheng *et al*., 2006; Ferreira *et al*., 1998; Kumar *et al*., 2010). For Ferreira *et al*. (1998) the benefits of using a hollow fibre membrane were that the CO_2 transfer rate per

membrane surface area was 10X higher than silicon tubing and that the module withdrew part of the dissolved oxygen in the algal culture. However, no difference was found in the cell concentration for the control (CO_2 supplied by bubbling) vs. the experiment (CO_2 supplied via membrane). In addition, the mass transfer coefficient dropped by 15% after the experiment which was attributed either to fouling of the membrane or to loss of the hydrophobic character of the membrane. Carvalho and Malcata (2001) found an improvement in the overall volumetric coefficients (K_La) for hollow-fiber modules compared to the K_La for bubbles. However, this failed to improve the algal growth significantly perhaps because the CO_2-rich and light-rich periods did not coincide with each other. Cheng *et al*. (2006) determined that the CO_2 fixation was 260 $mg.L^{-1}day^{-1}$ for a *Chlorella vulgaris* culture in a membrane-photobioreactor vs. 80 $mg.L^{-1}day^{-1}$ for an 'ordinary photobioreactor' (timeframe shown 100 minutes) (Cheng *et al*., 2006). They concluded by stating that 'membrane modules must resolve fouling, pressure resistance and other problems to make sure that high mass transfer rates are maintained for extended periods of operation' (Cheng *et al*., 2006). Eriksen *et al*. (1998) used a dual sparging method to improve the mass transfer of CO_2 to the algal culture. The air was provided continuously via orifice spargers while the CO_2 was provided in pulses in response to pH changes via a perforated membrane sparger. Thus, the air was supplied as larger bubbles (5-15 mm) which served to mix the culture while the CO_2 was supplied as small bubbles (< 5 mm) which served to facilitate mass transfer. The efficiency of CO_2 transfer was increased by 500% with this method however the independent control of aeration and mixing may create problems with scale-up (Eriksen, 1998; Fan *et al*., 2008).

2.5.2.4 Mixing

Adequate mixing is essential, for uniform distribution of CO_2 and O_2, for provision of a uniform average light exposure to all cells, and for prevention of sedimentation of the cells (Becker, 2004; Schenk, 2008). Mixing ensures that each algal cell will have access to light intermittently as it induces low light/high light cycles and prevents inhomogeneous distribution of light inside the algal cultures and the subsequent reduction of PE's (Eriksen, 2008; Schenk, 2008).

Air bubbles and high liquid velocities can cause shear stress which above a certain threshold can damage microalgae. Below this threshold shear stress can be beneficial in enhancing growth due to the physiological effect of this fluid shear stress and/or due to enhancement of heat and mass transfer rates (Contreras *et al*, 1998). In airlift reactors cell damage is most likely to occur at the sparger, in the riser and at the surface where bubble disengagement occurs (Fan *et al*., 2008). This can be reduced by supplying the algal culture with non-ionic surfactant which functions by preventing cell adhesion to gas bubbles (Eriksen, 2008).

Chapter 3 : Materials and Methods

3.1 Microorganism and culture conditions

Scenedesmus sp. was isolated as a contaminant from a pond in Upington, South Africa. The cells are spindle-shaped and cell walls appear smooth with no spines and would be tentatively classified in the non-spiny or 'obliquus' group according to Trainor et al's descriptors (Trainor et al., 1976). Stock cultures of *Scenedesmus* sp. were grown in 3NBBM medium (Appendix A) in 500 ml flasks at ambient temperatures (Figure 3.1). Illumination was provided continuously by two 30 W cool white fluorescent bulbs (Osram, SA) that provided an average light intensity of 185.27 $\mu mol.m^{-2}.s^{-1}$.KDG 1100 Rotameters (KDG Flowmeters, England) controlled the flow rates of CO_2 and air to supply a P_{CO2} of 0.01 atm (1%). The two gas lines were connected and filtered through a 0.2 µm Millipore autoclavable vent filter (Millex, USA) and the resultant CO_2-enriched air was humidified, by sparging through dH_2O. The CO_2-enriched air was then filtered again before entering the rotameter and being split to 8 lines. The CO_2-enriched air was bubbled through at 1 L/min to each flask of culture. Fresh cultures were prepared a few days prior to inoculation to ALRs in order to maintain the culture in log phase. Media was used to replace the culture taken and autoclaved distilled water (dH_2O) was used to replenish the evaporated water.

Figure 3.1: Stock culture apparatus

3.2 Cultivation in internal loop Air Lift Reactors

Scenedesmus sp. was cultivated in glass and stainless steel internal loop Air Lift Reactors (ALRs) (Figure 3.2). The ALRs were expressly designed for the purposes of microalgal cultivation and the specifications are illustrated in Figure B.1, Appendix B (Langley, 2010).

Scenedesmus sp. was inoculated from maintenance stock cultures to a concentration of 0.1 OD (0.05 g/L) within the 3.2 L working volume of each ALR. The appropriate volume of culture was transferred from the maintenance culture to a sterile measuring cylinder, and poured through a sterile funnel into the sampling tube of the reactor. Each reactor run was conducted for a period of 10 to 14 days. Light was supplied continuously to the cultures by three 18 W cool white fluorescent bulbs (Osram, SA) at a distance of 3 cm from the column surface. Cardboard cut-outs which were covered with aluminum foil flanked each ALR to reflect the light back to the ALR. The lights provided an average PPFD of 282.74 $\mu mol.m^{-2}.s^{-1}$.

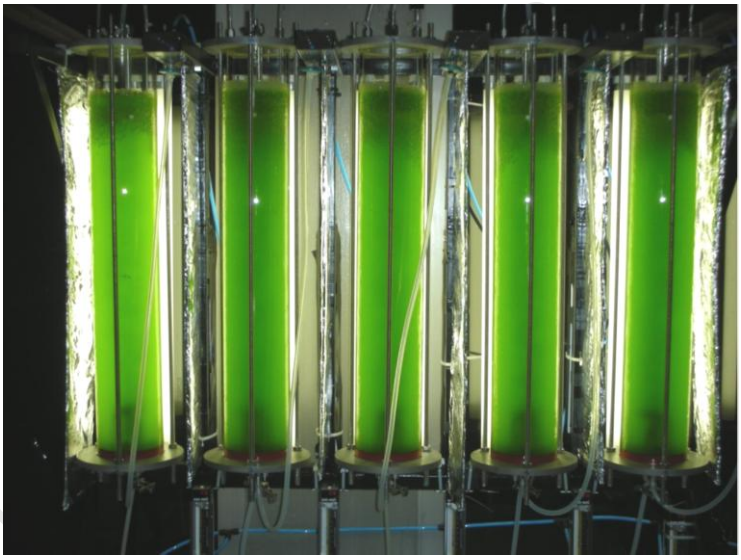

Figure 3.2: Photograph of ALRs in Bioreactor Laboratory, CeBER, U.C.T. (Langley, 2010)

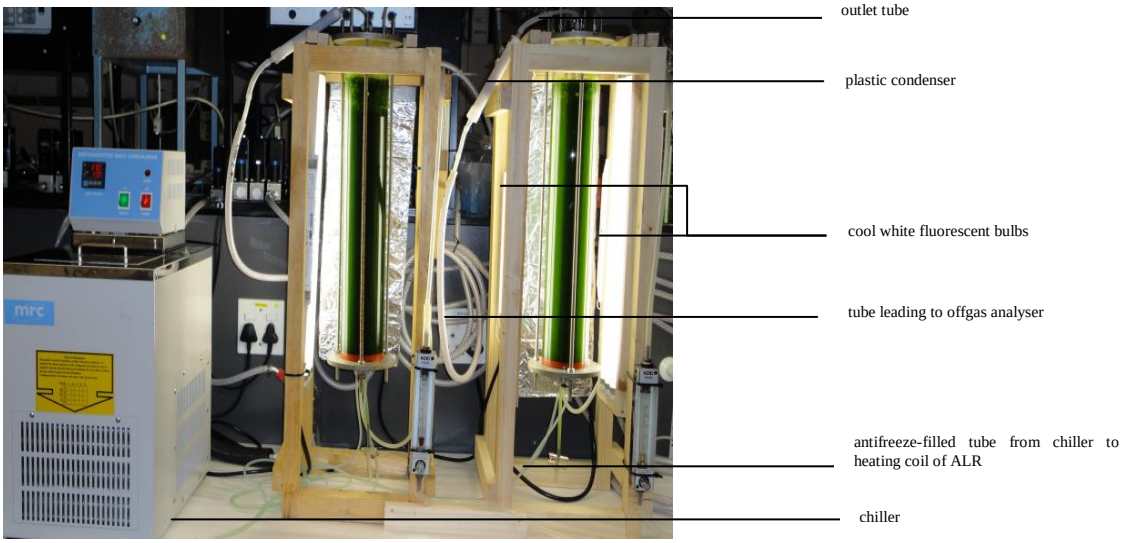

Figure 3.3: ALR experimental setup in Fe-S Laboratory, CeBER, U.C.T.

The *Scenedesmus* sp. culture (day 6) in R1 (LHS) was grown in fed-batch nutrient mode. The culture in R2 (RHS) was grown in batch mode and exposed to double the light intensity (aluminum flank removed for purpose of photograph).

Cultures were run at ambient temperatures which ranged from 25 °C to 27 °C. The ALR components were assembled and autoclaved with dH_2O, for 20 minutes at 121 °C (Everlight Vertical Type Autoclave, Laboratory Supplies, SA) prior to use. Each component of the 3NBBM media (Appendix A), was autoclaved separately and the vitamin solutions B1 (Thiaminhydrochloride) and B12 (Cyanocobalamin) were filtered through a 0.45 µm filter (Millipore, USA) and stored at 4 °C in the dark. The appropriate volumes were pipetted in a sterile bottle and poured through a sterile plastic funnel into each ALR.

The flow rates of the air and 100% CO_2 were each controlled by a Brooks 5850S Thermal Mass Flow Controller (Brooks Instrument B.V, U.S.A, assembled in Holland) and combined through an inline mixer. The flow rate through each controller was manipulated to supply gas at CO_2 partial pressures (P_{CO2}) from 0.00045 atm to 0.005 atm. For the experiments described in Chapter 5, rotameters (KDG Flowmeters, England; Sho-rate rotameters, Control Valve Technology, SA) were used to manipulate the flow rates to supply a P_{CO2} of 0.005 and 0.01 atm (Figure 3.3). At each ALR, the CO_2-enriched air was filtered through a 0.45 µm filter (Millipore, USA) and the flow rate was set to 2 $L.min^{-1}$ before being fed through a metal 0.22 µm stainless steel HPLC inlet filter sparger.

3.3 Analytical Methods

3.3.1 Determination of cell concentration

As accurate cell concentration determination was crucial to this study this topic is discussed in detail in Appendix C1. Two algal suspension samples were taken from each ALR at least once per day. To obey the linearity of the Beer-Lambert law the culture was diluted with dH_2O if the absorbance readings were more than 1. The biomass concentration was determined by taking the average of the 2 optical density readings at 750 nm (Helios intelliscan spectrophotometer/ mrc UV-200-RS, United Scientific (Pty) Ltd.) and converting this to concentration using the pertinent calibration curve. The wavelength of 750 nm was used rather than 680 nm, as the dominant pigment of *Scenedesmus* sp. is chlorophyll, and pigment content (measured at 680 nm) varies with age and culture conditions (Griffiths *et al*., 2011b).

Standard curves for the 1200 and 5000 ppm CO_2 growth conditions were generated by performing serial dilutions from a culture sample taken at the end of the run, measuring the absorbance values of these at 750 nm and taking at least 2 dry weight measurements to calculate the dry weight concentration of the culture. The absorbance values were then plotted against the dry weight value. A straight trendline was fitted to this and a R^2 value calculated by linear regression (Appendix C). The equation was then used to calculate the cell concentration ($g.L^{-1}$) from the measured absorbance values.

To calculate dry weight a known volume (10-20 mL) of culture was filtered through a pre-weighed 0.2 µM Millipore filter. The filter paper with algal biomass was dried in an 80°C oven (Memmert GmbH and Co., Germany) overnight. The following day this was weighed on a fine balance (Adventurer™ Ohaus, USA) and the concentration of the culture was calculated (Example in Appendix C).

3.3.2 Cell morphology

Scenedesmus sp. was inspected with the light microscope (Olympus BX40) regularly to examine cell morphology and to check that contamination with other algal species had not occurred. *Scenedesmus* sp. cells are spindle-shaped.

3.3.3 pH measurements

The pH was taken daily with a CyberScan 2500 pH meter (Wirsam Scientific, SA). The pH microelectrode and temperature probe were submerged in an undiluted sample and the pH recorded when reading stabilized. The pH meter was calibrated regularly with pH 4.0 and 7.0 buffers (Merck, SA).

3.3.4 Light measurements

For the experiments using 1 set of lights (three 18 W/640 k cool white fluorescent bulbs (Osram, SA), the average light intensity to the surface of the ALR was calculated as the average of 15 light intensity readings. Table 3-1 displays the readings, each a 15 s light intensity average, taken along 15 equidistant points distributed across the length and breadth of the light bank. Each reading was taken at a distance of 3 cm from the light bank as this is the distance between the light bank and the ALR. As the length of the light emitting portion of the bulb is 56.5 cm, the positions 1, 2, 3, 4 and 5 were taken at 53, 41, 28, 41 and 53 cm respectively.

Table 3-1: Average light intensity readings taken from the surface of the ALR positioned closest to the lights. I_{ext}= 282.7 µmol.m^{-2}.s^{-1}.

	L	M	R
1	198.0	207.6	193.0
2	259.3	308.4	286.0
3	358.2	353.7	334.7
4	324.4	336.0	295.9
5	276.4	267.8	241.7

To determine the average light intensity penetrating from all angles to the ALR, the average light intensity was calculated as the average of 15 to 20 light intensity readings. Table 3-2 and Table 3-3 display the readings for the experiments with 1 and 2 sets of lights respectively. Each reading, a 15 s light intensity average, was taken at equidistant points along the circumference and length of the surface of ALR. The ALR was filled with dH_2O, gas flow set to 2 $L.min^{-1}$ and aluminum flanks secured to ALR frame. Readings were taken with a submersible spherical micro quantum sensor (US-SQS/L) of a LI-COR LI-250 light meter (Heinz Walz GmbH, Germany). The light meter measures the Photosynthetic Photon Fluence Rate (PPFR), which is the total no of photons incident per time interval from all directions on a small sphere divided by the cross-sectional area of the sphere. PPFR is equivalent to PFD.

Table 3-2: Average light intensity readings, for 1 set of cool-white fluorescent lights, taken along the circumferential surface of the ALR. I_{avg}= 225.4 µmol.m^{-2}.s^{-1}.

	L	B	R	F
1	147.8	293.2	124.7	127.8
2	198.4	310.8	182.9	195.3
3	230.9	409.4	245.4	229.6
4	229.2	319.7	231.2	225.1
5	201.2	219.4	204.0	181.8

Table 3-3: Average light intensity readings, for 2 sets of cool-white fluorescent lights, taken along the circumferential surface of the ALR. I_{avg}= 560.0 µmol.m^{-2}.s^{-1}.

	L	F	R
1	445.4	539	373
2	528.2	616.6	531
3	551.8	743.3	617.6
4	547.7	740.2	568.9
5	468.3	587.7	537.9

3.3.5 Temperature measurements

The temperature was initially noted daily as each ALR had an online thermoccouple. When these thermoccouples malfunctioned temperature was monitored less frequently using a hand-held digital MT630 Thermometer (MajorTech, SA). However, it should be noted that the temperature values did not fluctuate by more than 2°C from the ambient temperature as the laboratory temperature was controlled. For the experiments described in Chapter 5, the temperature was controlled at 25 ± 1 °C

with a chiller (Model LTD6G, Grant Instruments, England) and monitored with a hand-held digital MT630 Thermometer (MajorTech, SA).

3.3.6 Spectrophotometric Anion measurements

To quantify the extracellular nitrate concentration in the algal media an ultraviolet spectrophotometric screening method was used according to Clesceri *et al*. (1998). The supernatant was taken from samples which had settled out in cuvettes and filtered with a 0.45 µM filter (Millipore, USA) attached to a 1 mL needless syringe (Uniqiao, Jiangsu Medical Instument Co., Ltd, China) so that interference from suspended particles did not occur. Acidification with 1N HCL was not done, as indicated in the method, since $CaCO_3$ concentrations were lower than 100 $mg.mL^{-1}$ for all samples. The samples were diluted between 10 and 200 fold with dH_2O and the absorbance read at 220 nm in a quartz cuvette. A standard curve was constructed by making serial dilutions from a 1000 ppm stock solution and measuring the absorbances with a mrc UV-200-RS spectrophotometer (United Scientific (Pty) Ltd., USA) (Appendix C).

3.3.7 High Performance Liquid Chromatography (HPLC) for Anion measurements

The concentration of extracellular nitrates and phosphates in the algal suspension was analysed by HPLC using a Waters IC-Pak Anion High Resolution column (Waters, SA), with a conductivity detector (Model 430, Millford, USA). Sodium Borate-Gluconate solution (Appendix A) was used as the mobile phase at a flow rate of 1 $mL.min^{-1}$. Samples were diluted and filter-sterilized with a 0.22 filter (Millipore, USA) prior to analysis. Standard curves were constructed by performing serial dilutions from $NaNO_3$ and KH_2PO_4 stock solutions and measuring the concentrations using HPLC (Appendix C).

3.3.8 Total Inorganic Carbon (TIC) analysis

The ANATOC Series II TOC analyser (SGE, Australia) was used to measure the inorganic and organic carbon present in the supernatant of the algae culture. A total carbon analysis was performed on each sample and the individual concentration of total inorganic and total organic carbon in the sample was reported. The inorganic carbon present in the sample is converted to CO_2 when injected

into the acidified catalyst suspension. The total CO_2 evolved is measured and reported as ppm ($mg.L^{-1}$). Once the TIC analysis is complete the near-UV lamp is automatically switched on and the organic carbon is oxidized to CO_2 by the conventional photocatalytic process. Photocatalytic oxidation refers to the ability of titanium dioxide to catalyze the oxidation of organic compounds in an aqueous medium in the presence of near UV light and oxygen. This mechanism is proposed to occur by formation of hydroxyl radicals at the surface of the titanium dioxide. This reaction yields CO_2, H_2O and either the acid, base or salt of any organically bound elements.

Samples were filtered before usage as solid organic components cannot be oxidized. Attempts were made to limit exposure of samples to the atmosphere. Samples were stored in sealed 40 mL sterile plastic containers in a 4°C fridge until analysis. The 200 ppm carbon standard solution using potassium hydrogen phthalate, working standard solution, catalyst suspension and perchloric acid solution (0.1M) were prepared as per the manufacturer's instructions (ANATOC Series II Total Organic Carbon Analyser Installation and Operation Manual).

3.3.9 Elemental analysis

Samples were taken on days 2, 4, 7, 10 and 14 of a *Scenedesmus* sp. culture grown under standard conditions, such that more than 2.5 mg of algae was obtained per sample. The samples were centrifuged for 10 minutes at 4000 rpm in a U-320 centrifuge (Boeco, Germany). The supernatant was retained and the pellets contained within the 50 ml sterile tube (grenier bio-one CELLSTAR®, USA) were stored at -60 °C. The samples were freeze-dried for two days using an Instravac vacuum (Air and Vacuum Technologies (Pty) Ltd, SA) and crushed with a metal spoon to grind the algal matter to a powder. Analysis was performed courtesy of the Department of Chemistry, UCT with a Thermo Flash EA 1112 series combustion analyser (Thermo Fisher Scientific, USA).

3.3.10 Spectrophotometric pigment quantification

A 2 mL sample of culture was centrifuged at 14000 rpm for 3 minutes (Eppendorf centrifuge 5415D, USA) and the supernatant was discarded. 2 ml of pre-warmed (60 °C) dimethyl sulphoxide (DMSO, 99%, SaarChem) was added to the pellet and the mixture was vortexed (Vortex-Genie 2, Scientific Industries, SA) until the cells were resuspended. The suspension was then incubated for 10 mins at 60 °C, vortexed and centrifuged at 14000 rpm to pellet the cells. The supernatant was transferred to cuvettes and OD read at 480 nm, 649 nm and 665 nm. DMSO was used as a blank and to dilute

samples if the OD reading was more than 1. To convert the absorbance readings to concentration the equations developed by Wellburn (1994) were used (Equations 3.1 to 3.3).

$$ChlA = 12.47 \times A665 \times -3.62 \times A649 \quad (3.1)$$

$$ChlB = 25.06 \times A649 - 6.5 \times A665 \quad (3.2)$$

$$Carotenoids = \frac{(1000 \times A480 - 1.29 \times ChlA - 53.78 \times ChlB)}{220} \quad (3.3)$$

Total pigment ($mg.L^{-1}$) equals to the sum of the chlorophyll *a* (ChlA), chlorophyll *b* (ChlB) and carotenoids. This was divided by the cell concentration ($mg.L^{-1}$) to express the pigment content as a percentage of dry weight.

3.3.11 CO_2 concentration readings

To increase the pressure within the reactor, a stopper was placed in the gas outlet of the stainless steel flange of the ALR (Appendix B). One end of a plastic condenser (Separations, SA) was attached to the output tube of the ALR and the other was attached to a plastic bag (devoid of gas). The discrete offgas samples were then fed to an offgas analyser manually (Hartmann and Braun, Germany) to determine the P_{CO2} of the output stream. Measurements were taken daily. The offgas analyser was purged with N_2 and calibrated with P_{CO2} of 0.000495 atm (0.0495%) CO_2 gas (Air Liquide, SA). The P_{CO2} in the input stream was recorded at the beginning of the run. For the ALR experiment using an input P_{CO2} of 0.005 atm (0.5%) and 0.01 atm (0.1%), data for the inlet and outlet gas was logged continuously with an ABB EL320 offgas analyser (ABB, Germany).

3.4 Data analysis

3.4.1 Calculation of characteristic consumption times

The characteristic mass transfer time (t_t) for CO_2 was calculated by:

$$t_t = \frac{1}{K_L a(CO_2)} \tag{3.4}$$

The mass transfer coefficient for the ALRs ($K_La(CO_2)$) was experimentally determined to be 0.0094 ± 0.00026 s^{-1} (Langley 2010). Thus, the t_t was calculated as 106.38 s.

The characteristic consumption time for CO_2 (t_r) was calculated as:

$$t_r = \frac{Y_{CO_2} C^*}{\mu X} \tag{3.5}$$

where: the yield coefficient (Y_{CO2}) is calculated to be 1.72 g CO_2.g X^{-1}($X_C \times M_{CO2}.M_C^{-1}$)

X_C, the average carbon content of *Scenedesmus* sp. =0.4696 (Appendix D)

M_{CO2}, the molar mass of CO_2 =44 $g.mol^{-1}$

M_C, the molar mass of carbon =12 $g.mol^{-1}$

C*, the saturation concentration of CO_2 =0.67 × 10^{-3} $g.L^{-1}$ at 0.045% CO_2

μ (s^{-1}) and X ($g.L^{-1}$) vary with time

The specific growth rate (μ) was plotted as a function of time and fitted to a three order polynomial (R^2=0.9149). The μ values predicted by this polynomial were used in the calculation of t_r. Mixing time is the time required to achieve a given degree of homogeneity starting from the completely segregated state (Doran, 1995). It can be measured by injecting a tracer into a vessel at one point and measuring its concentration at a different point (Doran, 1995). Fraser (2011) performed this experiment with the CeBER ALRs at the gas flow rate used in this study (2 $L.min^{-1}$(U_{GR} of 0.021 $m.s^{-1}$)) and the tracer response was used to determine the mixing time. The mixing time, which was taken as the time elapsed from the injection of the tracer to the time at which the concentration of the tracer normalized, was determined to be 53 s (Appendix E).

3.4.2 Thermodynamic modelling of carbon form concentration and speciation

The solubility of CO_2 in water was previously discussed (Section 2.2.3.3). However, when considering gas-absorption accompanied by chemical reaction, it is necessary to know the solubility of unreacted gas in the reacting solution. It is not convenient to measure the solubility by conventional methods during the course of algal culture. In the case of electrolyte solutions the solubility can be estimated by the method where the Henry's law constant of the solution is related to that of water at the same temperature by means of Equation 3.6 (Danckwerts, 1970).

$$\log_{10}\left(\frac{K_H}{K_H^{\,0}}\right) = hI \tag{3.6}$$

where: K_H = Henry's law constant of the solution

$K_H^{\,0}$ = Henry's law constant in water

h = sum of contributions referring to the species of positive and negative ions present and to the species of gas

I = ionic strength of the solution which is calculated by:

$$I = \frac{1}{2}\sum C_i Z_i^{\,2} \tag{3.7}$$

where: C_i = concentration of ions

z_i = valency of the ion

$$-\log y_i = A.z_i^{\,2}\left(\frac{\sqrt{I}}{I+\sqrt{I}} - B.I\right) \tag{3.8}$$

where: y_i = activity coefficient of species *i*

A = Debye-Huckel coefficient (temperature-dependent, 0.51 at 25 °C)

z_i = valency of the species

I = ionic strength

B = Davies B parameter = 0.3 in Visual Minteq

The thermodynamic package Visual Minteq (v3.0) was used to model the concentrations and speciation of the carbon forms in the algal suspension. The program uses Equation 3.7 to calculate ionic strength and uses the Davies equation (Equation 3.8) to calculate activity coefficients. As ionic strength does not exceed 0.5 mol.kg^{-1} for the modified Bold medium used for culturing *Scenedesmus* sp it is acceptable to use the Davies equation. Input values included pH, DIC (equivalent to TIC), P_{CO2}s and concentrations of the individual ions present in the algal suspension at that time point. The concentrations of the extracellular nutrients were estimated by relation to the measured concentrations of sodium nitrate and ion concentrations determined using molar mass ratios. The method relies on the assumptions that media component concentrations are utilized in the ratio provided in Appendix A and that the effect of trace elements and vitamins are negligible.

3.4.3 Calculation of CO_2 uptake rates and recoveries

To estimate the CO_2 uptake rate during the exponential phase of growth the natural logarithm of cell concentration (lnX) was plotted with time as a function of CO_2 inlet concentration. A linear trendline was fitted through the straight line region of this plot and the gradient was taken as the average specific growth rate. The CO_2 uptake rate was estimated using the growth rate, cell concentration, carbon content of *Scenedesmus* sp. and the molar masses of CO_2 and carbon:

$$Q_{CO_2} = \mu \times X \times X_c \times \frac{M_{CO_2}}{M_C} \tag{3.9}$$

where: μ = average specific growth rate (hr^{-1})

X = cell concentration (g.L^{-1}) at 24 hours

X_C = the average mass fraction of carbon in *Scenedesmus* sp.=0.4696 (Appendix D)

M_{CO2} = 44 g.mol^{-1}

M_C =12 g.mol^{-1}

The CO_2 flow rate (F_{CO2}) in $mg.hr^{-1}$ was calculated using the ideal gas law:

$$pV = nRT \tag{3.10}$$

where: p = 101325 Pa

V = 0.12 $mL.hr^{-1}$ × [CO_2] (ppm(v))

R = 8.314 $kJ.kmol^{-1}.K^{-1}$

T = 298 K

M_{CO2} = 44 $g.mol^{-1}$

The CO_2 uptake rate (Q_{CO2}) in $mg.hr^{-1}$ was estimated for the linear growth phase by using the biomass productivity, the carbon content and the molar masses of CO_2 and carbon:

$$Q_{CO_2} = \frac{(X_1 - X_2)}{(t_1 - t_2)} \times X_c \times \frac{M_{CO_2}}{M_C} \times V \tag{3.11}$$

where: X = cell concentration ($mg.L^{-1}$)

t = time (hours)

X_C = the average mass fraction of carbon in *Scenedesmus* sp.=0.4696 (Appendix D)

M_{CO2} = 44 $g.mol^{-1}$

M_C = 12 $g.mol^{-1}$

V = working volume of ALR=3.2 L

The CO_2 percentage recovery was estimated using biomass data (CR (X)):

$$CR(X) = \frac{Q_{CO_2}}{F_{CO_2}} \times 100 \tag{3.12}$$

The CO_2 percentage recovery was calculated using offgas data (CR (OG)):

$$CR(OG) = \frac{([CO_2]_{in} - [CO_2]_{out})}{[CO_2]_{in}} \text{ X } 100 \quad (3.13)$$

where: $[CO_2]_{in}$ = inlet CO_2 concentration (ppm)

$[CO_2]_{out}$ = outlet CO_2 concentration (ppm)

For the experiments outlined in Chapter 5, the CO_2 concentration in the offgas was measured. The offgas analyser operated cyclically; readings were taken for each reactor approximately every 2 hours. Between 69 and 119 readings were taken for each 2 hour interval and the total number of readings for the two-week growth period ranged from 6000 to 13000, depending upon the run. Each CO_2 inlet concentration was aligned to the CO_2 outlet concentration according to the time point and the CO_2 recovery calculated using Equation 3.13 in Microsoft Excel. The CO_2 recoveries were imported to MATLAB (R2010a, MathWorks Inc.) which was used to group and average data for each time interval. This data was then exported to Microsoft Excel where it was plotted.

3.4.4 Modelling of light intensities

An empirical light distribution model was used to predict average light irradiance (PFD) as a function of *Scenedesmus* sp. cell concentration (Fraser, 2011). The model is a modified Beer-Lambert law and uses two additional parameters to account for scattering effects which occur due to light path length and algal concentration.

$$I(C_x, z) = I_0.\exp\left[\frac{-K_{a,\max}.C_x.z}{(C_x + K_x)(z + K_z)}\right] \quad (3.14)$$

where: C_x is the biomass concentration ($g.L^{-1}$)

z is the distance from the illuminated surface (m)

I_0 is the light intensity at the surface ($\mu mol.m^{-2}.s^{-1}$)

$K_{a,\,max}$ is the Maximal absorption coefficient (m^{-1})

K_X is the constant for scattering by cells ($kg.m^{-3}$)

K_z is the constant for scattering by light path length (m)

The species specific model parameters $K_{a,max}$, K_x and K_z were determined experimentally for *Scenedesmus* sp. and are displayed in Table 3-4.

Table 3-4: Light distribution model parameters for *Scenedesmus* sp. (Fraser, 2011)

Parameter	Value	95% Confidence range	Unit
$K_{a,max}$	83.9	±9.64	-
K_x	7.51	±0.85	$g.L^{-1}$
K_z	9.53	±1.06	cm

Assumptions for the model include:

1. Light intensity does not vary vertically for the reactor

2. Light attenuation depends only on cell concentration and light path length.

3. The cells are homogeneously suspended in the medium, such that all properties that depend on cell concentration can be assumed constant throughout the reactor volume.

4. The external light source is constant at every external point around the reactor surface.

It should be noted that for the experimental setup in this study lights did not surround the ALR on all sides (Figure 3.3). However, 2 aluminum flanks were placed on opposite ends of the ALR which would reflect the light back to the ALR to a certain extent. Also, average surface light intensities were determined considering light penetrating from all angles to the ALR (Table 3-2 and Table 3-3).

3.5 Experimental Approach

The experimental work was compartmentalized into two sections. The first section, presented in Chapter 4, involved culturing *Scenedesmus* sp. at the CO_2 inlet concentrations of 450, 1200, 2900, 5000 and 10 000 ppm and examining the responses. The second section, presented in Chapter 5, involved optimizing CO_2 utilization by varying CO_2, light intensity and nutrient regime by means of a factorial design (Table 3-4).

Table 3-5: Matrix for the 2^3 factorial design

	Actual level			Coded level		
Run	**A** CO_2 **(ppm)**	**B** Incident light intensity (I_0) ($\mu mol.m^{-2}.s^{-1}$)	**C** Nutrient regime	**A**	**B**	**C**
1	10 000	225	Fed-batch	+1	-1	+1
2	10 000	225	Standard	+1	-1	-1
3	10 000	560	Fed-batch	+1	+1	+1
4	10 000	560	Standard	+1	+1	-1
5	5 000	225	Fed-batch	-1	-1	+1
6	5 000	225	Standard	-1	-1	-1
7	5 000	560	Fed-batch	-1	+1	+1
8	5 000	560	Standard	-1	+1	-1

Chapter 4 : Investigation into the CO_2 utilization of *Scenedesmus*

4.1 Introduction

This chapter involves the investigation of the response of *Scenedesmus* sp. across a range of CO_2 inlet concentrations. The aims for this chapter are to compare the capability of CO_2 fixation of *Scenedesmus* sp. to other microalgal species; to determine the $P_{CO2,CRIT}$ for *Scenedesmus* sp. in the CeBER laboratory, UCT at standard operating conditions and to examine the associated physiological responses of *Scenedesmus* sp. across the range of CO_2 inlet concentrations to delineate the limiting growth process.

4.2 Effect of CO_2 on growth

4.2.1 Algal growth as a function of CO_2 concentration

To study the effect of CO_2 availability on the production of algal biomass, *Scenedesmus* sp. was grown in batch mode for 288 to 336 hours in ALRs. Inocula were prepared a week prior to each experiment to ensure inoculation occurred with cells in the logarithmic growth phase of culture. Experiments were conducted at different CO_2 partial pressures viz. 0.00045, 0.0012, 0.0029, 0.0050 and 0.01 atm[3]. Figure 4.1 provides the profiles of biomass concentration with time as a function of CO_2 inlet concentration. Within the first 24 hours the cell concentration across all experiments increased similarly. Thereafter the growth curve on 450 ppm CO_2 deviated from exponential growth and biomass concentration increased at a lower linear rate than the other growth curves. The growth rates of the 1200, 2900 and 5000 ppm experiments increased similarly until the 96th hour whereupon the growth curve on 1200ppm CO_2 deviated from exponential to linear phase. The growth rates of the 2900 ppm and 5000 ppm experiments were similar up until the 240th hour whereupon the growth rate

[3] $P_{CO2} = y_{CO2} \times P$

where y_{CO2}=molar percentage of CO_2 in gas feed and P=total pressure (1 atm)

To convert from ppm(v) to molar percentage divide by 10^4

of the 2900 ppm experiment became zero. The growth rate of the 10 000 ppm experiment remained exponential until day 6, resulting in higher biomass concentrations. However at approximately 332 hours the cell concentration reached 3.7 $g.L^{-1}$ for the 5000 and 10 000 ppm experiments.

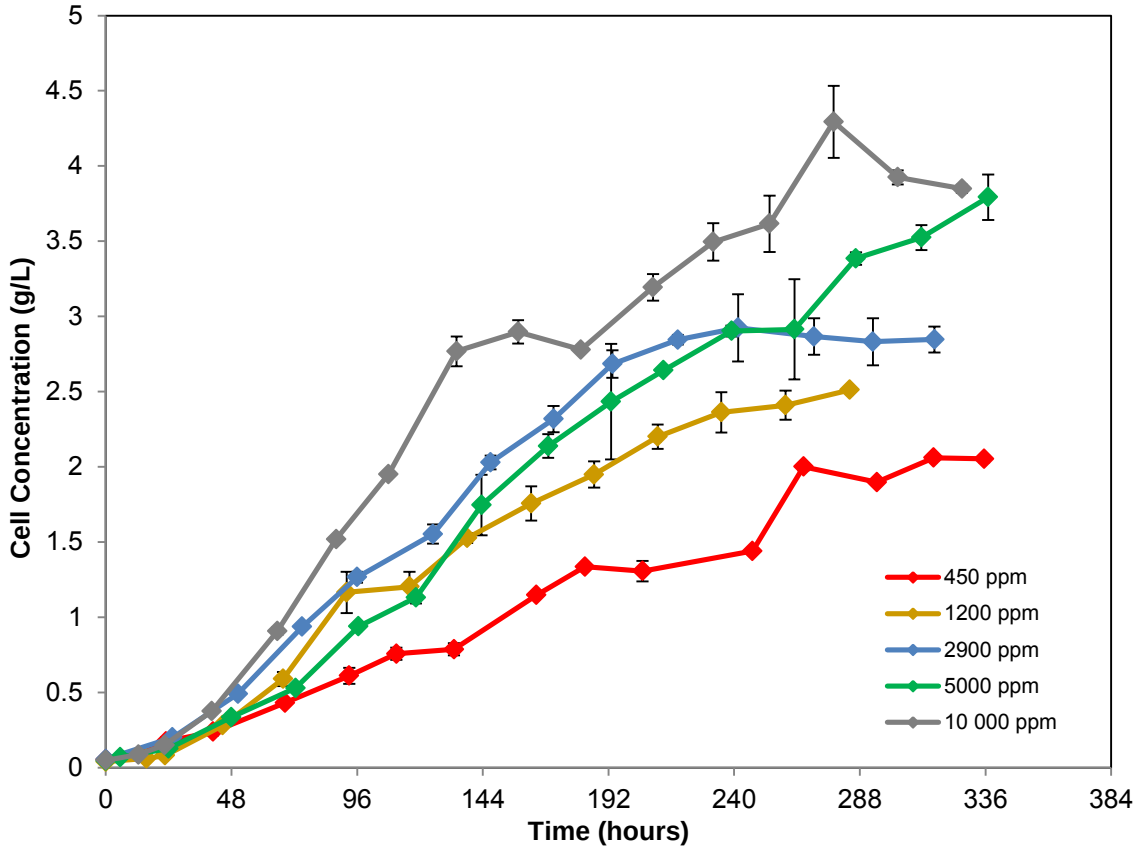

Figure 4.1: *Scenedesmus* sp. growth curves in ALRs at varied CO_2 inlet concentrations at 25 ± 2 °C

(Error bars for runs with 450, 1200 and 2900 ppm CO_2 represent standard deviations for duplicate ALR runs; error bars for the 5000 ppm experiment represent standard deviations for triplicate ALR runs and error bars for the 10 000 ppm run represent standard deviations for absorbance readings)

4.2.2 Characteristic Time Analysis of limiting process

It is presumed that the lowered growth at 450 ppm CO_2 was due to CO_2 mass transfer limitations. To confirm this, a characteristic time analysis was performed for *Scenedesmus* sp. cultured on 450 ppm CO_2 to determine whether mass transfer, mixing or physiological limitations were limiting growth (Contreras *et al.*, 1998; Fan *et al.*, 2008). Characteristic consumption times were determined as described in Section 3.4.1. As depicted in Figure 4.2 the maximum characteristic CO_2 consumption time (maximum t_r), calculated using the maximum specific growth rate, was higher than the mixing time (t_m) and the mass transfer time (t_t) at cell concentrations below 0.5 g/L. At higher cell

concentrations mass transfer became the limiting process as evidenced by the deviation of the 450 ppm growth curve from the 1200 ppm growth curve at 68.5 hours (Figure 4.1). Hence, at 450 ppm CO_2 growth would only be unconstrained by CO_2 at very low cell concentrations. The characteristic CO_2 consumption time (t_r) curve indicates that mixing does not inhibit growth as the mixing time of 53 s is less than the CO_2 consumption times. For the range of cell concentrations in this study (0.05 to 5.5 g/L) viscosity effects were negligible (Dicks, 2010). Hence, it is assumed that mixing would be unaffected by cell concentration in all experiments. Contreras *et al*. (1998) examined the effect of cell concentration (0-4 g/L) on the mass transfer coefficient in an ALR and found that k_La was not significantly affected. Thus, the possibility of an increased resistance at the gas-liquid interface for cell concentrations higher than 4 g/L cannot be excluded.

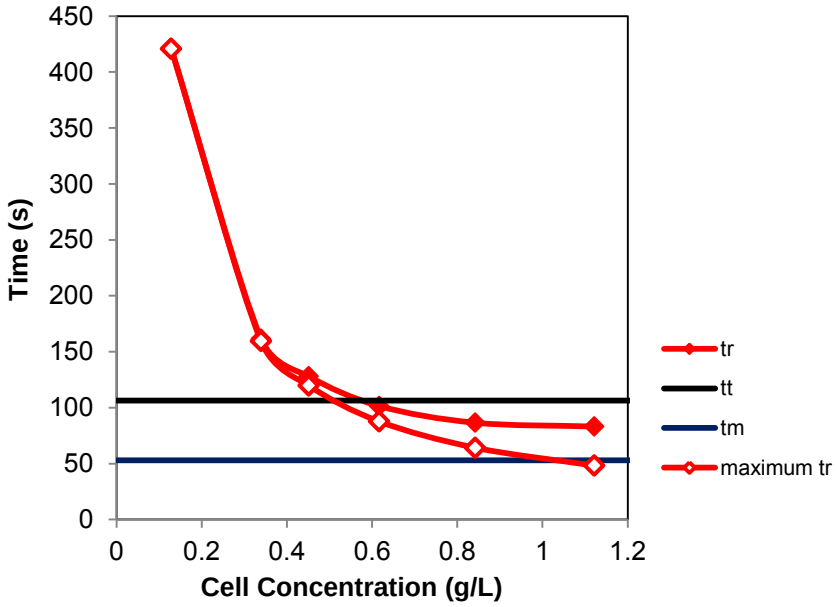

Figure 4.2: Characteristic mixing time (t_m), mass transfer time (t_t) and CO_2 consumption time (t_r) for *Scenedesmus* sp. cultured with 450 ppm CO_2

For batch cultures balanced growth occurs during the exponential phase i.e. the nutrient uptake provides the amount of nutrients required by the algal cell to maintain its current growth rate (Anderson, 2005; Borchardt, 1996). To estimate the CO_2 uptake rates during the exponential phase, the growth rate, carbon content, and cell concentration were used as described in Section 3.4.3. The CO_2 uptake rates were 17.69, 6.35, 17.03, 8.74 and 12.73 $mg.L^{-1}.hr^{-1}$ at 450, 1200, 2900, 5000 and 10 000 ppm CO_2 respectively. These values are lower than the average CO_2 uptake rates calculated during the linear phase of growth at all CO_2 levels except 450 ppm CO_2 (Section 4.6). Although growth rates are highest during the exponential phase, cell concentrations are very low initially and CO_2 uptake is a function of both growth rate and cell concentration.

4.3 Effect of CO_2 on nitrate uptake

4.3.1 Nitrate uptake as a function of CO_2 availability

The extracellular nitrate concentration was determined at intermittent time points for each experiment to establish whether the increased rate of growth at higher CO_2 concentrations was accompanied by a concomitant increase in nutrient uptake. A starting concentration of 750 mg/L $NaNO_3$ was used for all experiments. The high measured nitrate concentration for the 2900 ppm experiment on day 2 indicates that a starting concentration of higher than 750 mg/L $NaNO_3$ was used. This is possibly due to a pipetting error. Figure 4.3 illustrates the extracellular nitrate concentration with time as a function of CO_2 inlet concentration. The depletion of nitrate in the extracellular media was similar for the 450 and 1200 ppm CO_2 experiments while more rapid for the 2900, 5000 and 10 000 ppm experiments. On day 7 the extracellular nitrate concentration approached zero, (27 mg/L to 3 mg/L $NaNO_3$) for the 2900, 5000 and 10 000 ppm experiments respectively, whereas the depletion of nitrate for the 450 and 1200 ppm experiment occurred after day 9. Despite this the growth of *Scenedesmus* sp. continued after day 7 and day 9 for the respective experiments which implies that it used nitrogen from intracellular stores for growth thereafter.

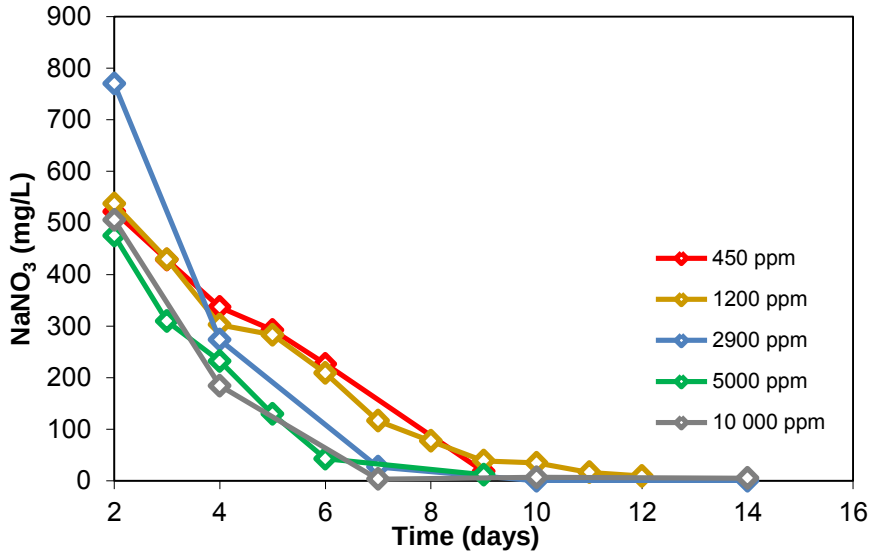

Figure 4.3: Depletion of extracellular sodium nitrate with growth of *Scenedesmus* sp. at varied CO_2 inlet concentrations

4.3.2 Selection of nitrate concentration

To determine which nitrate concentration to select for the increased nitrate experiments, the nitrogen fraction of cells (X_N), determined by elemental analysis (Section 3.3.9), was used to calculate the amount of $NaNO_3$ needed to form 1 g of *Scenedesmus* sp. Table 4-1 displays the nitrogen elemental composition for *Scenedesmus* sp. cultured on 2900 ppm CO_2 and 3NBBM (standard growth conditions) in the ALR on days 2, 4, 7, 10 and 14 of the growth curve. This was multiplied by the molar ratio of $NaNO_3$ to N to obtain the amount of sodium nitrate needed to form 1 g of *Scenedesmus* sp. Thus, for a cell concentration of 5 g/L a starting concentration in the range of 559 to 2899 mg/L $NaNO_3$ is predicted to be required for the batch process whereas 3NBBM contains 750 mg/L. This calculation was made based on the assumption that the nitrogen fraction of cells does not vary substantially when *Scenedesmus* sp. is cultured with higher CO_2 concentrations. Two thousand and 1450 mg/L of $NaNO_3$ were selected as intermediate concentrations between 750 mg/L and 2900 mg/L.

Table 4-1: Amount of sodium nitrate needed to form 1 g of biomass

Time (day)	X_N (%)	$NaNO_3$ / X (mg/g)
2	9.55	579
4	9.16	556
7	6.33	384
10	1.84	112
14	2.9	176

4.3.3 Effect of increased nitrate on *Scenedesmus* sp. growth

To investigate the role of nitrate availability in improving the growth of *Scenedesmus* sp. and the associated CO_2 uptake and recovery, experiments were conducted at two CO_2 concentrations. Growth was compared at the starting $NaNO_3$ concentrations of 750 and 2000 mg/L at a CO_2 concentration of 2900 ppm. Also, growth was studied at 750, 1450 and 2000 mg/L $NaNO_3$ at a CO_2 concentration of 5000 ppm. These results are presented in Figure 4.4 and 4.5 respectively.

At 2900 ppm CO_2, it was found that the rate of growth and the final cell concentration were lower at the increased nitrate concentration (Figure 4.4). At 5000 ppm CO_2 the higher concentrations of $NaNO_3$ impacted less negatively on growth in comparison to the 2900 ppm CO_2 experiment (Figure 4.5). When samples taken from cultures grown with high nitrate (2000 mg/L) were examined microscopically, multiple clusters of cells were observed and are shown in Figure 4.6. The flocculation of cells may be due to the interaction of the cations (Na^+ ions) with the negatively charged cells.

In a related study in the CeBER laboratory at UCT, Dicks and Harrison (in preparation) determined that the zeta potential of *Scenedesmus* sp. decreased steadily (below 0 mV) with increasing pH from 4.2 to 7.2 and thereafter stabilized until pH 13, beyond which the zeta potential decreased. He attributed this decrease to the increased conductivity of the solution and noted that salt loading impacts physical solution properties such as zeta potential, which in turn affect flocculation activities (Dicks and Harrison, in preparation). Figure 4.7 demonstrates that at 2900 ppm CO_2, the extracellular $NaNO_3$ concentrations were higher across the duration of growth when compared to the extracellular $NaNO_3$ concentrations at 5000 ppm CO_2 (Figure 4.7). The lowered rate of growth at higher nitrate concentrations at 2900 ppm CO_2 in comparison to 5000 ppm CO_2 can potentially be attributed to a higher salt loading, a decreased CO_2 transfer rate and/or to a higher DIC buffering capacity at 5000 ppm CO_2.

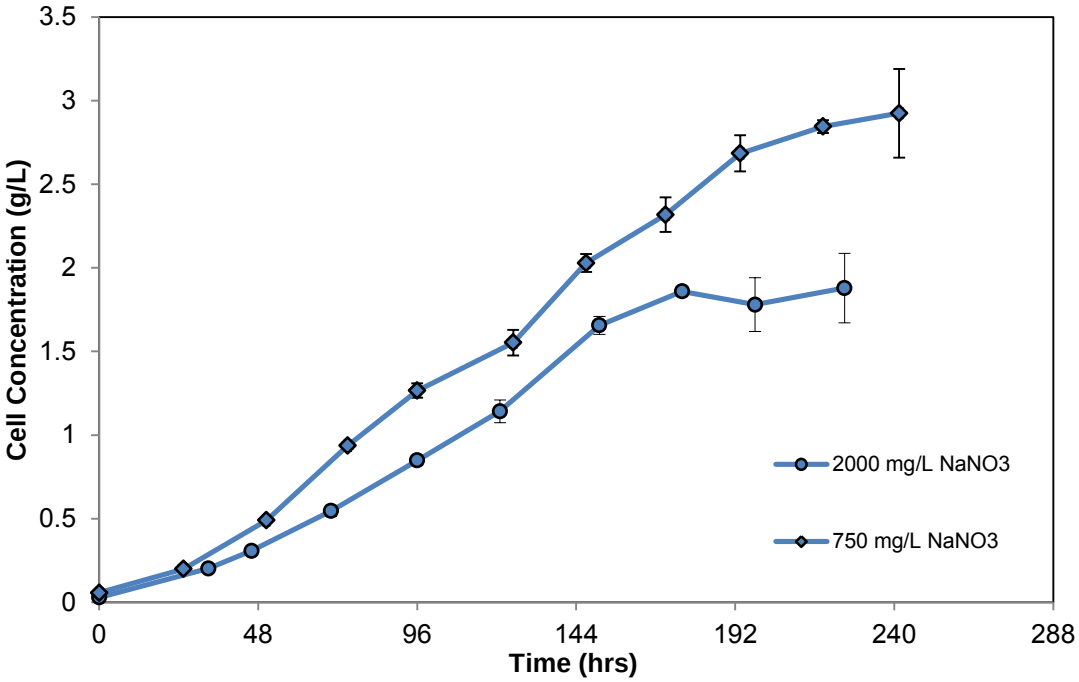

Figure 4.4: Growth curve of *Scenedesmus* sp. at 2900 ppm CO_2 in ALRs at 25 ± 2 °C

(Error bars represent standard deviations for duplicate ALR runs)

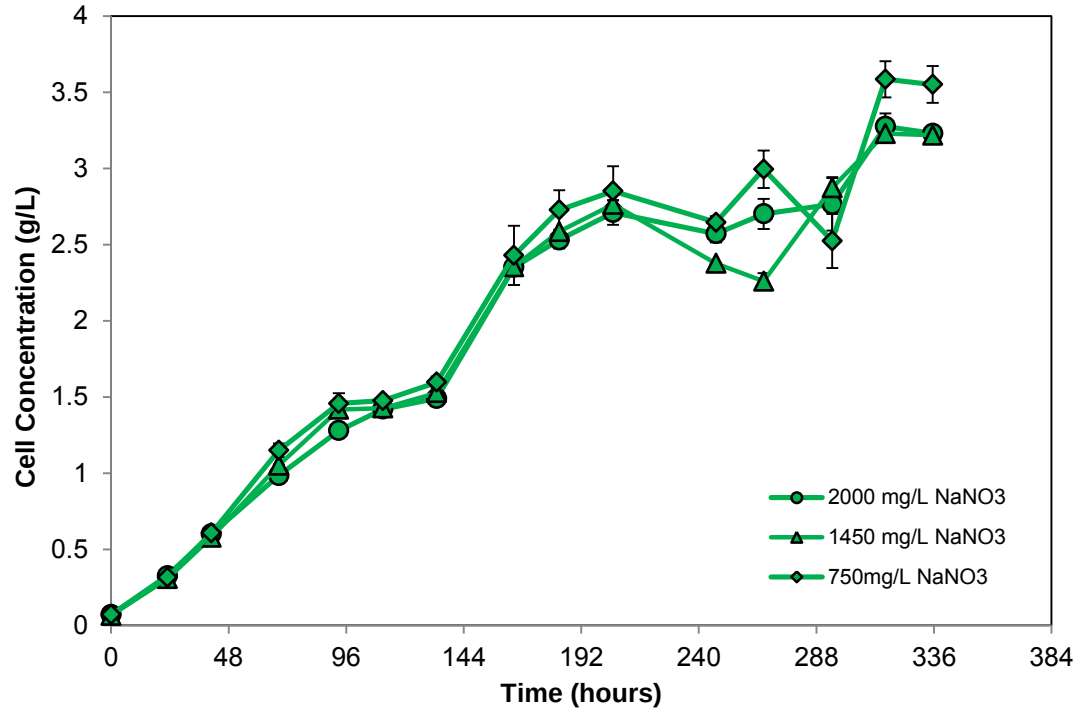

Figure 4.5: Growth curve of *Scenedesmus* sp. at 5000 ppm CO_2 in ALRs at 25 ± 2 °C

(Error bars for 2000 and 750 $mg.L^{-1}$ $NaNO_3$ conditions represent standard deviations for duplicate ALR runs)

A:

B:

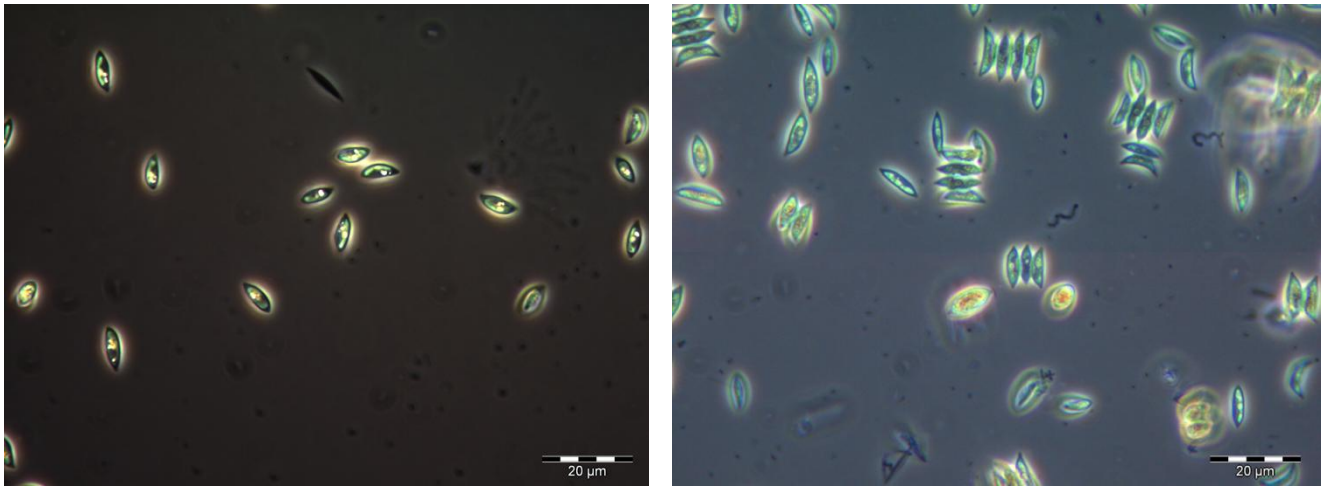

Figure 4.6: Micrographs of *Scenedesmus* sp. cultured for 10 days with (A) 2900 ppm CO_2 and 750 ppm $NaNO_3$ and (B) 2900 ppm CO_2 and 2000 ppm $NaNO_3$

(100X objective lens used)

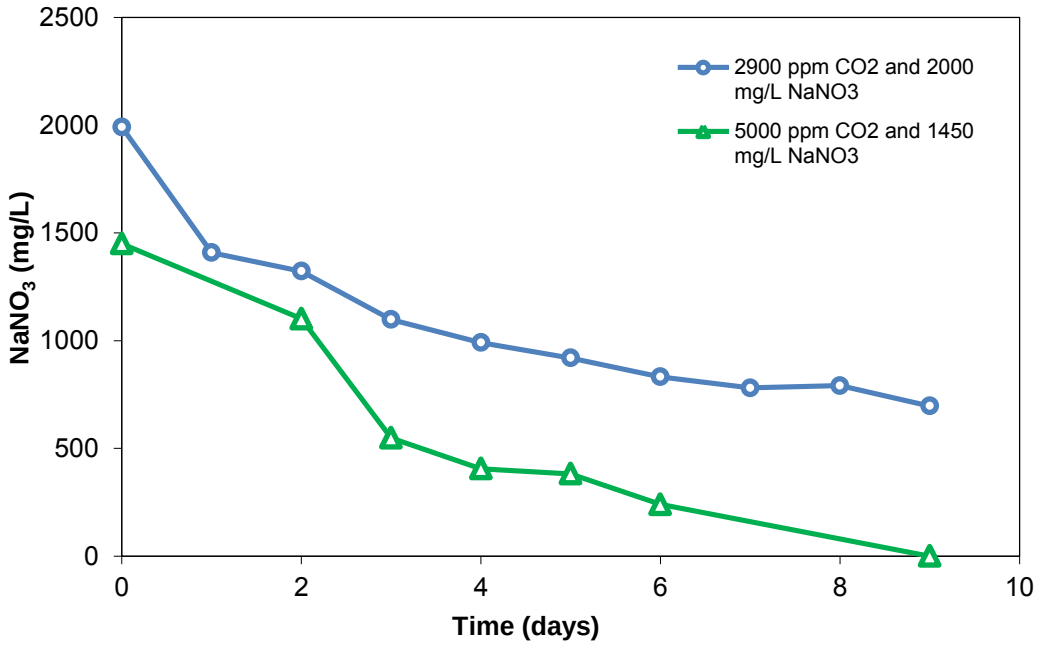

Figure 4.7: Depletion of extracellular sodium nitrate with growth of *Scenedesmus* sp. at 2900 and 5000 ppm CO_2 and nitrate concentrations of 1450 and 2000 $mg.L^{-1}$ respectively

4.4 Effect of CO_2 on pH

The pH profiles for growth experiments, across the range of CO_2 inlet concentrations are presented in Figure 4.8. The pH of the algal suspension increased rapidly within the first 48 hours in all experiments as the uptake rate of CO_2 was greater than the dissolution rate due to the rapid period of growth in the exponential phase (Figure 4.1). This is also evidenced by the low concentration of Dissolved Inorganic Carbon (DIC) in the cell-free media at the 48th hour of growth (Figure 4.10).

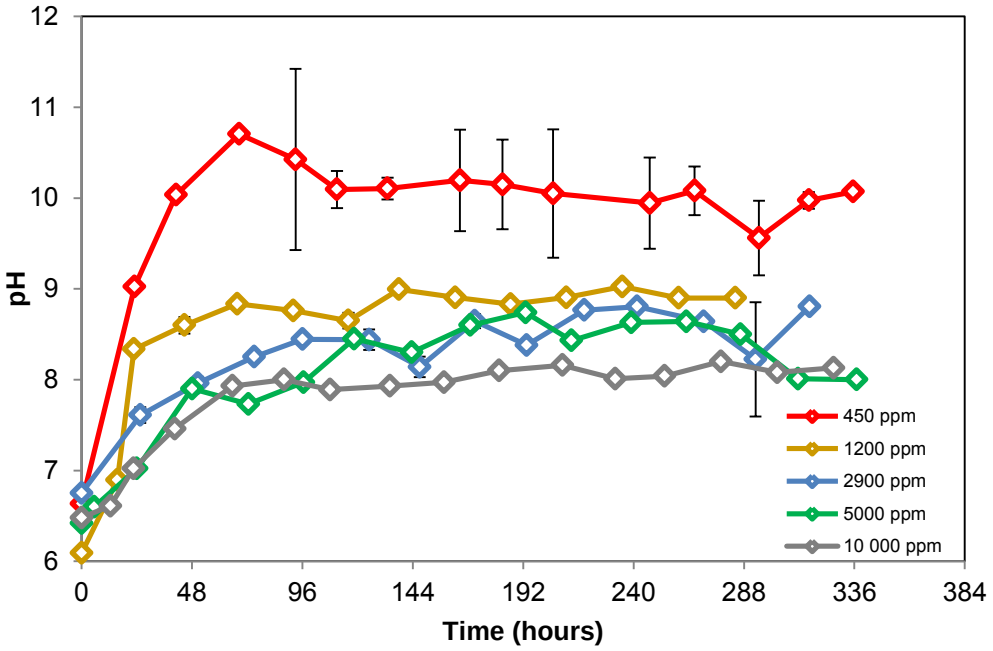

Figure 4.8: pH profiles of *Scenedesmus* sp. grown in ALRs at varied CO_2 inlet concentrations at 25 ± 2 °C
(Error bars for runs with 450, 1200 and 2900 ppm CO_2 represent standard deviations for duplicate ALR runs)

The pH profiles stabilized over the period of 100 to 240 hours across all experiments (Figure 4.1). Comparing the average pH[4] to the feed CO_2 concentrations and to the average CO_2 uptake rate it is evident that the pH decreases with increasing CO_2 uptake rates which are associated with increasing mass transfer (Figure 4.9). The exception for this is the average CO_2 uptake rate at 10 000 ppm CO_2, which is lower than both the average CO_2 uptake rates at 2900 and 5000 ppm CO_2 for this time period. This can be attributed to light limitation which occurs due to the higher cell concentrations at 10 000 ppm CO_2 (Section 5.5.3).

[4] Average pH and average CO_2 uptake rate calculated for 100 to 240 hours

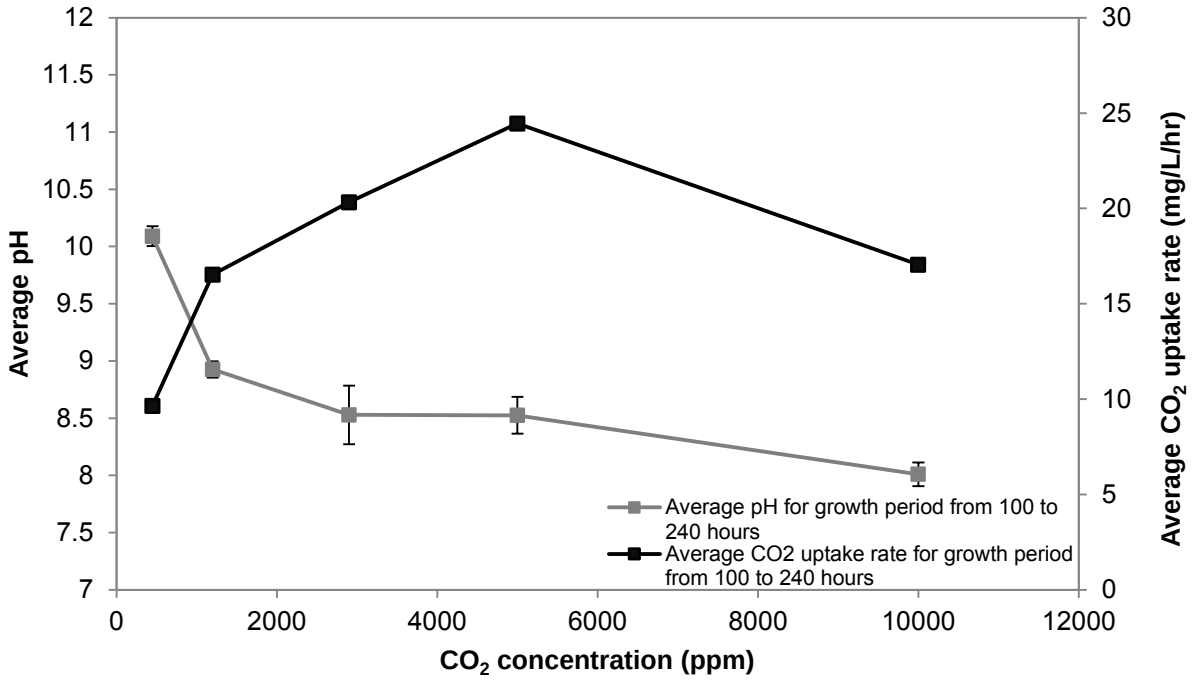

Figure 4.9: Relationship between average pH and average CO_2 uptake rate across all CO_2 inlet concentrations for the growth period of 100 to 240 hours

(Error bars on pH values represent average pH values for the period of 100 to 240 hours, R^2 values for the straight lines fitted to biomass data for the period of 100 to 240 hours range from 0.837 (at 10 000 ppm CO_2) to 0.988)

As *Scenedesmus* can tolerate pHs up to a maximum of 10 to 11.5 the pH range in this study is not expected to impede growth (Pott *et al*., 2009). Although this study did not decouple the effects of pH and DIC speciation, Azov (1982) supplied DIC to *S. obliquus* at pHs ranging from 8.1-9.3 (increments of 0.2) such that 0.1 mg of free CO_2 was provided for each of the seven assays. A constant specific carbon uptake rate of 0.3 mg C.g $PC^{-1}.min^{-1}$ was observed at all pHs for the high CO_2-adapted *S. obliquus* (Azov, 1982). The pH range for the 1200 to 10 000 ppm CO_2 experiments fell within the range investigated by Azov i.e. the physiological effect of pH is unlikely to affect the growth rate and the associated CO_2 uptake rate.

4.5 Effect of CO_2 on carbon form speciation

To examine the effect of varying CO_2 inlet concentrations, pH, DIC and ion concentrations on the solubility and speciation of carbon forms in the algal suspension, Visual Minteq (v3.0) was used according as described in Section 3.4.2. pH, nitrate concentrations and DIC were measured as described in Section 3.3.3, 3.3.6, 3.3.7 and 3.3.8 respectively. The concentrations of carbon species with time, across the range of CO_2 inlet concentrations are presented in Table 4-2. The CO_2/H_2CO_3 saturation concentrations which were estimated using Visual Minteq are higher in comparison to those calculated using Henry's Law (0.95, 6.1 and 20 $mg.L^{-1}$ versus 0.67, 4.3 and 15 $mg.L^{-1}$ for the 450, 2900 and 10 000 ppm CO_2 experiments respectively).

At a feed concentration of 450 ppm CO_2 the concentrations of bicarbonate and carbonate are very high due to the abundance of hydroxyl ions available at higher pHs (Equation 2.10, Section 2.5.2.2). As the stock culture was maintained on 1% CO_2 it would take about 4-6 hours for the CCM to become expressed once adapted to the low CO_2 environment (Thielmann *et al*., 1990). According to Pott *et al*., (2009) the *Scenedesmus* sp. used in this study is an active bicarbonate consumer. They demonstrated that, when *Scenedesmus* sp., *Spirulina platensis* and *Dunaliella salina* were supplied solely with bicarbonate, *Scenedesmus* sp. and *S. platensis* had a carbon uptake rate of 4.18 mmol C (g algae)$^{-1}$ h^{-1} whereas *C. vulgaris* took up 2.32 mmol C (g algae)$^{-1}$ h^{-1} and *D. salina* had a carbon uptake of 0.84 mmol C (g algae)$^{-1}$ h^{-1}. Thus, for the 450 ppm CO_2 experiment, *Scenedesmus* sp. should initially not be carbon limited. From day 2 onwards the concentration of the carbon species for the 450 ppm experiment is far lower in comparison to the 2900 and 10 000 ppm experiment (Table 4-2) which explains the lower growth rate (Figure 4.1). The bicarbonate and dissolved CO_2/H_2CO_3 is higher for the 10 000 ppm experiment in comparison to the 2900 ppm experiment for all time points with the exception being the higher bicarbonate concentration on the 7th day for the 2900 ppm condition. Additionally, Figure 4.9 illustrates that the rate of DIC accumulation is fastest for the 10 000 ppm experiment and that the DIC concentration plateaus on day 10 for the 2900 and 10 000 ppm experiment i.e. the algal suspension is saturated with DIC under these conditions.

The aforementioned information suggests that the higher growth rate of the 10 000 ppm experiment is not only due to the faster rate of DIC saturation for this condition but possibly due to a preference of *Scenedesmus* sp. to take up dissolved CO_2/H_2CO_3 rather than bicarbonate. As mentioned in Section 2.2.3.2 of the Literature Review, evidence suggests that the bicarbonate pump of *S. obliquus* is activated by ATP whereas the CO_2 pump is activated by light (Thielmann *et al*., 1990). Hence, usage of the CO_2 pump rather the bicarbonate pump may be the cell's least energetically expensive option i.e. the energy is rerouted to cell growth. Alternatively, each component of the CCM could be affected

differently during the partial expression or deactivation of the CCM of *Scenedesmus* sp. in response to higher DIC concentrations.

Table 4-2: Predicted concentrations of carbon forms in *Scenedesmus* sp. culture as a function of CO_2 inlet concentration and time

Experiment ($ppm\ CO_2$)	Time (Day)	CO_2/H_2CO_3 (g/L)	HCO_3^- (g/L)	CO_3^{2-} (g/L)
450	2	8.00×10^{-4}	6.23	8.05
	4	3.34×10^{-9}	3.96×10^{-9}	6.17×10^{-4}
	7	9.49×10^{-4}	788×10^{-4}	7.90×10^{-4}
2900	2	60.7×10^{-4}	24.2×10^{-4}	13.2×10^{-4}
	4	61.0×10^{-4}	84.2×10^{-2}	56.82×10^{-2}
	7	60.8×10^{-4}	2.52	60.8×10^{-4}
10 000	2	0.02	0.30	5.59×10^{-4}
	4	0.02	1.05	70.9×10^{-4}
	7	0.02	1.29	0.01

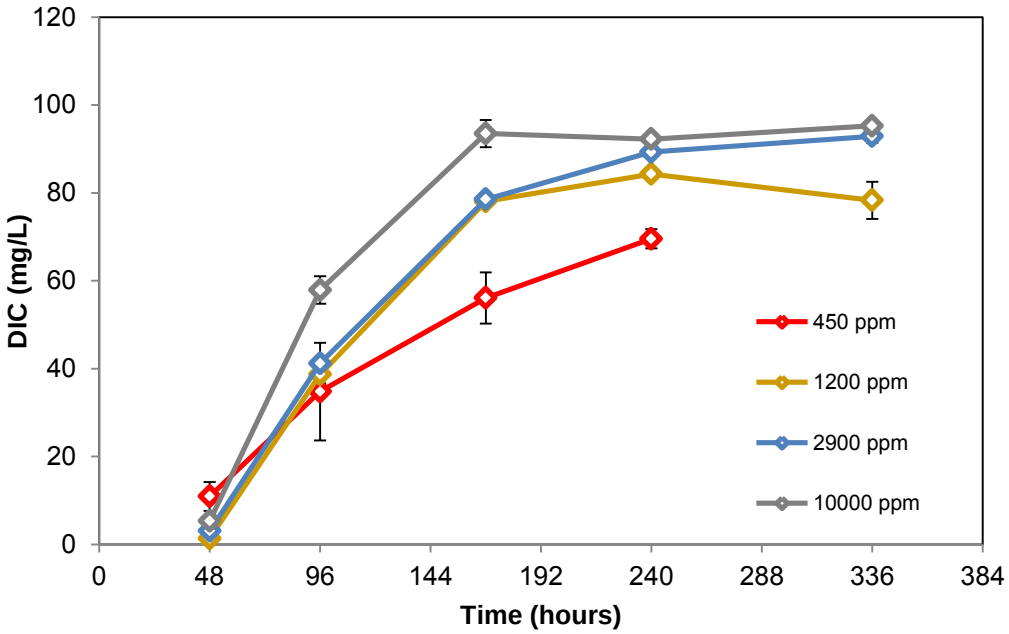

Figure 4.10: Accumulation of DIC in cell-free media as a function of CO_2 inlet concentration

(Error bars represent standard deviations of triplicate readings)

4.6 CO_2 fixation and recovery

Each growth curve was plotted such that an average productivity could be compared in the linear phase of growth across experiments (Figure 4.11). A straight trendline was fitted to each dataset and the slope, which represents the biomass productivity (Q_x), was determined by regression. The productivities were then converted to CO_2 uptake rates and recoveries as described in Section 3.4.3.

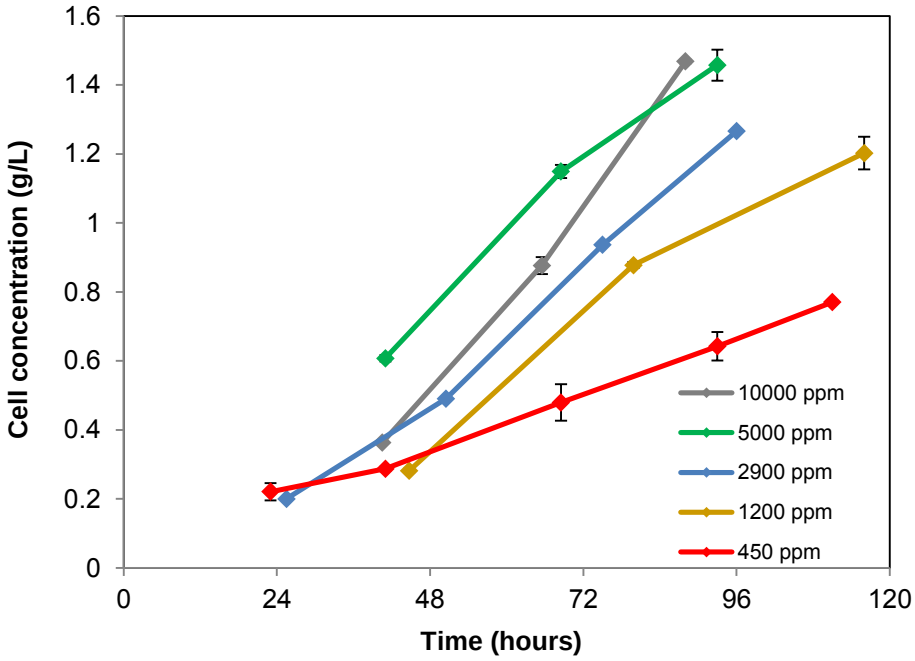

Figure 4.11: Linear-phase growth of *Scenedesmus* sp. as a function of CO_2 inlet concentration

Table 4-3 presents average biomass productivities (Q_x) and R^2 values across all CO_2 inlet concentrations. The maximum average productivity of 23.2 $mg.L^{-1}.hr^{-1}$ for *Scenedesmus* sp. surpasses the maximum average productivity of 13.1 $mg.L^{-1}.hr^{-1}$ for *C. vulgaris* (Langley, 2010). Both species were cultivated under the same operating conditions and using the same cultivation system. For *Scenedesmus* sp. the average productivities increased with higher inlet CO_2 concentrations (Table 4-3), whereas for *C. vulgaris* the maximum average productivity peaked at 3250 ppm CO_2 (Langley, 2010). He determined that the $P_{CO2,CRIT}$ for *C. vulgaris* was about 1200 ppm, as the Q_x increase was only 1.5% from 1200 to 3250 ppm CO_2 while the decrease in CO_2 recovery was substantial.

Table 4-3: Average biomass productivities for *Scenedesmus* sp. cultured with varied CO_2 inlet concentrations

Inlet CO_2 concentration (ppm)	Avg Q_x ($g.L^{-1}.hr^{-1}$)	R^2
450	0.0064	0.994
1200	0.0129	0.969
2900	0.0154	0.992
5000	0.0164	0.985
10000	0.0232	0.995

Table 4-4 presents the CO_2 uptake rates and recoveries across all CO_2 inlet concentrations, calculated based on the biomass productivity and carbon content of *Scenedesmus* sp. The average CO_2 uptake rates increased with higher CO_2 inlet concentrations and concomitant mass transfer rates, while the CO_2 recoveries decreased respectively. The inverse relationship between CO_2 uptake and recovery is displayed in Figure 4.12 and can be explained by the poor solubility of CO_2 in water and the mid-range mass transfer coefficient of the ALRs, for the operating conditions used in this study (Doran, 1995). Hence, use of higher P_{CO2}s is advantageous with respect to CO_2 uptake rates (due to an increase in mass transfer rate) and disadvantageous with respect to CO_2 recovery (excess CO_2 is not utilized). The CO_2 recovery of the ALRs can potentially be improved by increasing the retention time of CO_2 within the culture or by connecting reactors serially. The former could theoretically be achieved by decreasing the gas flow rate, decreasing the average bubble size or increasing the height of the reactor. However, decreasing the gas flow rate would decrease the mass transfer coefficient and lowering the bubble size may impair mixing and would be difficult practically (Langley, 2010). Connecting ALRs in series or increasing their heights requires gas compression and oxygen build-up needs to be taken into account. Due largely to the energetic burden of gas compression, more than 66 ALRs of the laboratory design used in this study (at a gas flow rate of 2 $L.min^{-1}$) would need to be connected in series in order to yield a positive energy balance (Richardson, 2011).

Table 4-4: Average CO_2 uptake rates and recoveries, calculated from biomass productivities, for *Scenedesmus* sp. cultured with varied CO_2 inlet concentrations

Inlet CO_2 concentration (ppm)	Avg. Q_{CO2} ($g.L^{-1}.day^{-1}$)	Avg. CO_2 recovery (%)
450	0.264	36.29
1200	0.533	27.43
2900	0.636	13.55
5000	0.677	8.369
10000	0.959	5.920

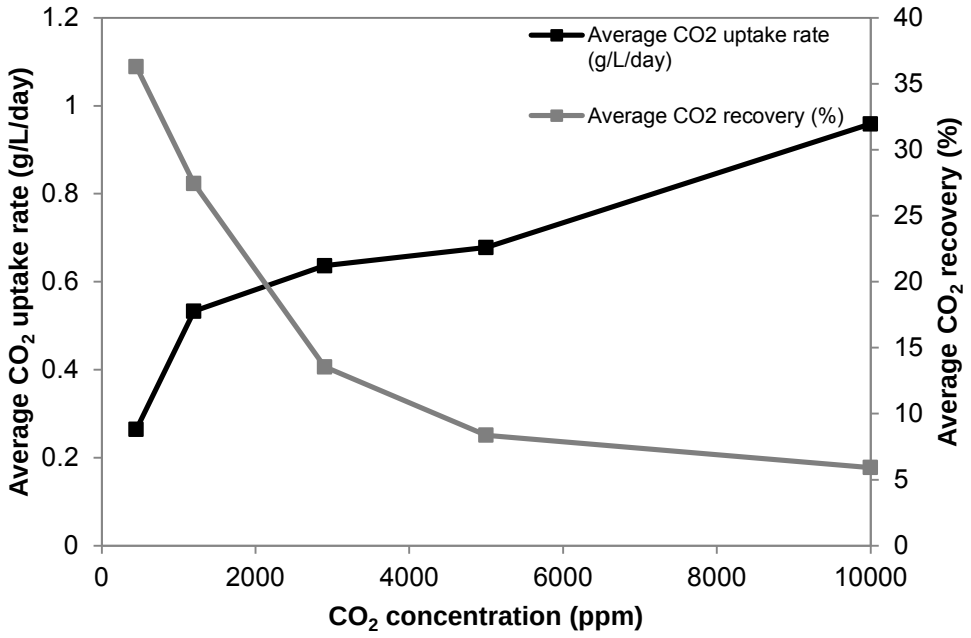

Figure 4.12: Relationship between average CO_2 uptake rate and recovery as a function of CO_2 inlet concentration

An overview of *Scenedesmus* sp. growth and CO_2 fixation and recovery indicators across all CO_2 inlet concentrations is presented in Table 4-5. The maximum cell concentration obtained (X_{max}) increased with higher influent CO_2 concentrations to a maximum of 4.2 g/L for 10 000 ppm. The average μ_{max}[5] was reasonably consistent for the different experiments; the average value was 0.045 hr^{-1} with a standard deviation of 0.003 hr^{-1}. The instantaneous maximum CO_2 recovery[6] calculated from biomass data (CR (X)) and offgas data (CR (OG)) are displayed to provide an indication of the maximum potential for CO_2 capture by *Scenedesmus* sp. The maximum CRs (X) correlate poorly to the maximum CO_2 recoveries calculated using offgas data and reasonably well to the average CO_2 recoveries (Table 4-4). It should be noted that the 5000 and 10 000 ppm experiments were conducted in another laboratory with a more technologically advanced offgas analyser using continuous data logging which resulted in data of improved reproducibility and accuracy.

Table 4-5: Data collated for *Scenedesmus* sp. cultured with varied inlet CO_2 concentrations

$[CO_2]$	**X_{max}**	**Max. Avg. μ_{max}**	**Instantaneous Max. CR (X)**	**Instantaneous Max. CR (OG)**	**Instantaneous Max. Q_{CO2}**
(ppm)	**($g.L^{-1}$)**	**(hr^{-1})**	**(%)**	**(%)**	**($g.L^{-1}.day^{-1}$)**
450	2.06 *(day 13)*	0.0449	70 ± 3.99 *(day 6)*	54.00 ± 2.67 *(day 5)*	0.467 *(day 6)*
1200	2.5 *(day 12)*	0.0428	43 ± 6.95 *(day 5)*	22.55± 11.99 *(day 5)*	0.98 *(day 5)*
2900	2.85 *(day 13)*	0.0427	20 ± 1 *(day 6)*	14.12± 2.90 *(day 6)*	0.89 *(day 6)*
5000	3.67 *(day 14)*	0.0472	12.45 *(day 6)*	6.951 *(day 3)*	1.02 *(day 6)*
10 000	4.29 *(day 11)*	0.0502	8 *(day 6)*	5.399 *(day 6)*	1.30 *(day 6)*

[5] average μ_{max} was taken as the maximum gradient value which was determined by the regression of a straight line drawn through three consecutive data points of the plot of lnX as a function of time during the first three days of growth

[6] The instantaneous max CO_2 recovery was calculated using Equation 3.12 and 3.13, and was taken as the average value for duplicate runs (except for the 10 000 ppm CO_2 condition)

4.7 Comparison of *Scenedesmus* sp. to other microalgal species

To compare the capability of CO_2 fixation of *Scenedesmus* sp. against other species, a literature review was performed and the results presented in Table 4-6. *Scenedesmus* sp.'s instantaneous maximum CO_2 uptake rate of 1.3 $g.L^{-1}.day^{-1}$ is relatively high in comparison to other Q_{CO2} data from literature, with the exception of Q_{CO2}s reported by Chiu *et al*. (2008), Douskava *et al*. (2009), Keffer and Kleinheinz (2002) and Martinez *et al*. (2010) (Table 4-6). Chiu *et al*. (2008) conducted their experiments using a semi-continuous culture mode, Douskava *et al*. (2009) used a threefold higher light intensity, Keffer and Kleinheinz (2002) used a fed-batch culture mode and Martinez *et al*. (2010) optimized CO_2 fixation with a factorial design, thus direct comparisons cannot easily be made. Douskava *et al*. (2009) and Martinez *et al*. (2010) did not report CO_2 recoveries. Chiu *et al*. (2008) reported a CO_2 recovery of 16% and a Q_{CO2} of 17.19 $g.L^{-1}.day^{-1}$ for a semi-continuous culture of a marine *Chlorella* sp. supplied with 15% CO_2. Keffer and Kleinheinz (2002) report a Q_{CO2} of 1.53 $g.L^{-1}.day^{-1}$ and a CO_2 recovery of 60% for a culture of *C. vulgaris* supplied with 0.0185% CO_2 in inlet gas.

Chiu *et al*. (2009) suggest using a porous centric-tube column, a high density culture and a low flow rate to improve CO_2 recoveries. A gas flow rate of 0.625 vvm was used in this study which is the second highest after Douskava *et al*., 2009 (Table 4-6). Although lowering the gas flow rate would improve the CO_2 recovery it would also decrease the mass transfer as sparging provides the function of mixing and CO_2 provision in the ALRs used in this study. Methods of obtaining a high density culture are discussed in Chapter 5.

Table 4-6: Comparison of microalgal species ability to fix CO_2.

Blue font indicates information which is taken from Wang *et al*., 2008. Black font indicates information which is assembled and modified from multiple references by this author. Bracketed volumes are working volumes.

Microalga	CO_2 (%)	T (°C)	Q_x ($g.L^{-1}.day^{-1}$)	Q_{CO2} ($g.L^{-1}.day^{-1}$)	Notes	Vol (L)	Gas flow rate (vvm)	CO_2 Recovery (%)	References
Aphanothece microscopica nagelli	15	35	0.770	0.0145	ALR- simple operation, 150 $\mu mol.m^{-2}.s^{-1}$	3	1 vvm	-	Jacob-Lopez *et al*., 2009a
Botryococcus braunii	–	25–30	1.100	>1.000	Accumulating hydrocarbon	-	-	-	Murakami and Ikenouchi, 1997
Chlorella sp.	air	26	0.169	-	Semi-continuous culture mode, 300 $\mu mol.m^{-2}.s^{-1}$	0.8	0.25 vvm	-	Chiu *et al*., 2008
"	2	"	0.874	7.830	"	"	"	58	"
"	5	"	0.808	9.480	"	"	"	27	"
"	10	"	-	13.98	"	"	"	20	"
"	15	"	-	17.19	"	"	"	16	"
Chlorella sp. *NCTU-2*	10	26	0.610	-	Semi-continuous culture mode (1/4), porous centric-tube photobioreactor, 300 $\mu mol.m^{-2}.s^{-1}$	(4)	0.25 vvm	63	Chiu *et al*., 2009
Chlorella sp. *UK001*	15	35	-	>1.000	-	-	-	-	Murakami and Ikenouchi, 1997
Chlorella sp.	6-8	31.2-33.2	0.116 - 0.137	-	Flue gas, open solar thin-layer photobioreactor (6 mm), 859-1750 $\mu mol.m^{-2}.s^{-1}$, fed-batch	400	varied	10-50	Doucha *et al*., 2005
C. vulgaris	0.012	25	0.307	0.497	ALR, 300 $\mu mol.m^{-2}.s^{-1}$	3.2	0.625	26	Langley, 2010
C. vulgaris	air	25	0.040	0.075	Watanabe's medium	-	-	-	Scragg *et al*., 2002
C. vulgaris	air	25	0.024	0.045	Low-N medium	-	-	-	Scragg *et al*., 2002
C. vulgaris	10-13	30	2.500	4.400	lower p.p of O_2 than control, Column Reactors, 1150 $\mu E.m^{-2}.s^{-1}$	0.3	0.83 vvm	-	Douskava *et al*., 2009
C. vulgaris	10	25	0.105 ±0.020	-	BG11 medium, 150 $\mu mol.m^{-2}.s^{-1}$	-	0.3 vvm	56-74	Yoo *et al*., 2010
C. vulgaris	0.185	-	-	1.530	Bubble column reactor, fed-batch	(2)	-	60	Keffer and Kleinheinz, 2002
C. vulgaris sp. *LEB-104*	5	30	0.310	0.252	Modified Bristol media, 12 hr light cycle	(8),11	-	-	Sydney *et al*., 2010

Microalga	CO_2 (%)	T (°C)	Q_x ($g.L^{-1}.day^{-1}$)	Q_{CO2} ($g.L^{-1}.day^{-1}$)	Notes	Vol (L)	Gas flow rate (vvm)	CO_2 Recovery (%)	References
Chlorococcum littorale	40	30	-	1.000	BG11 medium, 150 µmol.$m^{-2}.s^{-1}$	-	0.3 vvm	-	Murakami and Ikenouchi, 1997
Chlorella kessleri	18	30	0.087	0.163	Modified Bristol media, 12 hr light cycle	-	0.3 vvm for 15 mins. hr^{-1} during light phase	7-13	de Morais and Costa, 2007a
Chlorogeopsis	5	50	-	0.020	16 hr light cycle, 200 µmol.$m^{-2}.s^{-1}$	0.2	0.002 vvm	4-9	Ono, 2007
Dunaliella	3	27	0.170	0.313	High salinity, β-carotene	-	-	27-38	Kishimoto *et al*., 1994
Haematococcus pluvialis	16–34	20	0.076	0.143	Commercial scale, outdoor	-	-	-	Huntley and Redalje, 2007
Scenedexmus sp. *KCTC AG20831*	5.5	25	0.203	-	-	-	-	7-17	Yoo *et al*., 2010
S. obliquus	Air	-	0.009	0.016	Wastewater, outdoor, winter	-	-	-	Gomez-Villa *et al*., 2005
S. obliquus	Air	-	0.016	0.031	Wastewater, outdoor, summer	-	-	-	Gomez-Villa *et al*., 2005
S. obliquus	18	30	0.140	0.260	12 hr light cycle, 45 µmol.$m^{-2}.s^{-1}$	(1.8), 2	0.3 vvm for 15 mins. hr^{-1} during light phase	27.14-37.9	de Morais and Costa, 2007b
Spirulina sp.	12	30	0.220	0.413	12 hr light cycle, 45 µmol.$m^{-2}.s^{-1}$	(1.8), 2	0.3 vvm for 15 mins. hr^{-1} during light phase	-	de Morais and Costa, 2007b
Synecoccus aquilitis	-	-	-	1.500	mu increased from 0.19 hr^{-1} to 0.23 hr^{-1} with optimization	5	-	-	Murakami and Ikenouchi ,1997
Synechocystis sp.	10	35.3	-	2.070	Semi-continuous mode, bubble column, 686 µE.$m^{-2}.s^{-1}$	(1)	varied	-	Martinez *et al*., 2010

4.8 Conclusions

- The characteristic time analysis for the 0.045% CO_2 experiment revealed that the initial growth limitation was due to physiological constraints. Above a cell concentration of approximately 0.5 g/L, growth became limited by CO_2-transfer. This limitation occurred at higher cell concentrations for higher CO_2 concentrations in the inlet gas
- The linear biomass productivities and associated CO_2 uptake rates increased with increasing CO_2 partial pressures in the range of 450 to 10 000 ppm CO_2 in the ALRs, as higher CO_2 partial pressures drive higher mass transfer rates for CO_2, reducing limitations associated with active gas transfer
- Accordingly, CO_2 recoveries decreased in the range of 36 to 6% with increasing CO_2 partial pressures. The excess CO_2 served to drive mass transfer and remained largely unutilized
- The higher specific growth rate of *Scenedesmus* sp. maintained at 1% CO_2 correlated to a lower culture pH of below 8, compared with pH 8.5 to 9 for 0.12 to 0.5% CO_2 and pH 10 for 0.045% CO_2. Based on the speciation of carbon forms the better performance of *Scenedesmus* sp. at 1% CO_2 can potentially be attributed to a preference for uptake of dissolved CO_2 over bicarbonate
- The maximum average CO_2 uptake rate of 0.96 $g.L^{-1}.day^{-1}$ compared favourably to literature values with a few notable exceptions. These exceptions occurred under conditions with increased light supply or an increased retention time for the CO_2 gas
- Higher starting concentrations of $NaNO_3$ (1450 and 2000 $mg.L^{-1}$) failed to improve growth which indicates that nitrate was not the primary limiting reagent

4.9 Recommendations

- Where *Scenedesmus* sp. is cultured on air it is recommended that pH is controlled as higher pHs shift carbon speciation to carbonate which is not readily taken up by *Scenedesmus* sp.
- As the higher CO_2 liquid concentrations which are beneficial to growth can only be obtained at higher P_{CO2}s it is recommended that alternate methods of CO_2 delivery be investigated
- The postulation that *Scenedesmus* sp. takes up CO_2 in preference to bicarbonate should be verified through a fundamental study. This study should also quantify the potential for *Scenedesmus* sp. to utilize bicarbonate as this will inform whether *Scenedesmus* sp. should be

cultured in the integrated system developed by Langley (2010). If the above postulation is found to be true, then the high pH values associated with scrubbing CO_2 in the integrated system would result in low free CO_2 concentrations and would impede CO_2 uptake

Chapter 5 : Optimization of CO_2 utilization by *Scenedesmus*

5.1 Introduction

In this chapter the optimization of CO_2 utilization by *Scenedesmus* sp. is considered. This requires an examination of its growth-limiting factors. In Chapter 4, the effect of CO_2 concentration on growth was examined. The average maximum growth rate, CO_2 uptake rate and cell concentration occurred at the maximum CO_2 inlet concentration, 10 000 ppm CO_2 (Section 4.5).

To exclude the possibility of nutrient limitations a fed-batch nutrient culture mode was employed in experiments in this chapter. Additionally, considering that the light intensity provided is within a low to moderate range it was expected that light becomes limiting after a certain cell concentration has been attained. Experiments were therefore conducted with additional lighting, where 2 sets of lights were used instead of 1 set as in the standard operation. CO_2 concentrations of 0.5 and 1% CO_2 were used to ascertain whether the higher Q_{CO2s} at 1% CO_2 could justify the lower CO_2 recoveries. Thus, in this chapter the effect of CO_2, nutrient and light provision on algal growth is investigated using an experimental design to allow the impact of individual factors and their interactions to be considered.

5.2 Experimental Design

Figure 5.1 displays the 2^3 factorial design for this portion of the study. Each factor (A, B and C) was varied by two levels. CO_2 (A) was varied from 5000 to 10 000 ppm. Light intensity (B) was varied from 225 $\mu mol.m^{-2}.s^{-1}$ (1X Light Intensity) to 560 $\mu mol.m^{-2}.s^{-1}$ (2X Light Intensity). The nutrient regime (C) was either fed-batch or standard. For experiments with two sets of lights (2X Light Intensity) the second set of lights was switched on after 48 hours in order to avoid photoinhibition. For experiments operated with a fed-batch culture mode, nutrient aliquots were added on approximately the 48^{th}, 120^{th}, 192^{nd} and 264^{th} hour. Each nutrient aliquot consisted of 10% (w/v) of each component of the Modified Bold 3NBBM media (Appendix A). Temperature was controlled to 25 °C ± 1 °C with a chiller (Model LTD6G, Grant Instruments, England).

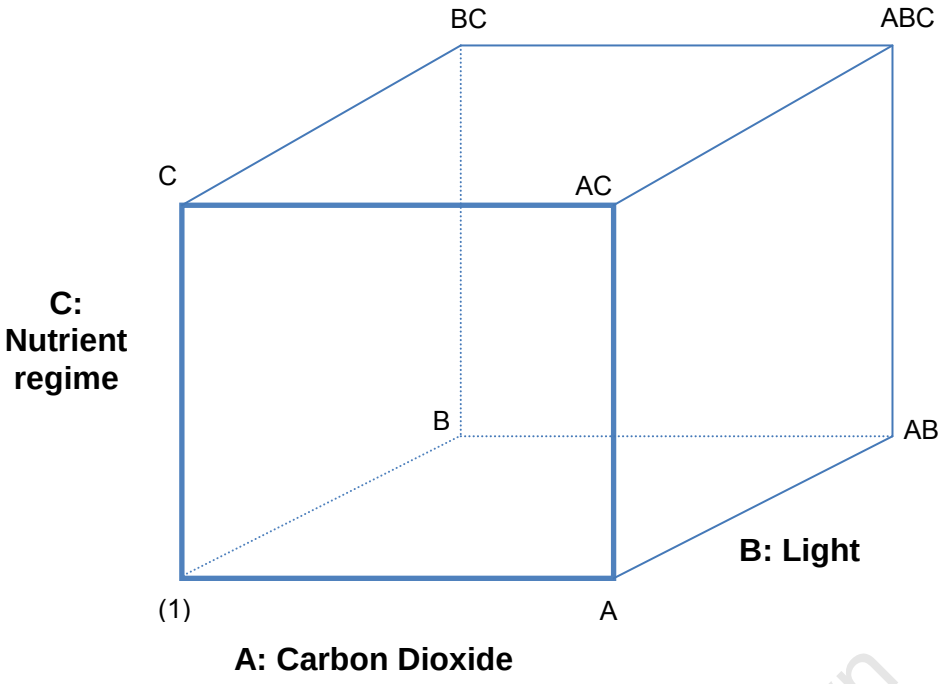

Figure 5.1: 2^3 Factorial Design for optimization of CO_2 utilization by *Scenedesmus* sp.

5.3 Effects of varying light, nutrient culture mode and CO_2 concentration on *Scenedesmus*

5.3.1 Growth rates, biomass productivities and biomass yields

To study the effects of the experimental conditions on biomass production, *Scenedesmus* sp. was cultured at 5000 and 10 000 ppm CO_2 in ALRs for 336 hours at both high and low conditions of nutrients and light. Table 5-1 presents the growth indicators for *Scenedesmus* sp. at 5000 ppm CO_2[7]. The maximum specific growth rates were lower for the 2X Light intensity, Fed-batch and 1X Light intensity runs than the 2X Light intensity and 1X Light intensity, Fed-batch runs. Due to equipment limitations all four runs could not be conducted simultaneously, the 2X Light intensity, Fed-batch and 1X Light intensity runs were conducted prior to the 2X Light intensity and 1X Light intensity, Fed-batch runs. Hence, the difference in μ_{max} was likely due to a difference in the physiological state of the inocula. The maximum cell concentration of 4.98 $g.L^{-1}$ was obtained for the 2X Light intensity, Fed-batch condition followed closely by 4.80 $g.L^{-1}$ of the 2X Light intensity condition. In Figure 5.2 the

[7]. These indicators were obtained by the methods used in Chapter 4, R^2 values for regressions for the 5000 and 10 000 ppm conditions ranged from 0.9782-0.9987.

growth profiles of *Scenedesmus* sp. at 5000 ppm CO_2 are given. The growth rate at 5000 ppm CO_2 inlet gas with no additional nutrients and standard light intensity (control) was the lowest. The growth rate for the 2X Light intensity condition initially superseded the growth of all other runs and attained its maximum cell concentration 118 hours earlier than all other runs.

Table 5-1: Data collated for *Scenedesmus* sp. cultured with 5000 ppm CO_2 under varying light and nutrient regimes

Factor	Experimental condition	Avg. μ_{max}(hr^{-1})	Avg. Q_x ($mg.L^{-1}.hr^{-1}$)	X_{max} ($g.L^{-1}$)
BC	2X Light intensity, Fed-batch	0.041	30.4	4.98
B	2X Light intensity	0.065	37.5	4.80
C	1X Light intensity, Fed-batch	0.061	22.3	4.47
(1)	1X Light intensity	0.040	11.9	3.79

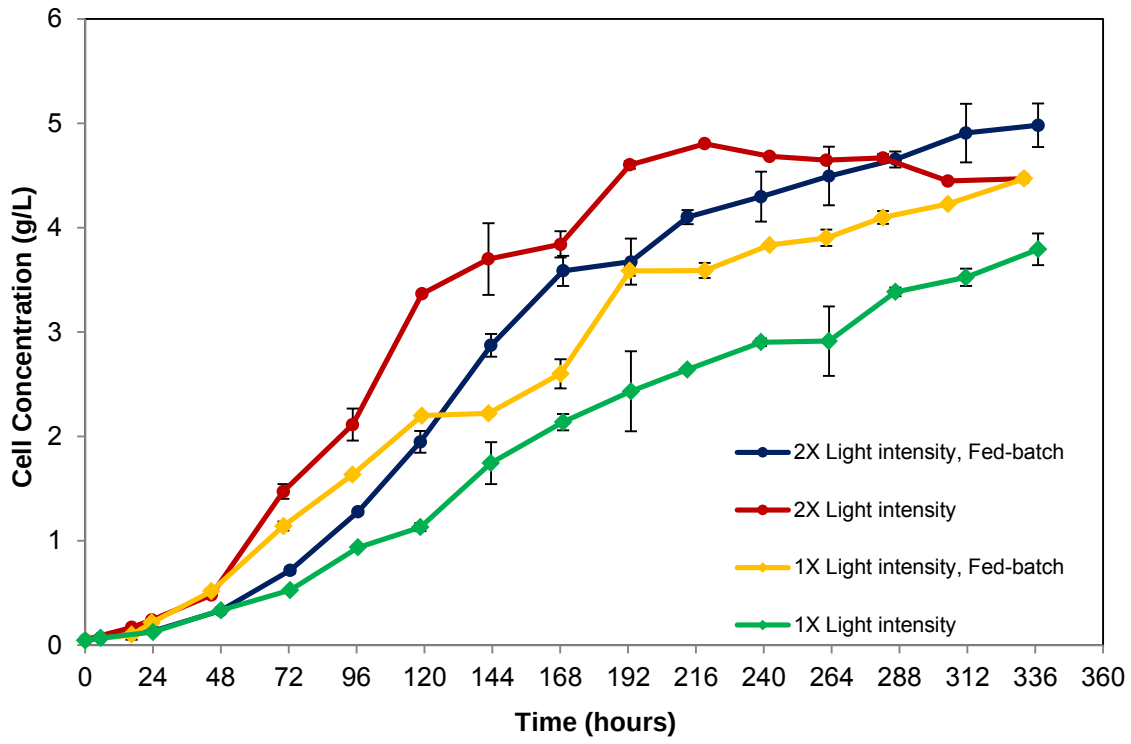

Figure 5.2: Growth curves of *Scenedesmus* sp. cultured in ALRs with 5000 ppm CO_2 (0.5%) at 25 ± 1°C under varying light and nutrient regimes

(Circles represent 2X Light intensity, diamonds represent 1X Light intensity, error bars represent standard deviations for absorbance readings. Extra light was introduced after 48 hours. Nutrients were supplied on approximately the 48th, 120th, 192nd and 264th hour)

Table 5-2: Data collated for *Scenedesmus* sp. cultured with 10 000 ppm CO_2 under varying light and nutrient regimes

Factor	Experimental condition	Avg. μ_{max} (hr^{-1})	Avg. Q_x ($mg.L^{-1}.hr^{-1}$)	X_{max} ($g.L^{-1}$)
ABC	2X Light intensity, Fed-batch	0.0495	29.3	5.32
AB	2X Light intensity	0.0535	44.6	5.09
AC	1X Light intensity, Fed-batch	0.0511	18.6	3.96
A	1X Light intensity	0.0502	23.7	4.29

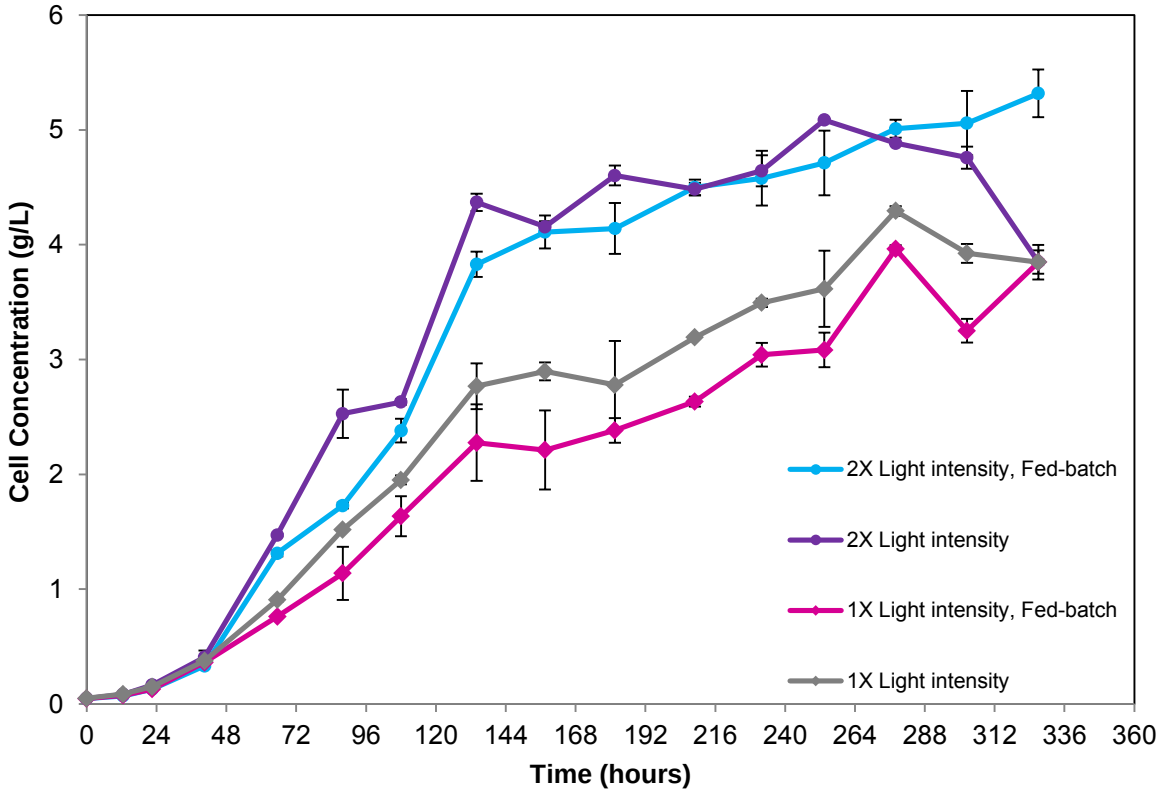

Figure 5.3: Growth curves of *Scenedesmus* sp. cultured in ALRs with 10 000 ppm CO_2 (1%) at 25 ± 1°C under varying light and nutrient regimes

(Circles represent 2X Light intensity, diamonds represent 1X Light intensity and error bars represent standard deviations for absorbance readings. Extra light was introduced after 48 hours. Nutrients were supplied on approximately the 48th, 120th, 192nd and 264th hour)

Table 5-2 presents the growth indicators for the 10 000 ppm CO_2 experiment. The maximum specific growth rates were similar for all runs. The maximum cell concentration of 5.32 $g.L^{-1}$ was obtained for the 2X Light intensity, Fed-batch condition followed closely by 5.09 $g.L^{-1}$ of the 2X Light intensity condition. The growth profiles of *Scenedesmus* sp. at 10 000 ppm CO_2 with varying light and nutrient regimes are presented in Figure 5.3. The rate of growth for the 1X Light intensity, Fed-batch condition was the lowest. The rate of growth for the 2X Light intensity condition superseded the growth of all other runs until the 254th hour whereupon it decreased.

5.3.2 pH and Dissolved Inorganic Carbon

The pH profiles of *Scenedesmus* sp. at 5000 ppm CO_2 under varying experimental conditions are presented in Figure 5.4. The pH curves for each condition generally fit the trend of the growth curves. The pH of *Scenedesmus* sp. when cultured with the 2X Light intensity, Fed-batch condition is higher than when cultured with the 2X Light condition during the period of growth from the 144th to the 263rd hour, as the growth rate for the 2X Light condition slows down during this time period whereas the growth rate of the 2X Light intensity, Fed-batch condition increases (Figure 5.2, Section 5.3.1).

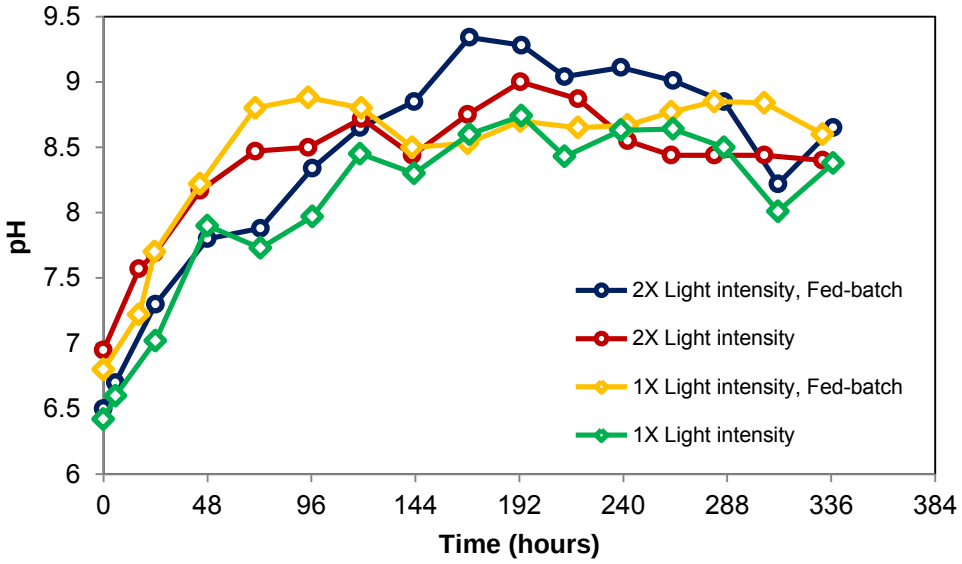

Figure 5.4: pH profiles of *Scenedesmus* sp. cultured in ALRs with 5000 ppm CO_2 (0.5%) at 25 ± 1°C as a function of varying light and nutrient regimes

The pH profiles of *Scenedesmus* sp. at 10 000 ppm CO_2 under varying experimental conditions are presented in Figure 5.5. The pH fluctuates closely around 8 for all conditions. All values (except one)

are lower than 8.3 (equivalence point of bicarbonate), hence DIC would occur predominantly as bicarbonate and to a lesser extent CO_2.

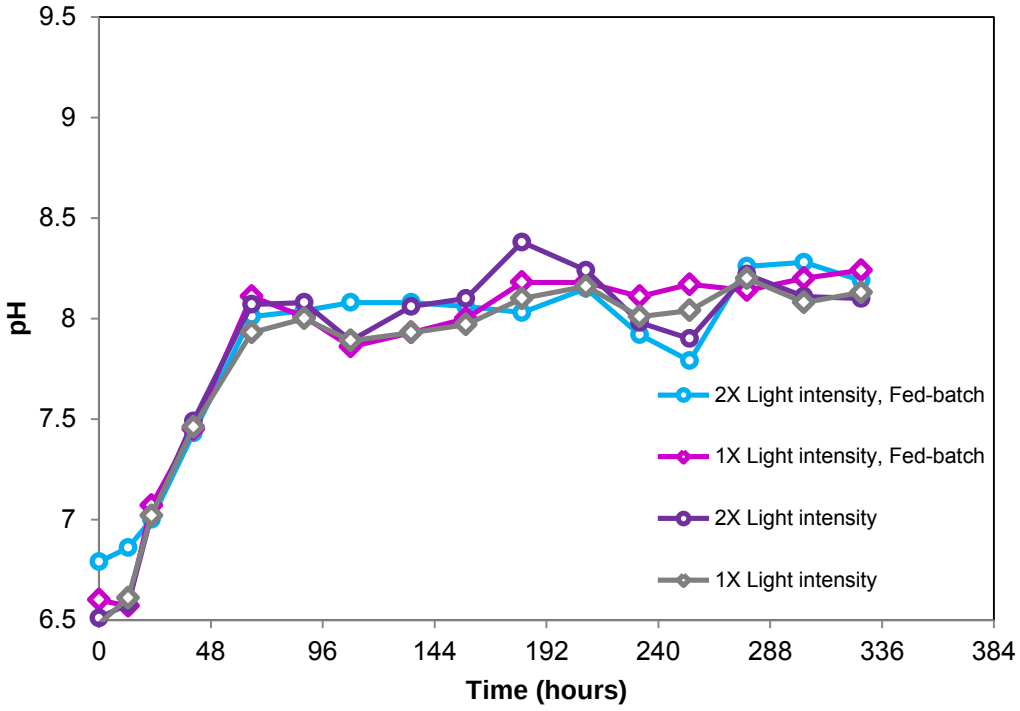

Figure 5.5: pH profiles of *Scenedesmus* sp. cultured in ALRs with 10 000 ppm CO_2 (1%) at 25 ± 1°C as a function of varying light and nutrient regimes

To determine the effect of higher light intensities and nutrient concentrations on the distribution and concentration of carbon forms, DIC was quantified as described in Section 3.3.8. The DIC accumulation over time for each experimental condition at 10 000 ppm CO_2 is displayed in Figure 5.6. Considering that the inoculum of *Scenedesmus* sp. is in log phase and that the cellular capacity for algal carbon storage is limited, the availability of carbon as DIC should be correlated with the patterns of growth (Borchardt, 1996). For the conditions where extra light was provided, the rate of DIC accumulation is greater. The rate of growth was initially higher when extra light was provided (during the period between 48 and 144 hours) which implies that the CO_2 uptake rate is greater and that the CO_2 concentration in the bulk liquid would be lower (Figure 5.3, Section 5.3.1). Subsequently, the CO_2 concentration driving force would be greater which would be expected to increase dissolution rates (Equation 2.12, Section 2.5.2.2). The effect of nutrient addition on CO_2 dissolution is discussed in Section 5.3.6.

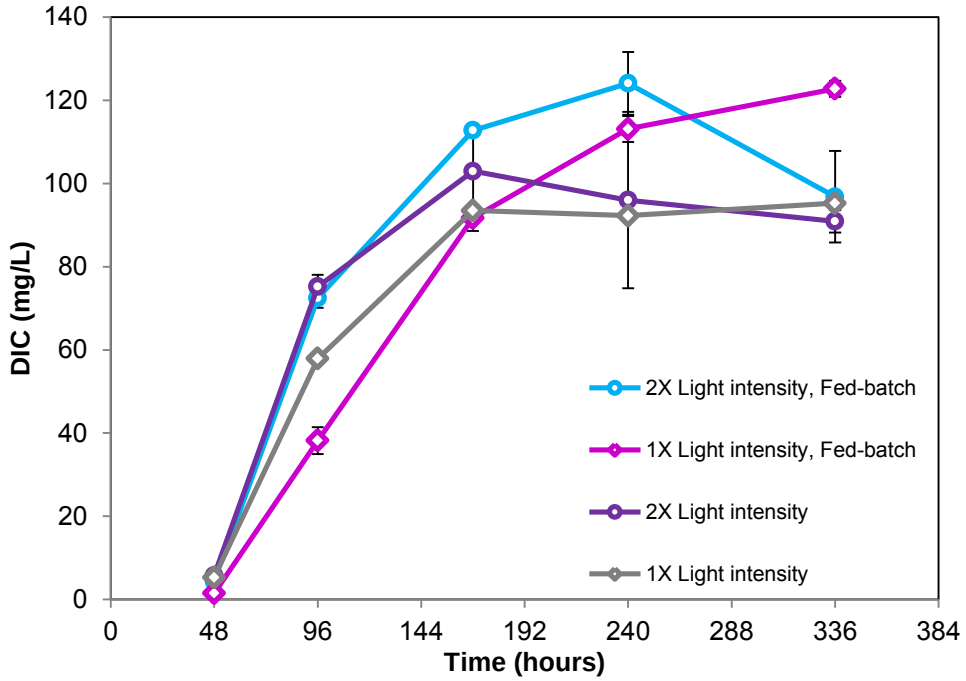

Figure 5.6: Accumulation of DIC in cell-free media as a function of varying light and nutrient regimes at 10 000 ppm CO_2

(Circles represent 2X Light intensity, diamonds represent 1X Light intensity, error bars represent standard deviations for triplicate DIC readings. Extra light was introduced after 48 hours. Nutrients were supplied on approximately the 48th, 120th, 192nd and 264th hour)

5.3.3 Light intensities

As the availability of light is critical to the growth of algae, the extent of light attenuation as a function of cell concentration and distance from light source was modelled using an empirical light distribution model as outlined in Section 3.4.4. This is graphically represented in Figure 5.7 for *Scenedesmus* sp. cultured at 10 000 ppm CO_2 at 1X Light intensity. Interestingly, even at the lowest cell concentration of 0.05 g.L^{-1}, the light intensity experienced by an algal cell travelling within the draft tube of the ALR is only about 85% of the incident light intensity. After 134 hours of growth at 10 000 ppm CO_2, 1X Light intensity the cell concentration increases beyond 2.7 g.L^{-1} whereupon the light intensity penetration in the draft tube tends to zero (Figure 5.3 and 5.7).

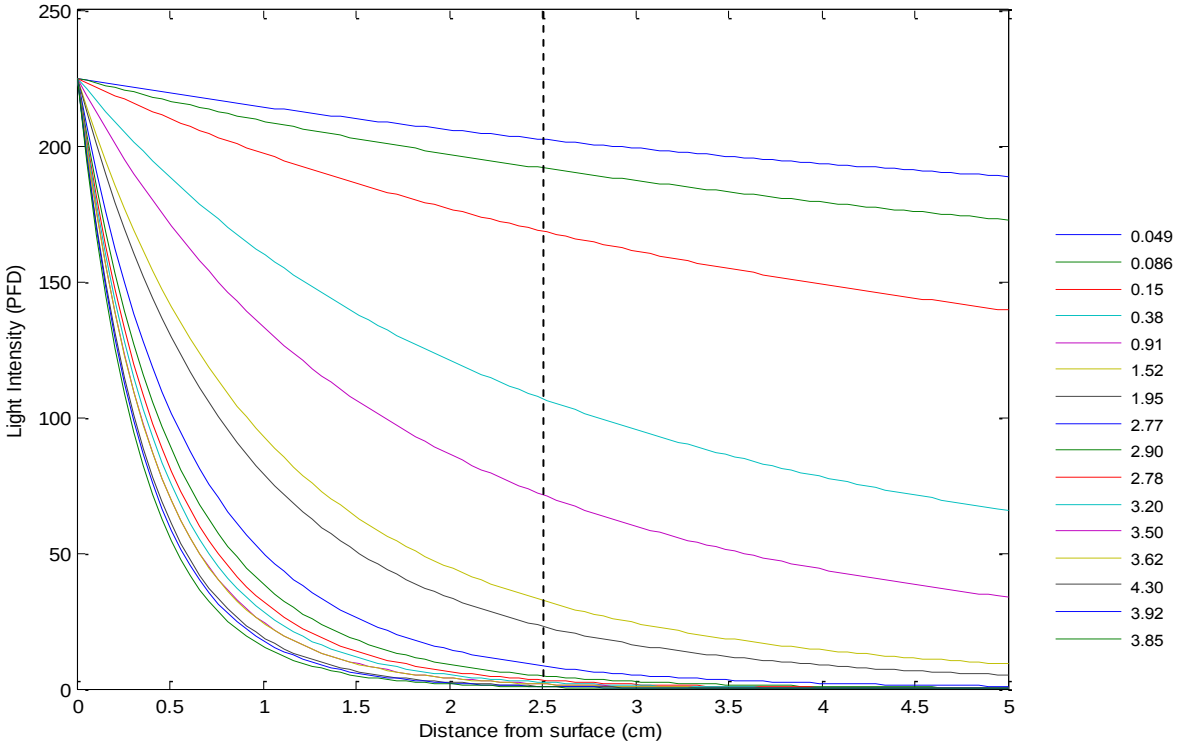

Figure 5.7: Attenuation of modelled light intensity with increase in distance from the illuminated ALR surface as a function of cell concentration

(Legend represents cell concentrations (g/L) of *Scenedesmus* sp. cultured with 10 000 ppm CO_2 and 1X Light intensity; 5 cm represents the centre of the ALR and the region to the right of the dotted line marks the location of the draft tube)

Figure 5.8 and 5.9 display the predicted light intensities relating to the range of cell concentrations at each growth condition at 5000 and 10 000 ppm CO_2 respectively. The average light irradiance (PFD) decays exponentially with the increasing cell concentration. The light profile is very similar for the Standard and Fed-batch conditions. When *Scenedesmus* sp. was cultivated at 5000 ppm CO_2 with high lights and high nutrients it was less responsive to the extra light provided than for the 2X Light intensity condition alone. This is reflected by the spike of the blue line in Figure 5.8. This was not the case when *Scenedesmus* sp. was cultivated at 10 000 ppm CO_2, as growth profiles for the 2X Light intensity condition and the 2X Light intensity, Fed-batch condition mirrored each other (Figure 5.9).

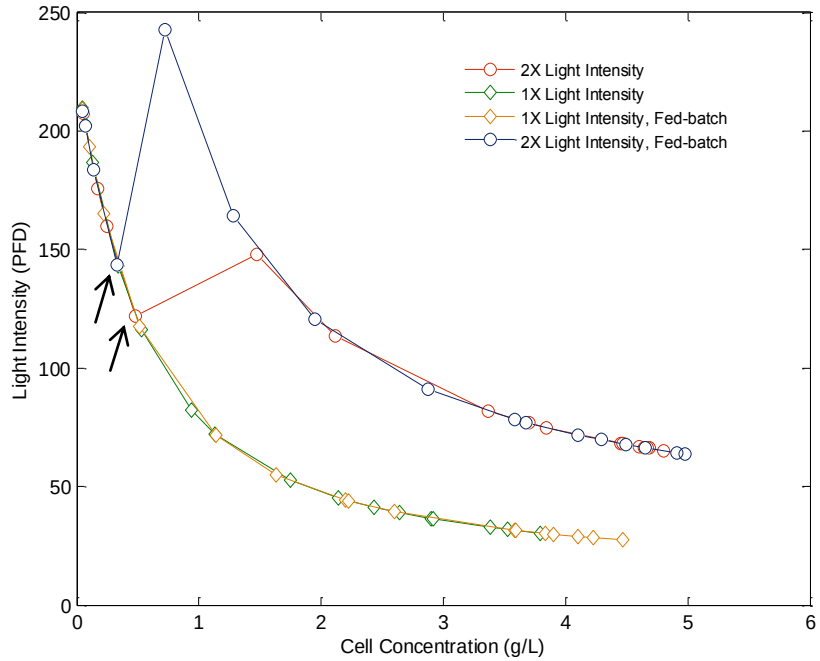

Figure 5.8: Attenuation of modelled light intensity in ALR with increasing cell concentrations of *Scenedesmus* sp. cultured at each experimental condition at 5000 ppm CO_2

(Arrows indicate the point at which extra light was introduced. Circles represent 2X Light intensity, diamonds represent 1X Light intensity)

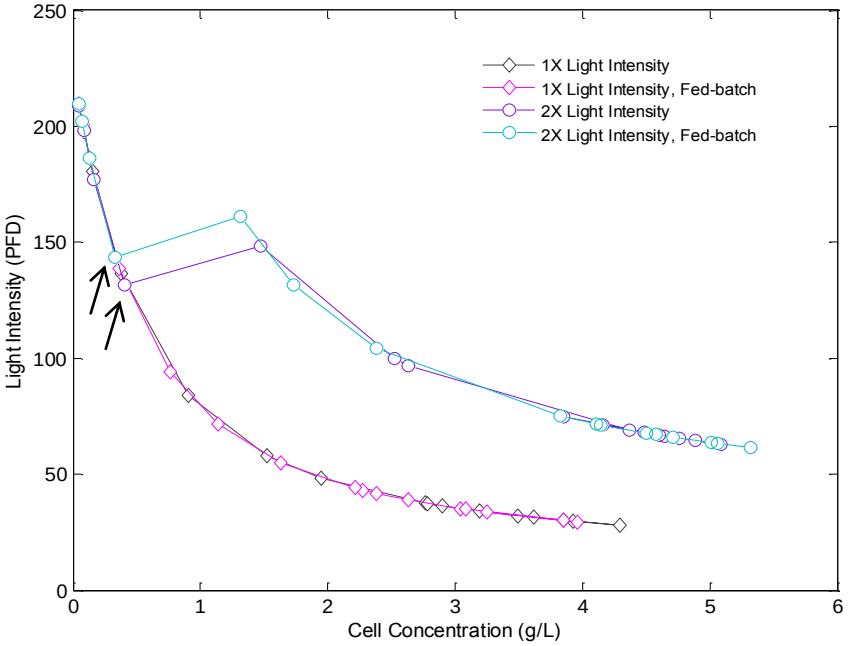

Figure 5.9: Attenuation of modelled light intensity in ALR with increasing cell concentrations of *Scenedesmus* sp. cultured at each experimental condition at 10 000 ppm CO_2

(Arrows indicate the point at which extra light was introduced. Circles represent 2X Light intensity, diamonds represent 1X Light intensity)

5.3.4 Pigment content

To study the effect of varying light intensity and nutrient concentration on the formation and distribution of pigments, a spectrophotometric method of pigment quantification was used as described in Section 3.3.10. Pigment content was determined as the sum of the chlorophyll *a*, chlorophyll *b* and carotenoid (xanthophylls and carotenes) concentrations, expressed relative to cell concentration (µg.mL^{-1} pigment/ µg.mL^{-1} cell concentration). Pigment content varied between 0.87 and 4.5%, which is within the 0.1 to 9.7% range reported in the literature (Griffiths *et al.*, 2011b; Nicholls and Dillon, 1978). Figure 5.10 illustrates that Chlorophyll *a* formed the greatest proportion of total pigment content at the 10 000 ppm CO_2, 2X Light intensity condition. This was observed across all experimental conditions.

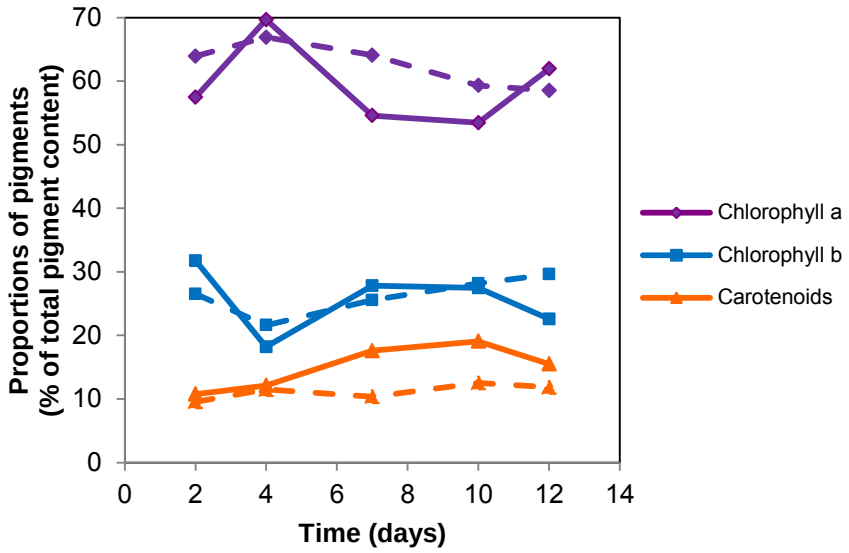

Figure 5.10: Proportions of pigments of *Scenedesmus* sp. with time

(Solid line represents *Scenedesmus* sp. when grown at 1% CO_2 with 2X Light intensity. Extra light was introduced on day 3. Dashed line represents *Scenedesmus* sp. when grown at 1% CO_2 with the fed-batch nutrient regime)

Figure 5.11 and 5.12 display the total pigment content for the 5000 and 10 000 ppm CO_2 experiments respectively. The specific pigment content for the 5000 ppm CO_2 conditions was generally higher than the 10 000 ppm CO_2 conditions (Figure 5.10 and Figure 5.11). The general trend in pigment content of the biomass under experimental conditions (after exposure to higher lights and nutrients, day 4 to 12) listed in decreasing order is 1X Light intensity, Fed-batch; 2X Light intensity, Fed-batch; 1X Light intensity and 2X Light intensity. The exception for this is the 1X Light intensity condition at 5000 ppm CO_2.

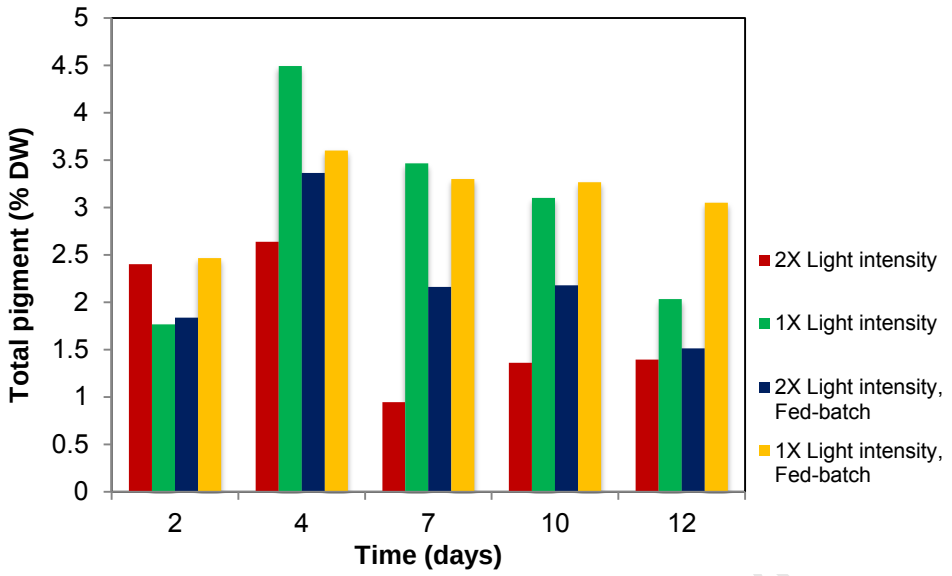

Figure 5.11: Concentration of pigments of *Scenedesmus* sp. cultured with 5000 ppm CO_2, in response to varying light and nutrient regimes

(Extra light was introduced on day 3 and extra nutrients were provided on day 3, 6, 9 and 12)

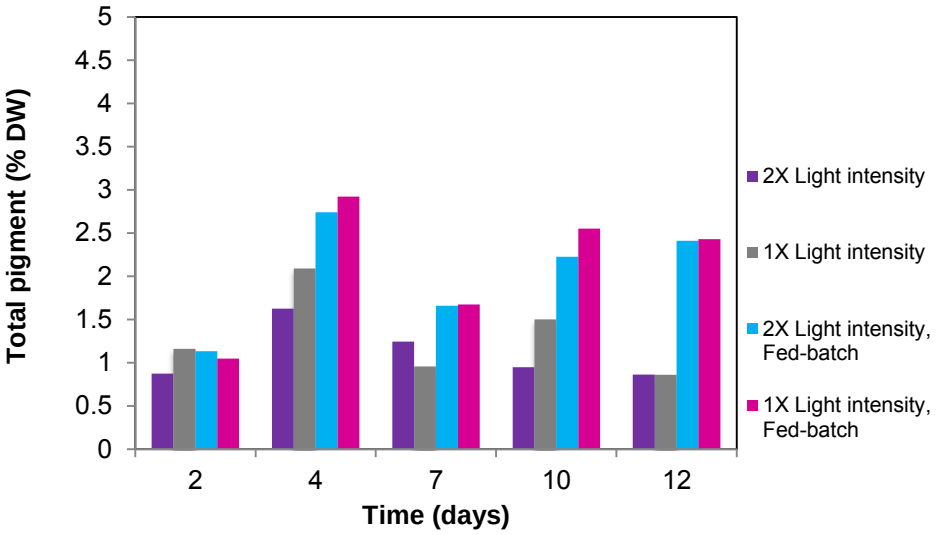

Figure 5.12: Concentration of pigments of *Scenedesmus* sp. cultured with 10 000 ppm, in response to varying light and nutrient regimes

(Extra light was introduced on day 3 and extra nutrients were provided on day 3, 6, 9 and 12)

The trend suggests that the additional nutrients provided during the Fed-batch nutrient regime are utilized to form pigments. Also, it was visually observed that the Fed-batch cultures were bottle-green whereas the 2X Light intensity cultures were khaki-green, at the same time point. Figure 5.13A displays the structures of chlorophyll *a* and *b* which are composed of the elements C, H, O, Mg and N; these are major elements that are supplied in the 3NBBM media (Appendix A). Additionally, the trend suggests that when *Scenedesmus* sp. was grown with higher light the pigment content was generally lower than the control. This demonstrates that *Scenedesmus* sp. adapts to the higher light environment by decreasing its capacity for capturing light. This adaptation is referred to as photoacclimation which is the graded reduction of photosynthetic pigment content in response to increased irradiance and can potentially involve changes in pigment complement, electron transfer components and Calvin Cycle enzymes (MacIntyre *et al*, 2002). As demonstrated by Figure 5.10 the Chlorophyll *a*/*b* ratio temporarily increased on day 4 after exposure to the higher light intensities provided on day 3. A higher Chlorophyll *a/b* ratio is correlated with a smaller sized light harvesting complex II (Logothetis, 2004; Sukenik *et al*., 1988). This suggests that the size of the light harvesting complex II for *Scenedesmus* sp. initially decreased in response to the higher intensities but thereafter increased in response to mutual shading.

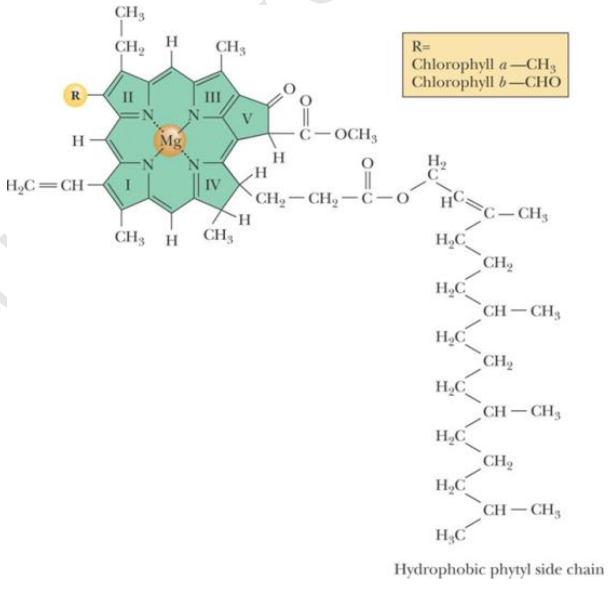

Figure 5.13: Structures of chlorophyll *a* and *b*. R is CH_3 in chlorophyll *a*; R is CHO in chlorophyll *b*

According to Masojídek *et al*. (1999), *Scenedesmus quadricauda* exhibited a higher capacity to adapt to high irradiances than *Chlorella sorokiniana*, due to an effective quenching mechanism and high photosynthetic capacity. They determined that *S. quadricauda* has a larger pool of xanthophyll-style pigments than *C. sorokiniana*. Xanthophylls, one of the two major groups of carotenoids, provide photoprotection against the damaging effects of light. In this study it was determined that the average carotenoid concentration was highest for the 2X light condition for both the 0.5% and 1% experiments, and that this increase occurred as a delayed response to the higher light intensity provided (Figure 5.10). Average maximum specific growth rates were 1.34 and 1.30 day^{-1} for *C. vulgaris* and 1.15 and 1.20 day^{-1} for *Scenedesmus* sp., cultured in CeBER ALRs at 2900 ppm CO_2, for nitrogen deficient (150 $mg.L^{-1}$) and nitrogen sufficient (1500 $mg.L^{-1}$) conditions respectively (Griffiths *et al*., 2011a). Therefore, the ability of *Scenedesmus* sp. to achieve higher cell concentrations is a reflection of its superior ability to adapt to a changing light environment and not due to an innate advantage over *Chlorella*. To put this from a perspective of evolutionary context, *Scenedesmus* represents the typical alga of fresh water microalgae which is often exposed to high irradiances while *Chlorella* species are mostly soil algae and are exposed to lower irradiances (Masojídek *et al*. 1999).

As the light model modified by Fraser (2011) does not account for changes in pigment concentrations it is difficult to determine to what extent pigment concentration affects light penetration in the ALR. However, this information serves to inform the discussion on the comparative assessment of growth using a feed gas containing 5000 and 10000 ppm CO_2 (Section 5.3.6).

5.3.5 Average CO_2 uptake rates and recoveries

The CO_2 uptake rates and recoveries, calculated as described in Section 3.4.3, are displayed for each experimental condition in Table 5-3. The compromise between increased CO_2 uptake with increased CO_2 mass transfer and decreased CO_2 recovery needs assessment. For instance, the CO_2 uptake rate increases by two-fold when increasing the CO_2 concentration from 5000 ppm to 10 000 ppm at 1X Light intensity, while the CO_2 recoveries are similar. However, the CO_2 uptake rate increases by 1.2 fold when increasing the CO_2 concentration from 5000 ppm to 10 000 ppm at 2X Light intensity, while the CO_2 recovery decreases by 1.7 fold. The increase in CO_2 uptake is proportional to the decrease in CO_2 recovery when examining the experimental effects at 5000 or 10 000 ppm CO_2 individually. Providing extra light to *Scenedesmus* sp. is the best strategy for improving the maximum average CO_2 uptake rate and recovery under these operating conditions, which highlights the light limitation in these reactors. The maximum average CO_2 uptake rate measured, 1.84 $g.L^{-1}.day^{-1}$ is high in comparison to literature values although the corresponding CO_2 recovery (CR (X)) is only 11.38% (Table 4-6, Section 4.7).

Table 5-3: Average CO_2 uptake rates and recoveries for *Scenedesmus* sp. under varying light and nutrient regimes

(Experiments conducted with 0.5% CO_2 are marked with an asterisk. Experiments conducted with 1% CO_2 are marked with a tilde)

Factor	Experimental condition	Avg. Q_{CO2} ($g.L^{-1}.day^{-1}$)	Avg. CR(X) (%)
BC	*2X Light intensity, Fed-batch	1.256	15.51
B	*2X Light intensity	1.550	19.14
C	*1X Light intensity, Fed-batch	0.921	11.38
(1)	*1X Light intensity	0.492	6.070
ABC	˜2X Light intensity, Fed-batch	1.211	7.476
AB	˜2X Light intensity	1.843	11.38
AC	˜1X Light intensity, Fed-batch	0.769	4.746
A	˜1X Light intensity	0.979	6.047

To determine the capacity of the cultivation system to remove CO_2, continuous offgas data was analysed to calculate CO_2 removal according to the method described in Section 3.4.3. The average CO_2 recoveries for each experimental condition at 5000 and 10 000 ppm are illustrated in Figure 5.14 and 5.15 respectively. Considering the CR (X) data and the fact that a pattern of the average CO_2 recoveries was not easily discernible for the 2X Light intensity, Fed-batch condition in comparison to the other conditions it is prudent to focus on the 2X Light intensity condition instead. During the linear phase of growth the average CO_2 recovery (CR(OG)) at 2X Light intensity was 9% which is far lower than the 19% calculated from biomass data(CR(X)). This discrepancy could potentially be due to variations between the relationship of cell concentration (g/L) and cell numbers for the different experimental conditions or experimental error. During the linear phase of growth the average CO_2 recovery at 2X Light intensity was 12.1% which is similar to the 11.5% calculated from biomass data. The patterns of CO_2 recovery for the Fed-batch conditions at 5000 and 10 000 ppm CO_2 were cyclical and the lower CO_2 recoveries corresponded to nutrient aliquot addition albeit with a time delay. This is possibly due to the salting-out effect where the addition of salt ions reduces the ability of water to hydrate gas molecules, as salt ions are strongly hydrated (Hangx, 2006). Thus, the addition of nutrients could have temporarily lowered the availability of DIC in the extracellular media and subsequently the CO_2 recovery.

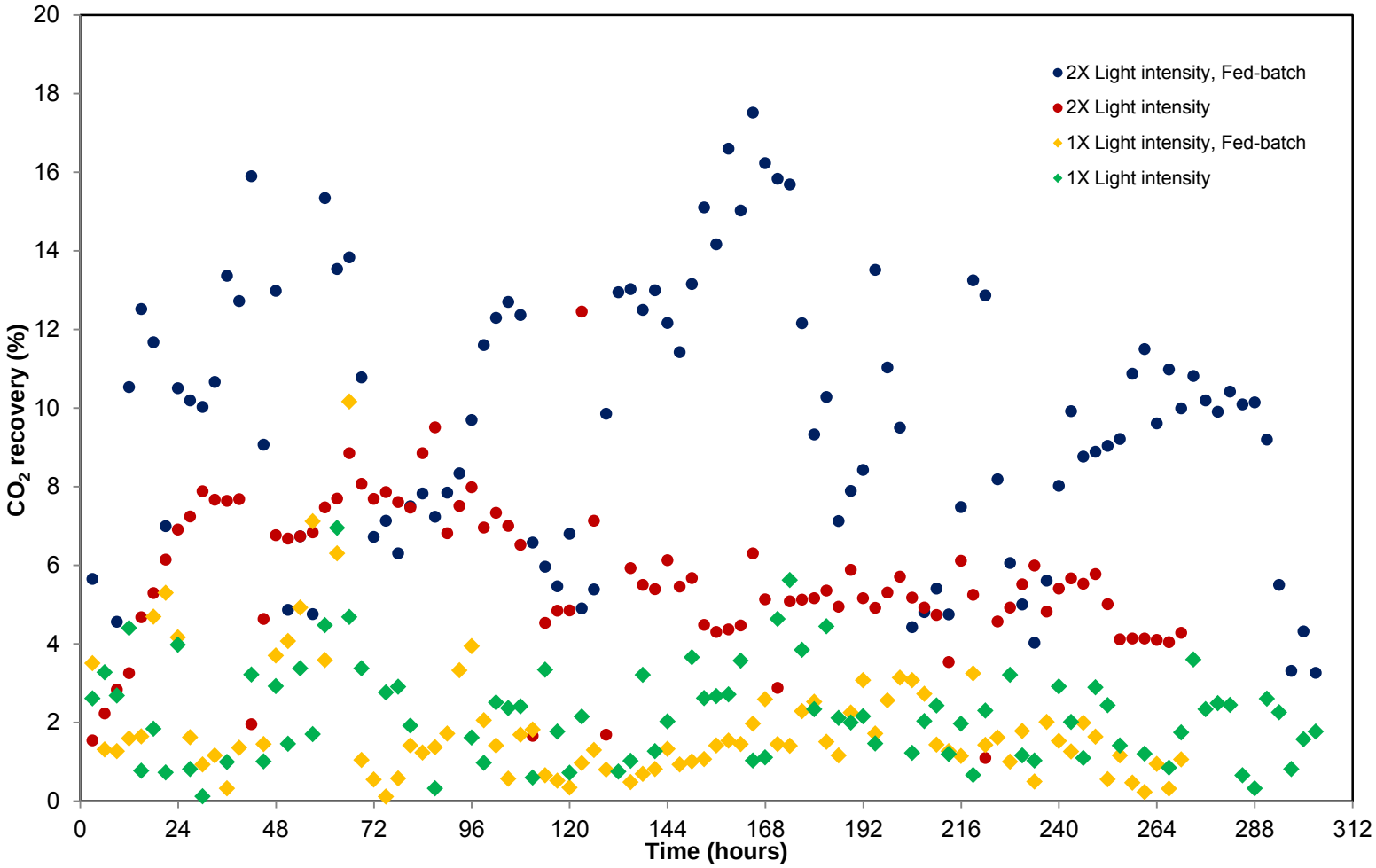

Figure 5.14: Average CO_2 recovery of *Scenedesmus* sp. for each experimental condition when cultured in ALRs with 5000 ppm CO_2

(Each marker represents an average CO_2 recovery for between 69-119 recoveries. Circles represent 2X Light intensity, diamonds represent 1X Light intensity Extra light was introduced after 48 hours. Nutrients were supplied on approximately the 48th, 120th, 192nd and 264th hour)

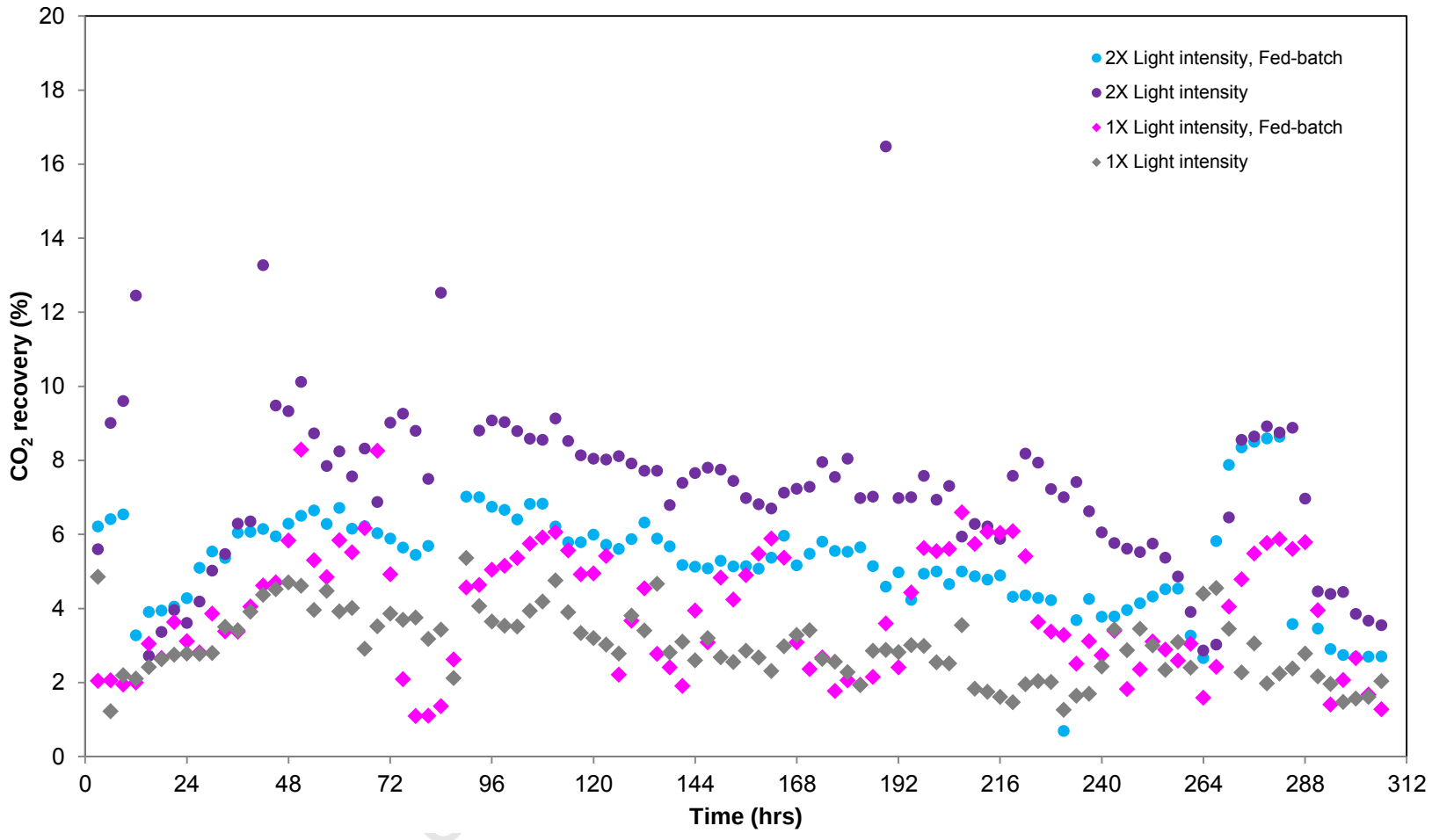

Figure 5.15: Average CO_2 recovery of *Scenedesmus* sp. for each experimental condition when cultured in ALRs with 10 000 ppm CO_2

(Each marker represents an average CO_2 recovery for between 69-119 recoveries. Circles represent 2X Light intensity, diamonds represent 1X Light intensity. Extra light was introduced after 48 hours. Nutrients were supplied on approximately the 48th, 120th, 192nd and 264th hour)

5.3.6 Overall assessment of experimental conditions on *Scenedesmus* sp.

To assess the overall effects of varying light and nutrient regimes on the growth of *Scenedesmus sp.* the growth curves of the 5000 and 10 000 ppm, experiments are presented in Figure 5.16. In comparision to the other experimental conditions, the 2X Light intensity, Fed-batch condition growth curves (blue lines) approximate the characteristic algal growth curve better. It is also evident that the nutrient addition prolonged the growth of *Scenedesmus* sp.; the growth rate of the 2X Light intensity curves (red and purple lines) declined at the 219th and 254th hour for the 5000 and 10 000 ppm CO_2 conditions respectively. The initial lower rates of growth for the 2X Light intensity, Fed-batch conditions in comparison the 2X Light intensity conditions could potentially be due the lower levels of light penetration due the formation of higher concentrations of pigments and/or due to diversion of energetic resources from replication (Section 5.3.4).

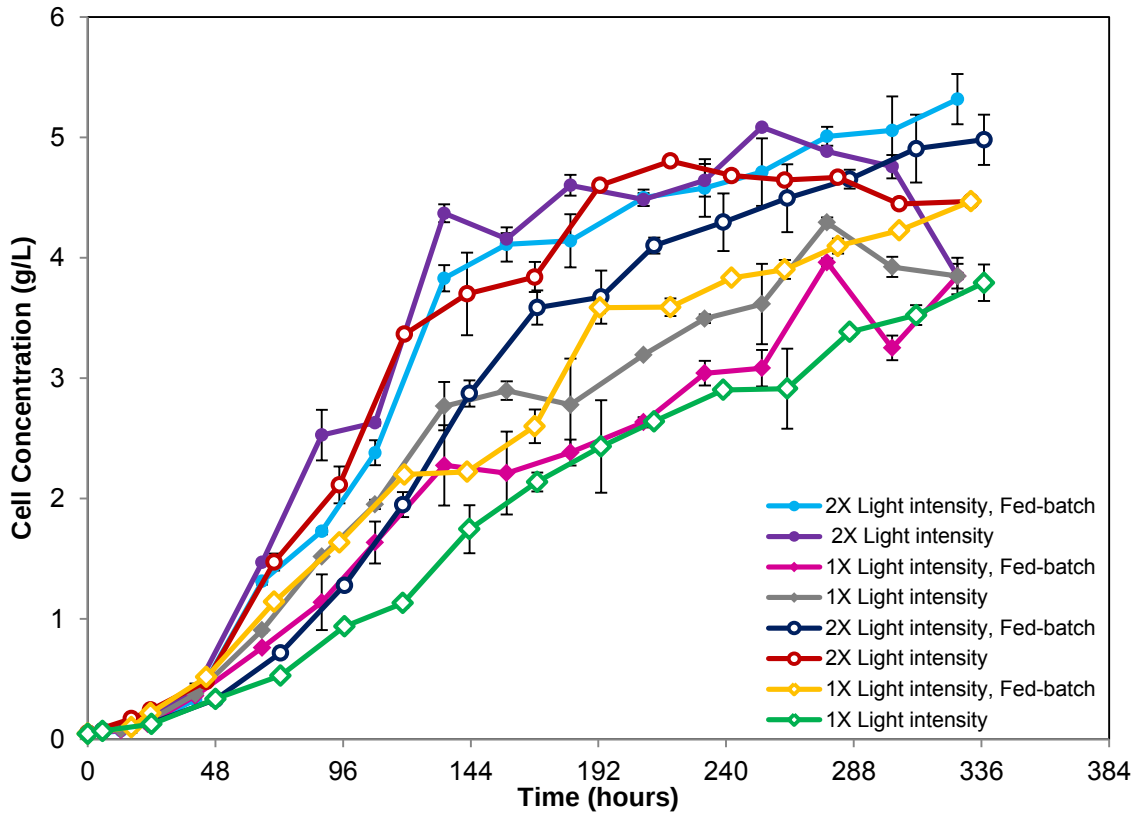

Figure 5.16: Growth curves of *Scenedesmus* sp. cultured in ALRs with varying light and nutrient regimes on 5000 and 10 000 ppm CO_2 at 25 ± 1°C

(Open symbols indicate growth at 5000 ppm CO_2. Closed symbols indicate growth at 10 000 ppm CO_2. Circles represent 2X Light intensity, diamonds represent 1X Light intensity. Error bars represent standard deviations for absorbance readings.)

The extra light provided had a larger effect on growth, than the extra CO_2 provided i.e. the difference in the green and grey curves is less than the differences for the green and red curves (5000 ppm CO_2) and for the grey and purple curves (10 000 ppm CO_2) (Figure 5.16). This is also reflected in Figure 5.17 which displays the response of CO_2 uptake rate against light intensity and CO_2 concentration.

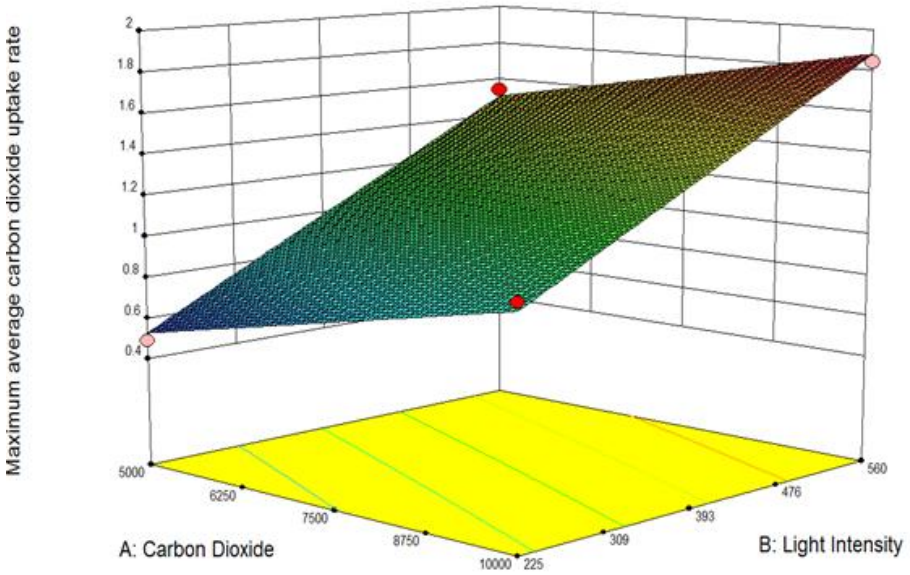

Figure 5.17: Response of maximum average CO_2 uptake rate to A: CO_2 (ppm) and B: Light Intensity ($\mu mol.m^{-2}.s^{-1}$)

An ANOVA was performed for the response of maximum average CO_2 uptake rate (Design-Expert trial v.8.05, Stat-Ease). The model was significant for the main effects at a 90% confidence level; there was an 8.7% chance that this model was generated due to noise.

$$Q_{CO_2} = +1.13 + 0.072A + 0.34B - 0.088C \quad (5.1)$$

Of the main effects the effect of light intensity was the only statistically significant factor (p=0.0247; Appendix F). The interactions were not included in the model as the effect of nutrient regime confounded the results as visualized by Figure 5.18, which displays the average carbon dioxide uptake rate for each experimental condition.

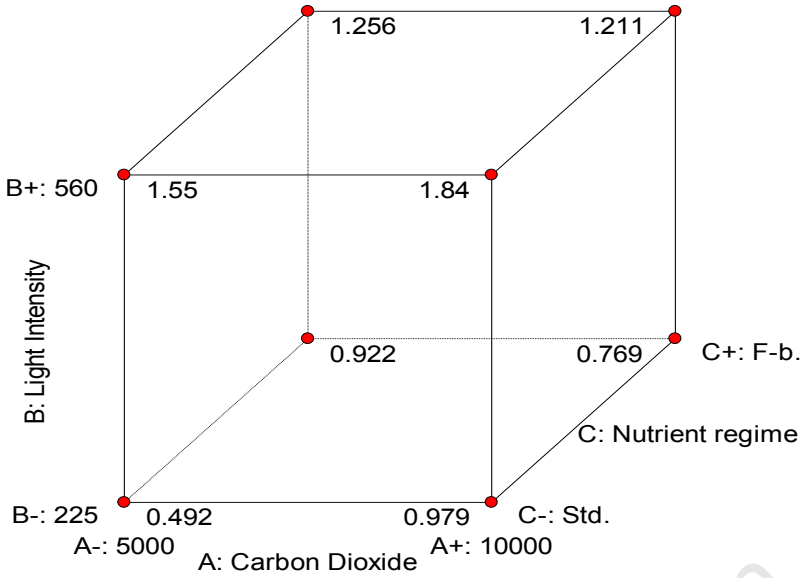

Figure 5.18: Average carbon dioxide uptake rates for all experimental conditions

(Units for CO_2 uptake rates are $g.L^{-1}.day^{-1}$. Units for CO_2 concentrations are ppm. Units for Light Intensity values are $\mu mol.m^{-2}.s^{-1}$. Nutrient regime is either Standard (Std.) or Fed-batch (F-b))

Figure 5.19 displays the micrographs of *Scenedesmus* sp. cultured at various experimental conditions at 10 000 ppm CO_2. Cells from the culture grown at the experimental condition of 10 000 ppm CO_2 and 2X light condition appear engorged when compared to cells from the 1X light condition, this could be due to a starch or lipid accumulation. Westerhoff *et al*. (2010) took measurements of starch, using transmission electron microscopy, for *Scenedesmus* sp. and *Chlorella* sp. before and after exposure to high CO_2 (20%). These authors determined that starch accumulates as a result of high CO_2 exposure for both species. When the cell volumes of *S. obliquus* cultured at h-light[8] were compared with the cell volumes of *S. obliquus* cultured at l-light it was determined that the h-light cells were on average 50% larger (Senger and Fleischhacker, 1977).

Prior to the experiments described in this chapter, a trial experiment was conducted where *Scenedesmus* sp. was cultured at 2900 ppm CO_2 with the 1X and 2X light conditions in ALRs. As temperature was not controlled the data was not shown here, although two interesting observations were made. Firstly, the cells were engorged for the extra light condition (from day 7 onwards) and secondly, a rapid spike in growth coincided with a 2°C increase in temperature. The growth at the 2X Light intensity, 2900 ppm CO_2 condition was considerably lower than the growth at the 2X Light intensity, 5000 ppm CO_2 condition i.e. the culture was CO_2-limited at 2900 ppm CO_2.

[8] h-light was 28 $W.m^{-2}$ and l-light was 5 $W.m^{-2}$. Distribution of cell volume was measured in a Coulter counter and cells were suspended in an azide-free balanced electrolyte solution. 100 cells were measured. (Senger and Fleischhacker, 1977).

A:

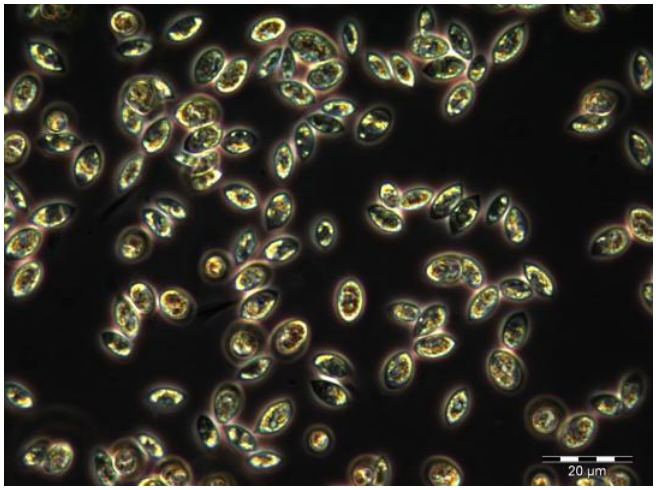

B:

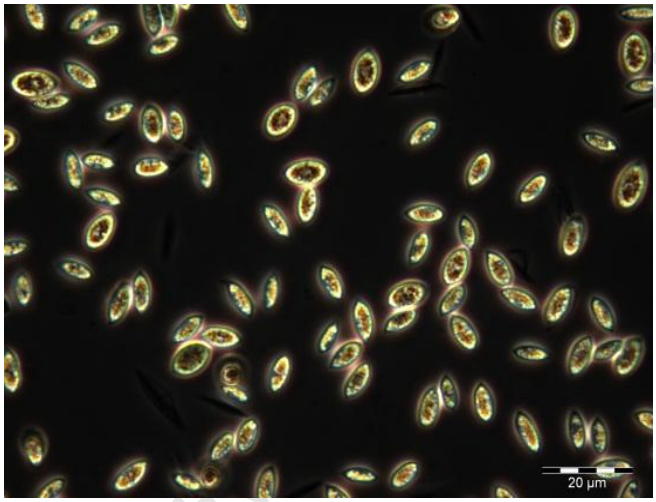

C:

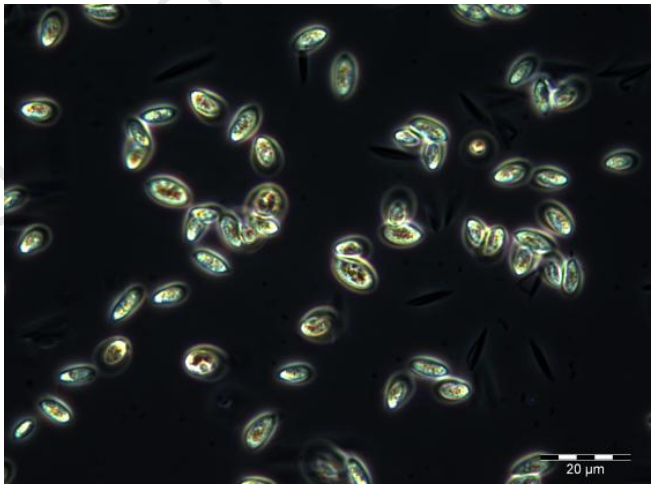

Figure 5.19: Micrographs of *Scenedesmus* sp. cultured for 10 days with 1% CO_2 under (A) 2X Light intensity, Fed-batch; (B) 2X Light intensity and (C) 1X Light intensity

(100X objective used)

To assess whether increases beyond 1% CO_2 resulted in improvements to CO_2 uptake rates, growth of *Scenedesmus* sp. cultured at 1% CO_2 was compared to data for *Scenedesmus* sp. cultured at 3% CO_2. Figure 5.20 displays the growth curves on 1 and 3% CO_2 at light intensities of 560 µmol.m^{-2}.s^{-1} and 590 µmol.m^{-2}.s^{-1} respectively. The growth rates were very similar for both conditions, although the maximum cell concentration of 5.12 g/L was attained 81 hours earlier at 3% CO_2. A CO_2 uptake rate of 1.84 g.L^{-1}.day^{-1} was calculated for the 3% CO_2 run (R^2=0.983). The same rate was obtained at 1% CO_2 and 2X Light intensity (R^2=0.999; Table 5-3). A CO_2 recovery (CR (X)) of 11.38% was obtained for the 1% CO_2, 2X Light intensity condition compared to 2.93% obtained for the 3% condition. Hence, the selection of a P_{CO2} beyond 1% cannot be justified.

Figure 5.21 displays the growth curves on 1 and 3% CO_2 at light intensities of 225 µmol.m^{-2}.s^{-1} and 590 µmol.m^{-2}.s^{-1} respectively. Interestingly, the growth for the 1% CO_2 condition appears to plateau at a cell concentration of 2.6 g/L and then recovers sufficiently to attain a maximum cell concentration of 4.15 g/L. Again, for the 1% CO_2, 1X Light intensity condition, light penetration in the draft tube tends to zero beyond a cell concentration of 2.7 g/L (Figure 5.7, Section 5.3.3). This occurred on approximately day 6. Further, the pigment concentration decreases from 2.09% to 0.95% from day 4 to 7, which would improve light penetration somewhat (Figure 5.12, Section 5.3.4). Thus, by adapting to the varying light intensities *Scenedesmus* sp. affords itself the opportunity to prolong growth. Contrastingly, the growth of *C. vulgaris* decreased steadily after attaining a cell concentration of 2.3 g/L when *Scenedesmus* sp. and *C. vulgaris* were cultured in CeBER ALRs at 2900 ppm CO_2 (Dicks and Harrison, in preparation).

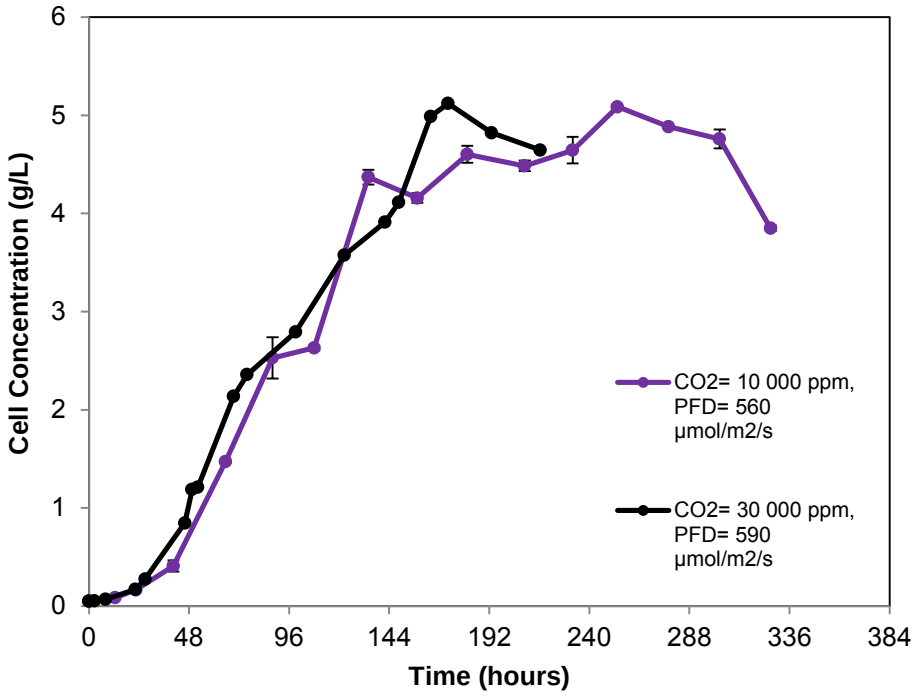

Figure 5.20: Growth curves of *Scenedesmus* sp. in ALRs at 1 and 3% CO_2 at a PFD of 560 and 590 µmol.m^{-2}.s^{-1} respectively

(3% CO_2 growth curve data was obtained at a temperature of ~27°C; Fraser, 2011)

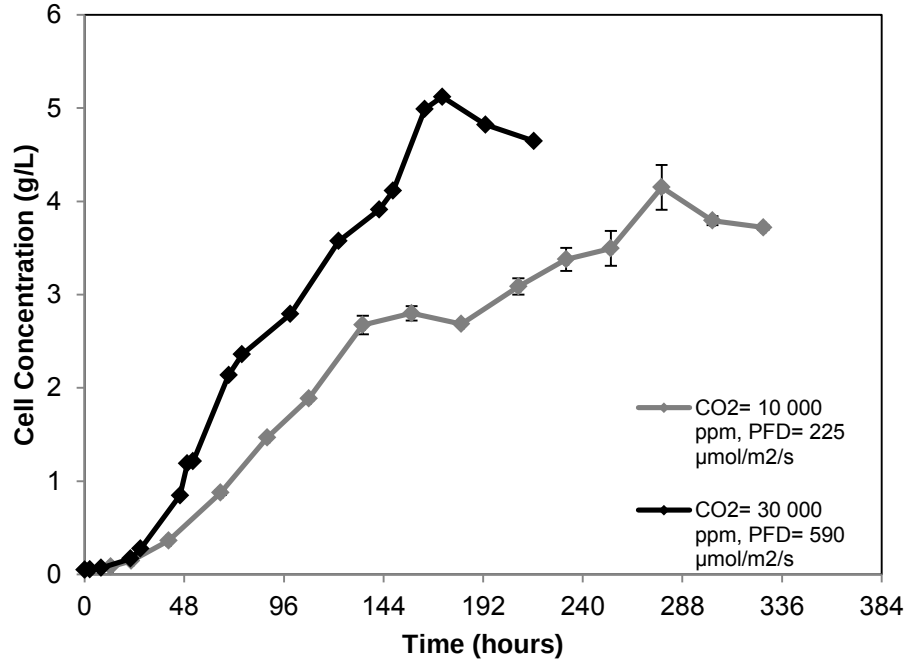

Figure 5.21: Growth curves of *Scenedesmus* sp. in ALRs at 1 and 3% CO_2 at a PFD of 225 and 590 µmol.m^{-2}.s^{-1} respectively

(3% CO_2 growth curve data was obtained at a temperature of ~27°C; Fraser, 2011)

5.4 Conclusions

- The provision of higher light intensities had a significantly positive effect on average CO_2 uptake rates and improved average CO_2 recoveries
- The Fed-batch nutrient regime did not significantly improve the average CO_2 uptake rate and potentially exacerbated the problem of mutual shading via formation of more pigments
- The combination of the Fed-batch nutrient regime and the 2X Light condition resulted in the highest biomass yields as growth was prolonged due to the addition of nutrients
- For cultivation of *Scenedesmus* sp. at the specified operating conditions for the 2X light experiment the $P_{CO2,\,CRIT}$ is within the range of 0.5 to 1% CO_2
- A higher CO_2 partial pressure of 3% failed to improve the maximum average CO_2 uptake rate and would reduce CO_2 recoveries substantially
- The biomass carrying capacity for *Scenedesmus* sp. is approximately 5 g/L when cultured in the ALRs at the specified operating conditions

5.5 Recommendations

- To validate and further improve the maximum CO_2 uptake rate for *Scenedesmus* sp., the experiment duration should be shortened and replicates performed. The categorical variable, nutrient regime should be replaced with the numerical variable temperature (25 °C to 30 °C). The Experimental Design could then be augmented with central and axial points to yield second-order interactions (i.e. a 2^3 second-order central composite design)
- The effect of higher light intensities should be tested, this will require new or modified equipment (the range of light intensities investigated here was limited by the reactor configuration/setup and the use of fluorescent bulbs)
- Additionally, as evidence suggests that higher light intensities and provision of higher CO_2 concentrations could improve lipid or starch productivity this should be quantified

Chapter 6 : Conclusions

This study investigated the CO_2 utilization of the microalgae *Scenedesmus* sp. via several approaches. Firstly, the $P_{CO2,CRIT}$ for *Scenedesmus* sp. at standard operating conditions was determined. Secondly, the physiological responses of *Scenedesmus* sp. were examined across a range of CO_2 partial pressures to delineate the limiting growth process. Thirdly, the CO_2 uptake rate for *Scenedesmus* sp. was optimized via manipulation of the light and nutrient regime. Lastly, the CO_2 fixation capability of *Scenedesmus* sp. was compared to other microalgal species.

Scenedesmus sp. was cultivated at a light intensity of 282.7 $\mu mol.m^{-2}.s^{-1}$ with 750 $mg.L^{-1}$ $NaNO_3$ (standard operating conditions) at the CO_2 partial pressures of 0.045, 0.12, 0.29, 0.50 and 1%, with 0.045% CO_2 regarded as the base case. Characteristic time analysis revealed that at a P_{CO2} of 0.045%, CO_2 becomes mass transfer limiting at cell concentrations higher than 0.5 g/L. This coincided with a shift in carbon speciation from CO_2/ H_2CO_3 to carbonate. When *Scenedesmus* sp. was cultured at a P_{CO2} of 0.12% the linear growth rate was increased by two-fold. However, after attaining a cell concentration of 1.27 g/L the growth rate decreased in comparison to the growth rates at the higher P_{CO2}s. Thus, *Scenedesmus* sp. is carbon-limited when cultured at the CO_2 partial pressures of 0.045 and 0.12% in the ALR after attaining a cell concentration of 0.5 and 1.27 g/L respectively.

The growth rates of *Scenedesmus* sp. at 0.29 and 0.5% CO_2 were similar while the growth rate at 1% CO_2 remained higher until a cell concentration of 2.7 g/L was attained. The rate of DIC accumulation was higher for the 1% CO_2 experiment although the DIC concentration tended to plateau after day 10 for all CO_2 partial pressures, albeit at significantly lower values for the 0.045 and 0.12% CO_2 experiments. This combined with the results attained from the thermodynamic modelling of carbon speciation and solubility suggested that *Scenedesmus* sp. preferentially takes up CO_2 over bicarbonate. Hence, the higher growth of *Scenedesmus* sp. at 1% CO_2 was due to the higher concentrations of DIC available and the distribution of DIC species.

The highest average maximum CO_2 uptake rate of 0.96 $g.L^{-1}.day^{-1}$ and highest cell concentration of 4.29 g/L was obtained at 1% CO_2. This was substantially higher than the 0.50 $g.L^{-1}.day^{-1}$ of *C. vulgaris* which was obtained at the $P_{CO2,\ CRIT}$ of 0.12%. This improvement was attributed to *Scenedesmus* sp.'s superior ability to grow in denser cultures which requires effective scavenging of light. For cultivation of *Scenedesmus* sp. under the standard set of operating conditions a $P_{CO2,CRIT}$ of 0.01 atm (1%) is advised.

To determine whether higher starting sodium nitrate concentrations could improve growth and the associated CO_2 uptake and recovery, *Scenedesmus* sp. was cultured at 0.29% CO_2 with 2000 $mg.L^{-1}$ and at 0.5% with 1450 and 2000 $mg.L^{-1}$ $NaNO_3$. When *Scenedesmus* sp. was cultured at 0.29% CO_2 with 2000 $mg.L^{-1}$ $NaNO_3$, settling was observed. This was attributed to a higher salt loading which prompted flocculation. Growth was also not improved at 0.5% CO_2 with 1450 and 2000 $mg.L^{-1}$ $NaNO_3$. Hence, experiments performed with higher starting nitrate concentrations failed to improve biomass productivities and associated CO_2 uptake rates and recoveries.

Manipulation of the light and nutrient regimes demonstrated that CO_2 uptake rates were significantly improved with provision of higher light intensities. The Fed-batch nutrient regime resulted in higher concentrations of pigment being formed which presumably exacerbated the problem of mutual shading. The highest average CO_2 uptake rate of 1.84 $g.L^{-1}.day^{-1}$ occurred with 1% CO_2 and 560 $\mu mol.m^{-2}.s^{-1}$. The corresponding average CO_2 recovery was 12.1% (CR (OG)). Providing a P_{CO2} of 3% did not improve the average CO_2 uptake rate of 1.84 $g.L^{-1}.day^{-1}$ and resulted in a substantial decrease in CO_2 recovery. For cultivation of *Scenedesmus* sp. at the light intensities of 560 to 590 $\mu mol.m^{-2}.s^{-1}$, a P_{CO2} within the range of 0.5 to 1% is advised.

The maximum average CO_2 uptake rate of 1.84 $g.L^{-1}.day^{-1}$ is the fourth highest when compared to twenty-two literature reported values of various microalgal species (Table 4-6, Section 4.7). This study concludes that *Scenedesmus* sp. has great capability for CO_2-fixation due to its ability to attain high cell densities. Overall, *Scenedesmus* sp. is a promising candidate for large-scale production of CO_2-neutral fuels due to its comparatively good lipid productivity and CO_2-fixation capability (Griffiths *et al*., 2011a[9]). To fully harness the CO_2-fixation capability of *Scenedesmus* sp. it is recommended that these results be replicated in an algal cultivation system where the CO_2 recovery is greater.

[9] Of 11 microalgal species (selected on the basis of lipid productivity) *Scenedesmus* sp. ranks in the top three in terms of lipid productivities and settling rates (Griffiths et al., 2011a).

References

Abanades, J.C., Akai, M., Benson, S., Caldeira, K., de Coninck, H., Cook, P., Davidson, O., Doctor, R., Dooley, J., Freund, P., Gale, J., Heidug, W., Herzog, H., Keith, D., Mazzoti, M., Metz, B., Meyer, L., Osman-Elasha, B., Palmer, A., Pipatti, R., Rubin, E., Smekens, K., Soltanieh, M. and Thambimuthu, K. 2005. *IPCC Special Report Carbon Dioxide Capture and Storage.*

Andersen, R.A. 2005. *Algal Culturing Techniques.* Elsevier Academic Press, London.

ANATOC Series II Total Organic Carbon Analyser Installation and Operation Manual. Australia: SGE International Pty Ltd.

Azov, Y. 1982. Effect of pH on inorganic carbon uptake in algal cultures. *Applied and Environmental Microbiology*. 43(6):1300-1306.

Bailey, J.E. and Ollis, D.F. 1986. *Biochemical Engineering Fundamentals.* McGraw-Hill, New York.

Barsanti, L. and Gualtieri, P. 2006. *Algae: Anatomy, Biochemistry, and Biotechnology.* Taylor and Francis Group, LLC CRC Press, Boca Raton.

Becker, E.W. 1994. *Microalgae: Biotechnology and Microbiology.* Press Syndicate of the University of Cambridge, London.

Ben-Amotz, A. and Avron, M. 1973. The role of glycerol in the osmotic regulation of the halophilic alga *Dunaliella parva*. *Plant Physiology*. 51(5):875-878.

Borchardt, M.A. 1996. Nutrients. In *Algal Ecology Freshwater Benthic Ecosystems.* J.R. Stevenson and Bothwell, M.L. and Lowe, R.L. Academic Press, Inc, San Diego.

Borkenstein, C.G., Knoblechner, J., Fruhwirh, H. and Schagerl, M. 2010. Cultivation of *Chlorella emersonii* with flue gas derived from a cement plant. *Journal of Applied Phycology.* 23(1):131-135.

Brown, L.M. 1996. Uptake of carbon dioxide from flue gas by microalgae. *Energy Conversion and Management.* 37(6-8):1363-1367.

Campbell, M.N. 2008. Biodiesel: algae as a renewable source for liquid fuel. *Guelph Engineering Journal*.1:2–7.

Carroll, J.J. and Mather, A.E. 1992. The system carbon dioxide-water and the Krichevsky-Kasarnovsky equation. *Journal of Solution Chemistry.* 21(7):1201-1209.

Carvalho, A.P. and Malcata, X. 2001. Transfer of carbon dioxide within cultures of microalgae: plain bubbling versus hollow-fiber modules. *Biotechnology Progress.* 17(2):265-272.

Chapel, D.G., Mariz, C.L. and Earnest, J. 1999. Recovery of CO_2 from flue gases: commercial trends. [Online]. Available:
http://prod75-inter1.netl.doe.gov/publications/proceedings/01/carbon_seq/2b3.pdf [2011, 4/23].

Chelf, P., Brown, L.M. and Wyman, C.E. 1993. Aquatic biomass resources and carbon dioxide trapping. *Biomass Bioenergy*. 4(3):175-183.

Cheng, L., Zhang, L., Chen, H. and Gao, C. 2006. Carbon dioxide removal from air by microalgae cultured in a membrane-photobioreactor. *Separation and Purification Technology.* 50(3):324-329.

Chiu, S., Tsai, M., Kao, C., Ong, S. and Lin, C. 2008. Reduction of CO_2 by a high-density culture of *Chlorella* sp. in a semicontinuous photobioreactor. *Bioresource Technology.* 99(9):3389-3396.

Chiu, S., Tsai, M., Kao, C., Ong, S. and Lin, C. 2009. The air-lift photobioreactors with flow patterning for high-density cultures of microalgae and carbon dioxide removal. *Engineering in Life Sciences.* 9(3):254-260.

Clesceri, L.S., Greenberg, A.E. and Eaton, A.D. 1998. Inorganic Nonmetallic Constituents. In *Standard Methods for the Examination of Water and Wastewater.* M.H. Franson, Ed. 20th ed. 1015 Fifteenth Street, NW Washington, DC 200005-2605: American Public Health Association. 4-1.

Coal. [Online]. Available: http://www.energy.gov.za/files/coal_frame.html [2011, 02/11].

Colman, B., Huertas, I.E., Bhatti, S. and Dason, J.S. 2002. The diversity of inorganic carbon acquisition mechanisms in eukaryotic microalgae. *Functional Plant Biology.*29(3):261-270.

Contreras, A., García, F., Molina, E. and Merchuk, J.C. 1998. Interaction between CO_2-mass transfer, light availability, and hydrodynamic stress in the growth of *Phaeodactylum tricornutum* in a concentric tube airlift photobioreactor. *Biotechnology and Bioengineering.* 60(3):317-325.

de Morais, M.G. and Costa, J.A.V. 2007a. Isolation and selection of microalgae from coal fired thermoelectric power plant for biofixation of carbon dioxide. *Energy Conversion and Management.* 48(7):2169-2173.

de Morais, M.G. and Costa, J.A.V. 2007b. Biofixation of carbon dioxide by *Spirulina* sp. and *Scenedesmus obliquus* cultivated in a three-stage serial tubular photobioreactor. *Journal of Biotechnology.* 129(3):439-445.

Danckwerts, P.V. 1970. Solubility of Gases in Liquids. In *Gas-Liquid Reactions.* McGraw-Hill Book Company, New York.

Dicks, R.G.and Harrison, S.T.L. 2011. Surface and suspension effects on microalgae bioflocculation. *Biochem Eng J*. In Preparation.

Dicks, R.G. 2010. Experimental data from CeBER Laboratory, Department of Chemical Engineering, University of Cape Town. Unpublished.

Doran, P.M. 1995. *Bioprocess Engineering Principles.* Elsevier Academic Press, London.

Doucha, J., Straka, F. and Livansky, K. 2005. Utilization of flue gas for cultivation of microalgae (*Chlorella* sp.) in an outdoor open thin-layer photobioreactor. *Journal of Applied Phycology.* (17):403–412.

Douskava, L., Doucha, J., Livansky, K., Machat, J., Novak, P., Umysova, D., Zachleder, V. and Vitova, M. 2009. Simultaneous flue gas bioremediation and reduction of microalgal biomass production costs. *Applied Microbiology Biotechnology*. 82:179–185.

Electricity. [Online]. Available: http://www.energy.gov.za/files/electricity_frame.html [2011, 2/14].

Eriksen, N.T. 2008. The technololology of microalgal culturing. *Biotechnology Letters*. 30(9):1535-1536.

Eriksen, N.T., Geest, T. and Iversen, J.J.L. 1996. Phototrophic growth in the lumostat: a photo-bioreactor with on-line optimization of light intensity. *Journal of Applied Phycology*. 8(4-5):345-352.

Eriksen, N.T. 1998. Dual sparging laboratory-scale photobioreactor for continuous production of microalgae. *Journal of Applied Phycology*. 10(4):377-382.

Fan, L., Zhang, Y., Zhang, L. and Chen, H. 2008. Evaluation of a membrane-sparged helical tubular photobioreactor for carbon dioxide biofixation by *Chlorella vulgaris*. *Journal of Membrane Science*. 325(1):336-345.

Fernández, F.G.A., Camacho, F.G., Pérez, J.A.S., Sevilla, J.M.F. & Grima, E.M. 1997. A model for light distribution and average solar irradiance inside outdoor tubular photobioreactors for the microalgal mass culture. *Biotechnology and bioengineering*. 55(5):701-714.

Ferreira, B.S. B.S., Fernades, H.L., Reis, A. and Mateus, M. 1998. Microporous hollow fibres for carbon dioxide absorption: Mass transfer model fitting and the supplying of carbon dioxide to microalgal cultures. *Journal of Chemical Technology and Biotechnology*. 71(1):61-70.

Fraser, M. 2011. Modelling airlift photobioreactors for algal bioenergy, using *Scenedesmus* sp. as the model species. Cape Town: University of Cape Town (MSc thesis).

Galan, M., Bonet, J., Sire, R., Reneaume, J. and Pleşu, A.E. 2009. From residual to useful oil: Revalorization of glycerine from the biodiesel synthesis. *Bioresource Technology*. 100(15):3775-3778.

Garrett, R.H. and Grisham, C.M. 2005. *Biochemistry*. Thomson Brooks/Cole, Belmont.

Geckler, R.P., Sane, J.O. and Tew, R.W. 1962. Highly concentrated carbon dioxide as a carbon source for continuous algae cultures [Online].
Available: http://contrails.iit.edu/DigitalCollection/1962/AMRLTDR62-116article06.pdf [2009, 03/11].

Gibbons, B.H. and Edsall, J.T. 1963. Rate of hydration of carbon dioxide and dehydration of carbonic acid at 25 °C. *The Journal of Biological Chemistry*. 238(10):3502-3507.

Gordon, J.M. and Polle, J.E.W. 2007. Ultrahigh bioproductivity from algae. *Applied Microbiology and Biotechnology*. 76(5):969-975.

Griffiths, M.J. and Harrison, S.T.L. 2009. Lipid productivity as a key characteristic for choosing algal species for biodiesel production. *Journal of Applied Phycology*. 21(5):493-507.

Griffiths, M.J., Harrison, S.T.L. and van Hille, R.P. 2011a. Lipid productivity, settling potential and fatty acid profile under nitrogen sufficient and deficient conditions of 11 microalgal species promising for biodiesel production. Unpublished.

Griffiths, M.J., Garcin, C., van Hille, R.P. and Harrison, S.T.L. 2011b. Interference by pigment in the estimation of microalgal biomass concentration by optical density. *The Journal of Microbiological Methods.* 85(2):119-23.

Haiduc, A., Brandenberger, M., Suquet, S., Vogel, F., Bernier-Latmani, R. and Ludwig, C. 2009. SunCHem: an integrated process for the hydrothermal production of methane from microalgae and CO_2 mitigation. *Journal of Applied Phycology.* 21(5):529-541.

Hangx, S.J.T. 2006. *Subsurface Mineralisation: Rate of CO_2 mineralization and geomechanical effects on host and seal formations.* CATO Workpackage WP 4.1.

Hsueh, H.T., Chu, H. and Yu, S.T. 2007. A batch study on the bio-fixation of carbon dioxide in the absorbed solution from a chemical wet scrubber by hot spring and marine algae. *Chemosphere.* 66(5):878-886.

Hufton, J.R., Allam, R.J., Chiang, R., Middleton, P., Weist, E.L. and White, V. 2005. Development of a process for CO_2 capture from gas turbines using a sorption enhanced water gas shift reactor system. In *Greenhouse Gas Control Technologies 7.* E.S. Rubin, Eds. Oxford: Elsevier Science Ltd. 253-261.

Huntley M.E. and Redalje D.G. 2007. CO_2 mitigation and renewable oil from photosynthetic microbes: a new appraisal. *Mitigation and Adaption Strategies for Global Change*. 12:573–608.

Jacob-Lopes, E., Revah, S., Hernández, S., Shirai, K. and Franco, T.T. 2009a. Development of operational strategies to remove carbon dioxide in photobioreactors. *Chemical Engineering Journal.* 153(1-3):120-126.

Jacob-Lopes, E., Scoparo, C.H.G., Lacerda, L.M.C.F. and Franco, T.T. 2009b. Effect of light cycles (night/day) on CO_2 fixation and biomass production by microalgae in photobioreactors. *Chemical Engineering and Processing: Process Intensification.* 48(1):306-310.

Kadam, K.L. 1997. Power plant flue gas as a source of CO_2 for microalgae cultivation: Economic impact of different process options. *Energy Conversion and Management.* 38(Supplement 1):S505-S510.

Keffer, J.E. and Kleinheinz, G.T. 2002. Use of *Chlorella vulgaris* for CO_2 mitigation in a photobioreactor. *Journal of Industrial Microbiology and Biotechnology.* 29(5):275-280.

Kumar, A., Yuan, X., Sahu, A.K., Dewulf, J., Ergas, S.J. and Van Langenhove, H. 2010. A hollow fiber membrane photo-bioreactor for CO_2 sequestration from combustion gas coupled with wastewater treatment: a process engineering approach. *Journal of Chemical Technology and Biotechnology*. 85(3):387-394.

Kurano, N., Ikemoto, H., Miyashita, H., Hasegawa, T., Hata, H. and Miyachi, S. 1995. Fixation and utilization of carbon dioxide by microalgal photosynthesis. *Energy Conversion and Management.* 36(6-9):689-692.

Kyoto Protocol to the United Nations Framework Convention on Climate Change. [Online]. Available: http://unfccc.int/kyoto_protocol/status_of_ratification/items/2613.php [2011, 2/14].

Kishimoto M., Okakura T., Nagashima H., Minowa T., Yokoyama S.Y. and Yamaberi K. 1994. CO_2 fixation and oil production using microalgae. *Journal of Fermentation and Bioengineering.* 78:479–482.

Langley, N. 2010. Strategies for Carbon Dioxide Delivery to Microalgal Cultures and their Potential for the Reduction of Emissions. Cape Town: University of Cape Town (MSc thesis).

Lee, Y.K. 2001. Microalgal mass culture systems and methods: Their limitation and potential. *Journal of Applied Phycology*. 13(4):307-315.

Loewenthal, R.E. and Marais, G.v.R. 1973. *The Carbonic System in Water Treatment.* Research Report no. W.4. for the Department of Civil Engineering, University of Cape Town.

Logothetis, K., Dakanali, S., Ioannidis, N. and Kotzabasis, K. 2004. The impact of high CO_2 concentrations on the structure and function of the photosynthetic apparatus and the role of polyamines. *Journal of Plant Physiology.* 161(6):715-724.

MacIntyre, H.L., Kana, T.M., Anning, T. and Geider, R.J. 2002. Photoacclimation of photosynthesis irradiance response curves and photosynthetic pigments in microalgae and cyanobacteria. *Journal of Phycology.* 38(1):17-38.

Martínez, L., Redondas, V., García, A. and Morán, A. 2010. Optimization of growth operational conditions for CO_2 biofixation by native *Synechocystis* sp. *Journal of chemical technology and biotechnology.* 86(5):681-690.

Masojídek, J., Torzillo, G., Koblížek, M., Kopecký, J., Bernardini, P., Sacchi, A. and Komenda, J. 1999. Photoadaptation of two members of the Chlorophyta (*Scenedesmus* and *Chlorella*) in laboratory and outdoor cultures: changes in chlorophyll fluorescence quenching and the xanthophyll cycle. *Planta.* 209(1):126-135.

Michiki, H. 1995. Biological CO_2 fixation and utilization project. *Energy Conversion and Management.* 36(6-9):701-705.

Miyasaka, H., Ohnishi, Y., Akano, T., Fukatso, K., Mizoguchi, T., Yagi, K., Maeda, I., Ikuta, Y., Matsumoto, H. and Shioji, N. and Miura, Y. 1998. Excretion of glycerol by the marine *Chlamydomonas* sp. strain W-80 in high CO_2 cultures. *Journal of Bioscience and Bioengineering.* 85(1):122-124.

Moroney, J.V. and Somanchi, A. 1999. How do algae concentrate CO_2 to increase the efficiency of photosynthetic carbon fixation? *Plant Physiology.* 119:9–16.

Murakami, M. and Ikenouchi, M. 1997. The biological CO_2 fixation and utilization project by RITE (2) — Screening and breeding of microalgae with high capability in fixing CO_2. *Energy Conversion and Management.* 38(Supplement 1):S493-S497.

Nakas J.P., Schaedle, M., Parkinson, C.M., Coonley, C.E. and Tenenbaum, S.W. 1983. System Development for Linked-Fermentation Production of Solvents from Algal Biomass. *Applied Environmental Microbiology.* 46(5):1017-1023.

Nicholls, K.H. and Dillon, P.J., 1978. An evaluation of phosphorus–chlorophyll–phytoplankton relationships for lakes. *International Review of Hydrobiology*. 63 (2), 141–154.

Nielsen, E.S. 1955. Carbon dioxide as carbon source and narcotic in photosynthesis and growth of *Chlorella Pyrenoidosa*. *Physiologia Plantarum.* 8(2):317-334.

Ono, E. and Cuello, J.L. 2007. Carbon Dioxide mitigation using thermophilic cyanobacteria. *Biosystems Engineering*. 96(1):129-134.

Packer, M. 2009. Algal capture of carbon dioxide; biomass generation as a tool for greenhouse gas mitigation with reference to New Zealand energy strategy and policy. *Energy Policy.* 37(9):3428-3437.

Pegels, A. 2010. Renewable energy in South Africa: Potentials, barriers and options for support. *Energy Policy*. 38(9):4945-4954.

Pehnt, M. and Henkel, J. 2009. Life cycle assessment of carbon dioxide capture and storage from lignite power plants. *International Journal of Greenhouse Gas Control*. 3(1):49-66.

Posten, C. 2009. Design principles of photo-bioreactors for cultivation of microalgae. *Engineering in Life Sciences.* 9(3):165-177.

Pott, R., Fagan, M. and van Hille, R.P. 2009. Development of an assay system for external carbonic anhydrase in whole cell algal systems. Unpublished.

Richardson, C. 2011. Investigating the Role of Reactor Design to Maximise the Environmental Benefit of Algal Oil for Biodiesel. Cape Town: University of Cape Town (MSc thesis).

Rosenberg, J.N. 2008. A green light for engineered algae: redirecting metabolism to fuel a biotechnology revolution. *Current Opinion in Biotechnology.* 19(5):430-436.

Satoh, A., Kurano, N. and Miyachi, S. 2001. Inhibition of photosynthesis by intracellular carbonic anhydrase in microalgae under excess concentrations of CO_2. *Photosynthesis Research.* 68(3):215-224.

Schenk, P., Thomas-Hall, S., Stephens, E., Marx, U., Mussgnug, J., Posten, C., Kruse, O. and Hankamer, B. 2008. Second Generation Biofuels: High-Efficiency Microalgae for Biodiesel Production. *Bioenergetics Research.* 1(1):20-43.

Seckbach, J. and Libby, W.F. 1970. Vegetative life on Venus? Or investigations with algae which grow under pure CO_2 in hot acid media at elevated pressures. *Origins of Life and Evolution of the Biosphere.* 2(2):121-143.

Senger, H. and Fleischhacker, P.H. 1977. Adaptation of the photosynthetic apparatus of *Scenedesmus obliquus* to Strong and Weak Light Conditions. *Plant Physiology*. 43:35-42.

Sialve, B., Bernet, N. and Bernard, O. 2009. Anaerobic digestion of microalgae as a necessary step to make microalgal biodiesel sustainable. *Biotechnology Advances.* 27(4):409-416.

Silberberg, M. 2003. *Chemistry: The Molecular Nature of Matter and Change.* 3rd ed. McGraw Hill, New York.

Spijkerman, E. 2008. What physiological acclimation supports increased growth at high CO_2 conditions? *Physiologia Plantarum.* 133(1):41-48.

Stevenson, J.R., Bothwell, M.L. and Lowe, R.L. Eds. 1996. *Algal Ecology Freshwater Benthic Ecosystems*. Elsevier Academic Press, San Diego.

Stewart, C. and Hessami, M. 2005. A study of methods of carbon dioxide capture and sequestration–the sustainability of a photosynthetic bioreactor approach. *Energy Conversion and Management.* 46(3):403-420.

Sukenik, A., Bennett, J. and Falkowski, P. 1988. Changes in the abundance of individual apoproteins of light-harvesting chlorophyll a/b-protein complexes of photosystem I and II with growth irradiance in the marine chlorophyte *Dunaliella tertiolecta*. *Biochimica et Biophysica Acta.Bioenergetics.* 932:206-215.

Sung, K., Lee, J., Shin, C., Park, S. and Choi, M. 1999. CO_2 fixation by *Chlorella* sp. KR-1 and its cultural characteristics. *Bioresource Technology.* 68(3):269-273.

Sydney, E.B. 2010. Potential carbon dioxide fixation by industrially important microalgae. *Bioresource Technology*. 101(15):5892-5896.

Tans, P. and Keeling, R. *Trends in Atmospheric Carbon Dioxide - Mauna Loa* [Online]. Available: http://www.esrl.noaa.gov/gmd/ccgg/trends/ [2010, 5/22].

Thambimuthu, K., Soltanieh, M., Abanades, J.C., Allam, R.J., Bolland, O., Davison, J., Feron, P., Goede, F., Herrera, A., Iijima, M., Jansen, D., Leites, I., Mathieu, P., Rubin, E., Simbeck, D., Warmuzinski, K., Wilkinson, M., Williams, R., Jaschik, M., Lyngfelt, A., Span, R. and Tancyzk, M. 2005. Capture of CO_2. In *IPCC Special Report on Carbon dioxide Capture and Storage*. Z. Abu-Ghararah and T. Yashima.

The tree of life. [Online]. Available: http://gapanalysis.nbii.gov [2009, 5/20].

Thielmann, J., Tolbert, N.E., Goyal, A. and Senger, H. 1990. Two systems for concentrating CO_2 and bicarbonate during photosynthesis by *Scenedesmus*. *Plant Physiology.* 92(3):622-629.

Trainor, F.R., Cain, J.R. and Shubert, L.E. 1976. Morphology and nutrition of the colonial green alga *Scenedesmus*: 80 years later. *The Botanical Review.* 42(1)1-21.

Usui, N. and Ikenouchi, M. 1997. The biological CO_2 fixation and utilization project by RITE(1) — Highly-effective photobioreactor system. *Energy Conversion and Management.* 38(Supplement 1):S487-S492.

Vunjak-Novakovic, G., Kim, Y., Wu, X., Berzin, I. and Merchuk, J.C. 2005. Air-lift bioreactors for algal growth on flue gas: Mathematical modeling and pilot-plant studies. *Industrial and Engineering Chemistry Research.* 44(16):6154-6163.

Wang, B., Li, Y., Wu, N. and Lan, C. 2008. CO_2 bio-mitigation using microalgae. *Applied Microbiological Biotechnology.* 79(5):707-718.

Wellburn, A.R. 1994. The spectral determination of chlorophylls a and b, as well as total carotenoids, using various solvents with spectrophotometers of different resolution. *Plant Physiology.* 144:307-313.

Westerhoff, P., Hu, Q., Esparza-Soto, M. and Vermaas, W. 2010. Growth parameters of microalgae tolerant to high levels of carbon dioxide in batch and continuous-flow photobioreactors. *Environmental Technology.* 31(5):523-532.

Wiltshire, K.H., Boersma, M., Möller, A. and Buhtz, H. 2000. Extraction of pigments and fatty acids from the green alga *Scenedesmus obliquu*s (Chlorophyceae). *Aquatic ecology.* 34(2):119-126.

Winkler, H. and Marquand, A. 2009. Changing development paths: From an energy-intensive to low-carbon economy in South Africa. *Climate and Development.* 1(1):47-65.

van Beilen, J.B. 2010. Why microalgal biofuels won't save the internal combustion machine. *Biofuels, bioproducts and biorefining.* 4(1):41-52.

Yeh, A.C. and Bai, H. 1999. Comparison of ammonia and monoethanolamine solvents to reduce CO_2 greenhouse gas emissions. *The Science of the Total Environment.* 228(2-3):121-133.

Yoo, C., Jun, S., Lee, J., Ahn, C. and Oh H.M. 2010. Selection of microalgae for lipid production under high levels carbon dioxide. *Bioresource Technology.* 101(Supplement 1):S1:S71-S74.

Zhu, X., Long, S.P. and Ort, D.R. 2008. What is the maximum efficiency with which photosynthesis can convert solar energy into biomass? *Current Opinion in Biotechnology.* 19(2):153-159.

Appendices

Appendix A: Recipes for Stock Solutions

Table A-1: Modified Bold (3NBBM) medium

Component	Quantity (g/L)
$NaNO_3$	0.75
$CaCl_2.3H_2O$	0.025
$MgSO_4.7H_2O$	0.075
$K_2HPO_4.3H_20$	0.075
KH_2PO_4	0.175
NaCl	0.025
PIV metal solution	6 mL/L
Vitamin B12 (Cyanocobalamin)	1 mL/L
Vitamin B1 (Thiamine)	1 ml/L

Table A-2: Provasoli's trace (PIV) metal solution

Component	Quantity (g/L)
Na_2EDTA	0.75
$FeCl_3.6H_2O$	0.025
$MnCl2.4H_2O$	0.075
$ZnCl_2$	0.025
$CoCl_2.6H_2O$	0.075
$Na_2MoO_4.2H_2O$	0.175

Table A-3: Vitamin stock solutions

Component	Quantity (g/L)
Vitamin B1	1.2
Vitamin B12	0.1 then 1:100 dilution

Filter sterilize and store in the dark at 4 °C.

Table A-4: Sodium Borate-Gluconate mobile phase

Component (HPLC-grade)	Quantity (mL/L)
Borate gluconate concentrate	40
n-butanol	40
Acetonitrile	240

Fill to 1 L with dH_2O and mix thoroughly. Filter and degas

Table A-5: Sodium Borate-Gluconate concentrate

Component (HPLC-grade)	Quantity (g/L)
Sodium gluconate	16
Boric acid	18
Sodium tetraborate decahydrate	25
Glycerine	250 mL

Prior to adding the glycerine add about 500 mL dH_2O and mix until dissolved. Fill to 1 L with dH_2O. Autoclave before storage.

Appendix B: Diagram of ALR

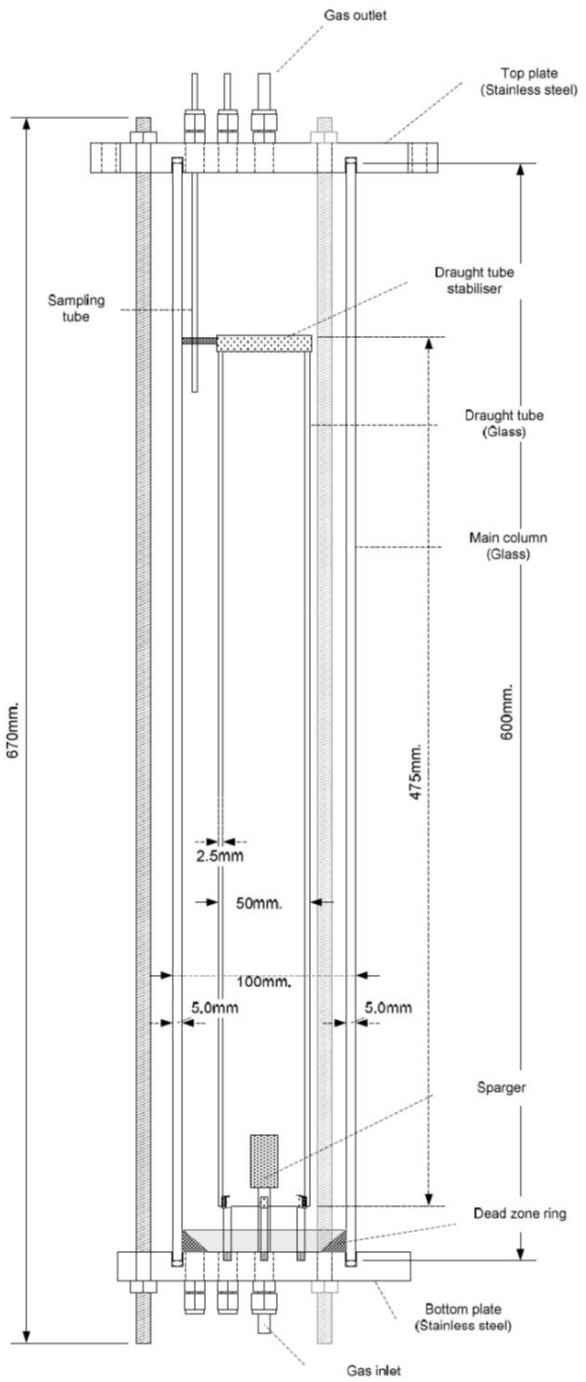

Figure B.1: Diagram of ALR showing dimensions of key components (Langley, 2010)

Appendix C: Calibration curves

Appendix C1: Note on accurate cell concentration determination

In this study, accurate determination of cell concentration was complicated by the fact that several growth conditions were employed. Cell shape, cell size, cell clustering and pigment content vary according to the growth phase and condition which affects the relationship between absorbance and cell dry weight. Hence, using a coefficient from a standard curve generated from a single point during the growth cycle can result in inaccurate predictions of cell concentrations. This was observed for the 1200 ppm CO_2 experiment in this study; the coefficient used from the standard curve generated at the end of the growth cycle resulted in cell concentrations which correlated poorly with cell concentrations determined by dry weight measurements.

To circumvent the risks associated with this method, Griffiths *et al*. (2011b) suggest generating a standard curve in the middle of the growth curve or across the entire growth cycle. Dicks (2010) generated standard curves across the entire growth cycle for *Scenedesmus* sp. for the 2900 and 450 ppm CO_2 conditions. The coefficients were plotted and a polynomial trendline was fitted to this to generate a coefficient curve (Figure C.2 and Figure C.3). This equation is then used to identify the coefficient according to the day of cultivation such that the cell concentration ($g.L^{-1}$) can be calculated from the measured absorbance values. However, due to time constraints coefficient curves could not be generated for all the different conditions that were employed. Thus, dry weight measurements were taken at regular time points of the growth curve to validate the cell concentrations calculated from absorbance values (Table C-1). If the cell concentrations calculated from the standard curve correlated poorly with the cell concentrations calculated using dry weight measurements, an alternate coefficient was used. Additionally, absorbance was measured at 750 nm to avoid interference by pigment absorption (Figure C.1).

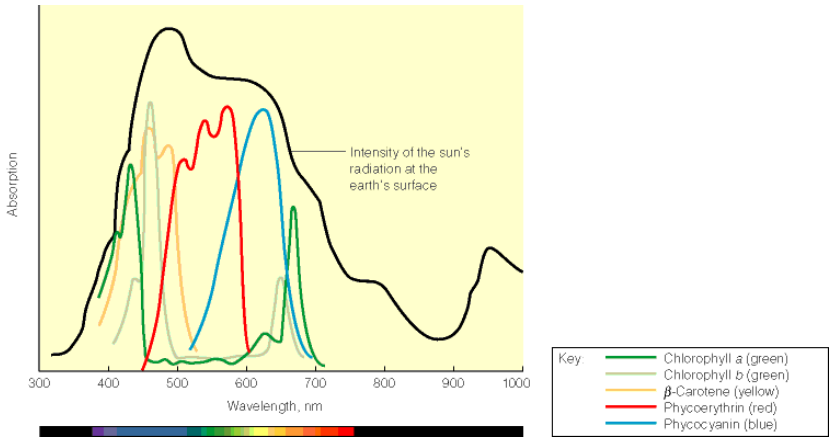

Figure C.1: Absorption spectra of plant pigments (Garrett and Grisham, 2005)

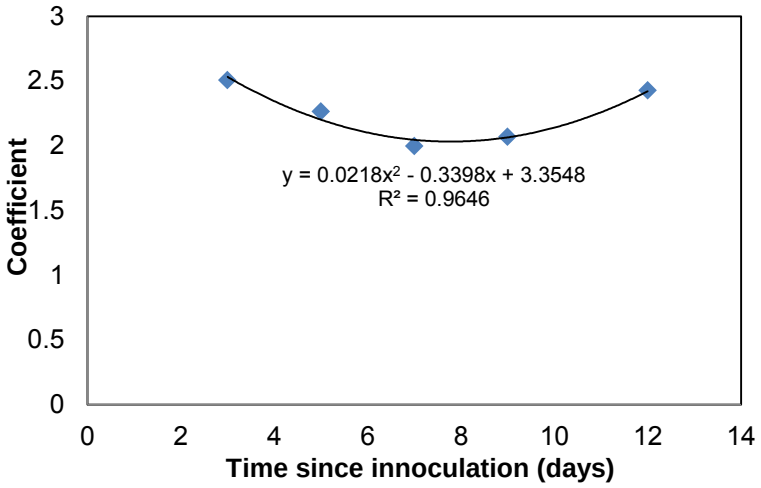

Figure C.2: Coefficient curve for *Scenedesmus* sp. cultured with 2900 ppm CO_2, absorbance taken at 750 nm (Dicks, 2010)

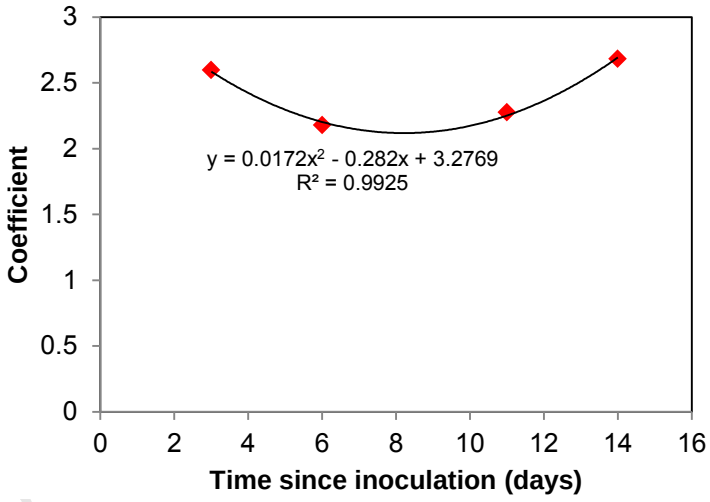

Figure C.3: Coefficient curve for *Scenedesmus* sp. cultured with 450 ppm CO_2, absorbance taken at 750 nm (Dicks, 2010)

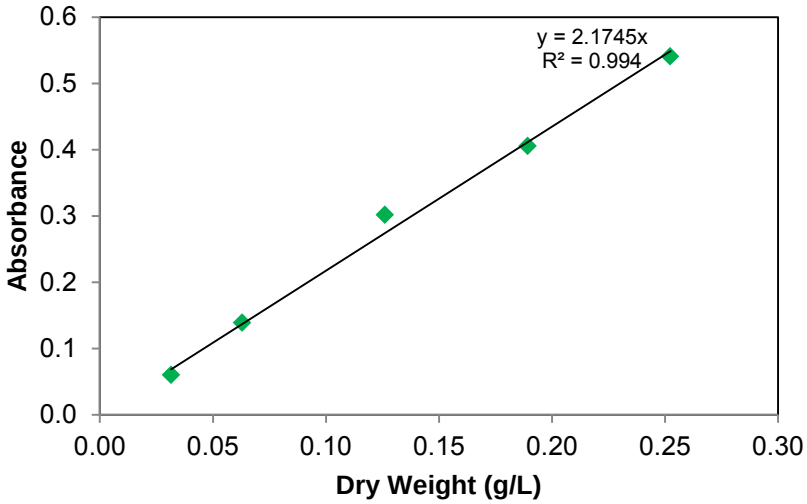

Figure C.4: Standard curve of *Scenedesmus* sp. cultured with 5000 ppm CO_2, absorbance taken at 750 nm

Table C-1: Example of calculation of cell concentrations using dry weight measurements

(Taken with samples of *Scenedesmus* sp. across the growth cycle at 10 000 ppm CO_2. DW, FP, X and Δ stand for dry weight, filter paper, biomass concentration and difference between the dry weight of cell sample with filter paper and filter paper respectively)

multiplier	50				
Reactor 1: 2X Light intensity, Fed-batch					
Day	**DW**	**DW FP**	Δ	**X (g/L)**	
2	0.0974	0.0945	0.0029	0.145	
4	0.1123	0.0931	0.0192	0.96	
7	0.1438	0.0929	0.0509	2.545	
10	0.1623	0.0931	0.0692	3.46	
14	0.2008	0.0925	0.1083	5.415	
14	0.2012	0.0937	0.1075	5.375	
				Avg. final conc	**St. dev.**
				5.395	0.028
Reactor 2: 1X Light intensity, Fed-batch					
Day	**DW**	**DW FP**	Δ	**X (g/L)**	
2	0.098	0.0921	0.0059	0.295	
4	0.108	0.0956	0.0124	0.62	
7	0.1202	0.09	0.0302	1.51	
10	0.137	0.0936	0.0434	2.17	
14	0.1614	0.0922	0.0692	3.46	
14	0.1619	0.0946	0.0673	3.365	
				Avg. final conc	**St. dev.**
				3.413	0.067
Reactor 3: 2X Light intensity					
Day	**DW**	**DW FP**	Δ	**X (g/L)**	
2	0.0941	0.092	0.0021	0.21	
4	0.1146	0.092	0.0226	1.13	
7	0.1468	0.0934	0.0534	2.67	

10	0.1702	0.0968	0.0734	3.67	
14	0.1848	0.0927	0.0921	4.605	
14	0.1863	0.0946	0.0917	4.585	
				Avg. final conc	**St. dev.**
				4.595	0.014
Reactor 4: 1X Light intensity					
Day	**DW**	**DW FP**	**Δ**	**X (g/L)**	
2	0.0933	0.0904	0.0029	0.145	
4	0.1097	0.0951	0.0146	0.73	
7	0.1282	0.0936	0.0346	1.73	
10	0.1441	0.0942	0.0499	2.495	
14	0.1687	0.0945	0.0742	3.71	
14	0.1635	0.093	0.0705	3.525	
				Avg. final conc	**St. dev.**
				3.618	0.130

Appendix C2: Calibration curves for determination of anion concentrations

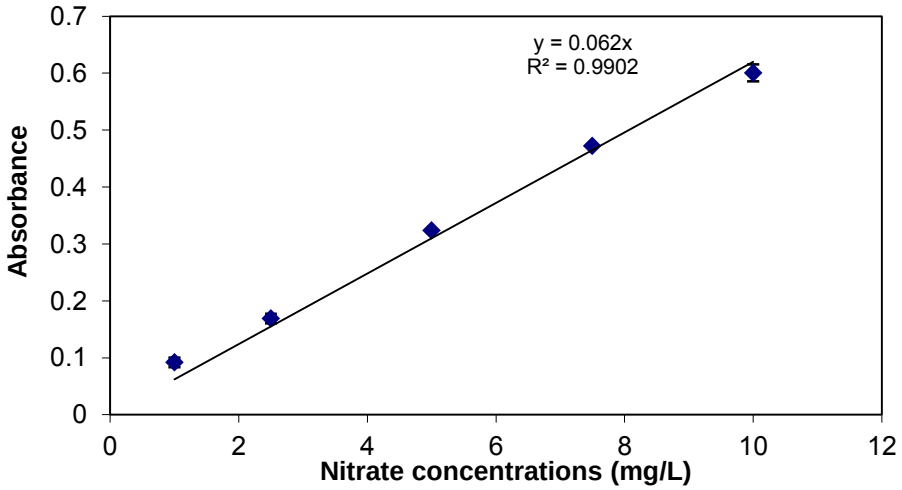

Figure C.5: Nitrate Standard Curve (spectrophotometric), absorbance read at 220 nm

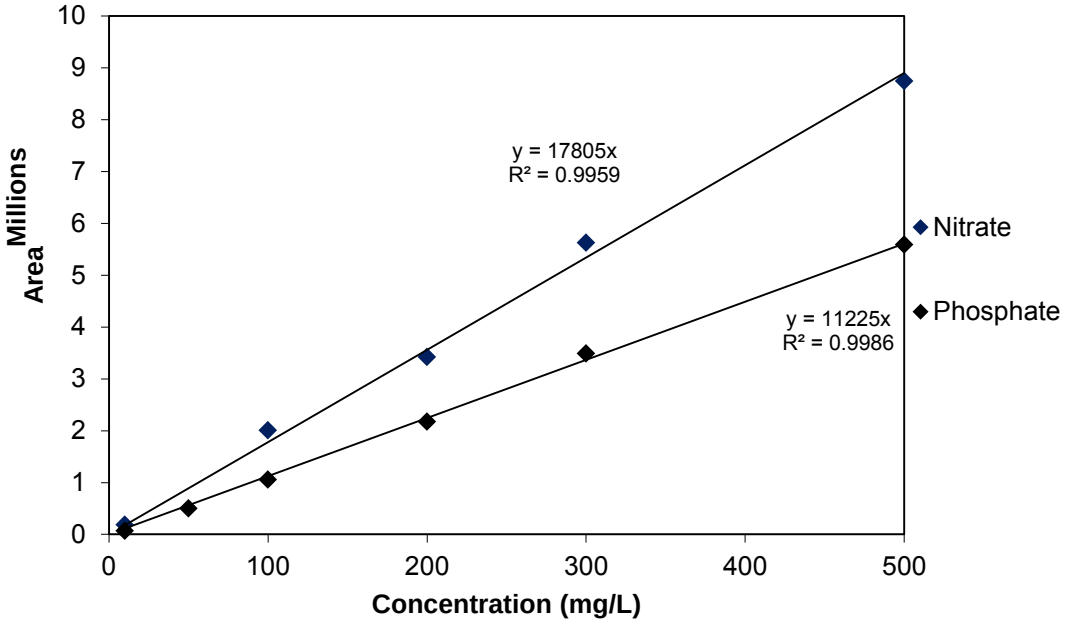

Figure C.6: Nitrate and Phosphate Standard Curves (HPLC)

Appendix D: Elemental mass fractions of *Scenedesmus* sp.

Table D-1: Elemental mass fractions of *Scenedesmus* sp. when cultured with 2900 ppm CO_2

(Values on the left hand side of the table are when *Scenedesmus* sp. was cultured at 1X Light intensity and values on the right hand side of the table are when *Scenedesmus* sp. was cultured at 2X Light intensity)

Day	C	H	N		C	H	N
2	45.69	6.4	9.55		45.91	6.55	9.53
4	49.69	6.81	9.16		48.24	7.11	7.26
7	47.53	6.76	6.33		44.77	6.51	2.95
10	46.96	6.94	1.84		45.34	6.58	4.25
14	44.95	6.25	2.9		48.54	7.19	1.24
Average	46.96	6.63	5.96		46.56	6.79	5.05
St. dev.	1.83	0.29	3.52		1.72	0.33	3.34

Appendix E: Determination of Mixing Time (t_m)

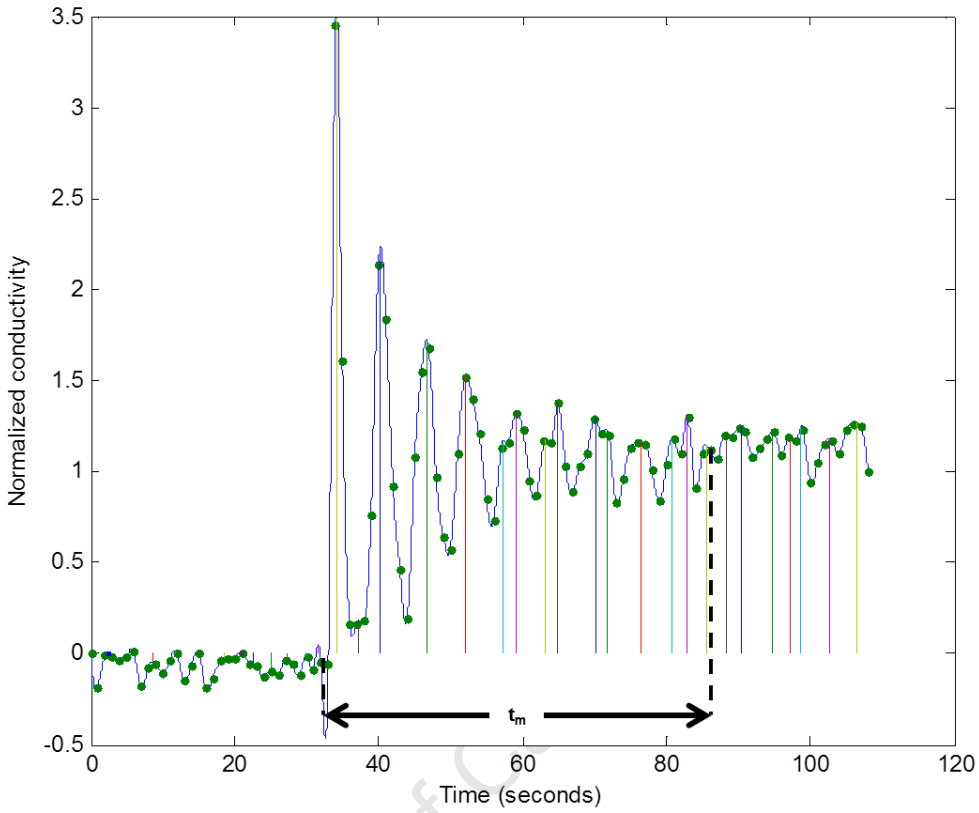

Figure E.1: Normalized tracer response signal graph at U_{GR}=0.021 m.s^{-1} in ALR (Fraser, 2011)

Appendix F: ANOVA for main effects of 2^3 model

Table F-1: ANOVA for main effects model

Source	Sum of Squares	df	Mean square	F value	p-value Prob>F
Model	1.02	3	0.34	4.57	0.088
A:CO_2	0.042	1	0.042	0.57	0.4911
B:Light intensity	0.91	1	0.91	12.31	0.0247
C:Nutrient regime	0.062	1	0.062	0.84	0.4107
Residual	0.3	4	0.074		
Cor Total	1.31	7			